

# Rotational Isomerism in *trans*-1,2-Diarylethylenes

UGO MAZZUCATO\*<sup>†</sup> and FABIO MOMICCHIOLI<sup>‡</sup>

Dipartimento di Chimica, Università di Perugia, I-06100 Perugia, Italy, and Dipartimento di Chimica, Università di Modena, I-41100 Modena, Italy

Received January 2, 1991 (Revised Manuscript Received July 22, 1991)

## Contents

I. Introduction	1679
II. Methods of Investigation	1682
A. Techniques Based on Emission Spectroscopy	1682
1. Excitation Wavelength Effect	1682
2. Lifetime Measurements	1683
3. Time-Resolved Spectroscopy	1683
4. Frozen-In Nonequilibrium Mixtures of Rotamers	1684
5. Quantitative Methods of Fluorescence Analysis	1684
6. Differential Quenching	1687
7. Emission from "Dilute Cold Gases"	1687
B. Other Experimental Techniques	1688
1. Direct Detection Techniques	1688
2. Conventional and Laser Flash Photolysis	1689
C. Quantum Mechanical Calculation Techniques	1689
III. Survey of Studies on Rotamerism of Various DAE Compounds	1691
A. Hydrocarbon Compounds	1691
1. Naphthyl Derivatives	1691
2. Phenanthryl Derivatives	1700
3. Benzophenanthryl Derivatives	1703
4. Anthryl Derivatives	1704
5. Pyrenyl Derivatives	1708
6. Chrysenyl Derivatives	1709
7. Distyrylnaphthalenes and -benzenes	1709
8. Dimethylstilbenes	1709
B. Heteroatom-Containing Compounds	1710
1. Azastilbenes	1710
2. Naphthyl-Pyridyl Derivatives	1712
3. Phenanthryl-Pyridyl Derivatives	1713
4. Quinoyl and Isoquinoyl Derivatives	1713
5. Quinoxaly and Pyrazyl Derivatives	1715
6. Pyrrolyl and Indoyl Derivatives	1715
7. Thienyl and Furyl Derivatives	1715
C. Solvent Effects	1716
IV. Conclusions	1717

## I. Introduction

Information on the behavior of many molecules thought to undergo conformational equilibration in the ground state is abundant in the scientific literature.

As an example, the physicochemical properties (e.g., photoreactivity) of polyenes can be rationalized by assuming that these compounds exist in the ground state as equilibrium mixtures of almost planar conformers,

named *s*-cis and *s*-trans isomers by Mulliken,<sup>1</sup> differing from one another by a 180° rotation around one or more of their quasisingle C-C bonds<sup>2</sup> (Figure 1a).

In the early 1960s, the existence of equilibrated mixtures of *s*-cis and *s*-trans isomers was proposed by Cherkasov<sup>3,4</sup> to explain the spectroscopic behavior of *n*-vinylanthracene (*n* = 1,2,9) (Figure 1b). This case of isomerism, which is related to internal rotation of the molecule around the quasi single bond connecting the anthryl and vinyl groups, is the direct precursor of the rotational isomerism (rotamerism) in *trans*-1,2-diarylethylenes (DAEs).

A little later, Fletcher<sup>5</sup> showed that certain fluorescence anomalies (band shift with variation of excitation wavelength) observed with compounds containing rotatable chromophoric (or auxochromic) groups (e.g., 6-methoxyquinoline, *o,o'*-biphenol), are due to the molecule existing in at least two different conformations (Figure 1c) with slightly shifted spectra.

A rather different, but yet related, phenomenon occurs in flexible aromatic molecules like bi(poly)phenyls where distinct *s*-cis and *s*-trans isomers cannot occur because of symmetry reasons. These molecules exist in the ground state as a broad distribution of nonplanar conformations centered at a sizable value of the twist angle of the interannular quasi single bond(s). Provided the degree of nonplanarity is greatly reduced in the pertinent excited state, these systems exhibit structureless absorption bands which can be considered as resulting from the overlapping of a large number of individual transitions slightly shifted with respect to one another.<sup>6,7</sup>

On the other hand, certain biaryls where the existence of discrete rotamers can be postulated (e.g., 2,2'-binaphthyl, Figure 1d) exhibit spectroscopic anomalies clearly referable to the presence of rotameric equilibria.<sup>8</sup>

While examples of rotamerism are numerous in the literature, direct measurements of the actual distinct properties of rotameric species have been reported mostly for DAEs. These nonrigid, stilbene-like compounds are good candidates for rotamerism similar to vinylanthracenes.<sup>3</sup> In fact, *s*-cis/*s*-trans isomerism is, in principle, allowed in DAEs of the general formula Ar-CH=CH-Ar' whenever Ar and/or Ar' do not have *C*<sub>2v</sub> symmetry with respect to the bond axis. Thus, asymmetrical substitution at the ortho/meta positions of the phenyl group of *trans*-stilbene (Figure 2a) or replacement of one (or both) phenyl group(s) with a polycyclic group (Figure 2, parts b and c) allows the existence of distinct rotamers interconvertible by rotation of one (or both) aryl group(s) around the quasi single bond(s) with the ethylenic bridge. Let us adopt the following contracted notations for DAEs: *n*-St-

<sup>†</sup> Università di Perugia.

<sup>‡</sup> Università di Modena.



Ugo Mazzucato was born in Padua in 1929. He received a degree in chemistry from the University of Padova in 1955. He was lecturer in physical chemistry and related subjects at the Universities of Padua (1955–68), L'Aquila (1968–69), and Perugia (1969–present). At Perugia, he has been a full professor of physical chemistry since 1969 and the chairman of the Chemistry Department of the Science Faculty since 1986. He is one of the founding members of the European Photochemistry Association, the Italian Group of Photochemistry, the national divisions of Physical Chemistry and Chemical Education, and the regional section of the Italian Chemical Society. He is a member of the editorial boards of the *Gazzetta Chimica Italiana* and *Journal of Photochemistry and Photobiology, A: Chemistry*. In the first part of his career he spent brief periods at the Universities of Sheffield (working under G. Porter), Orsay (S. Leach), and Moscow (L. A. Tumerman) to learn about photophysical and photochemical techniques. He has authored over 130 scientific papers on kinetics, spectroscopy, acid–base and charge–transfer equilibria, photographic science, chemical education and, primarily, on photochemistry. His principal research interest is focused on the processes of rotation around double bonds (cis–trans photoisomerization) and single bonds (ground-state rotamerism) in stilbene-like compounds and their heteroanalogues and on their bimolecular processes with energy, electron and proton donors or acceptors. His hobbies include stamp collection, mountain excursions, and wine tasting.



Fabio Momicchioli was born in Siena, Italy, in 1937. He studied in the Faculty of Industrial Chemistry at Bologna University, where he graduated in 1961. Soon afterward he joined the Department of Chemistry at the University of Modena. There, he was first assistant professor and lecturer of theoretical chemistry (1965–1975) and of other topics related to physical chemistry. Since 1976, he has been a full professor of physical chemistry. In 1986, he was a visiting professor at the Chemistry Laboratory of the Ecole Normale Supérieure, Montrouge, France. His research interests are centered on the electronic spectroscopy and the photophysics of conjugated systems. He has been primarily involved in the optimization of semiempirical calculation techniques for studying conformational and dynamic properties of nonrigid molecules in their ground and excited electronic states. Since 1981, his research group has also been engaged in experimental photophysics and photochemistry by both stationary and time-resolved spectroscopy.

(styryl)Ar if  $Ar' = \text{phenyl}$ ;  $n,n'$ -D(di)ArE(ethylene) if  $Ar = Ar'$  and  $n,n'$ -ArAr'E if  $Ar \neq Ar'$ , where  $n,n'$  denote

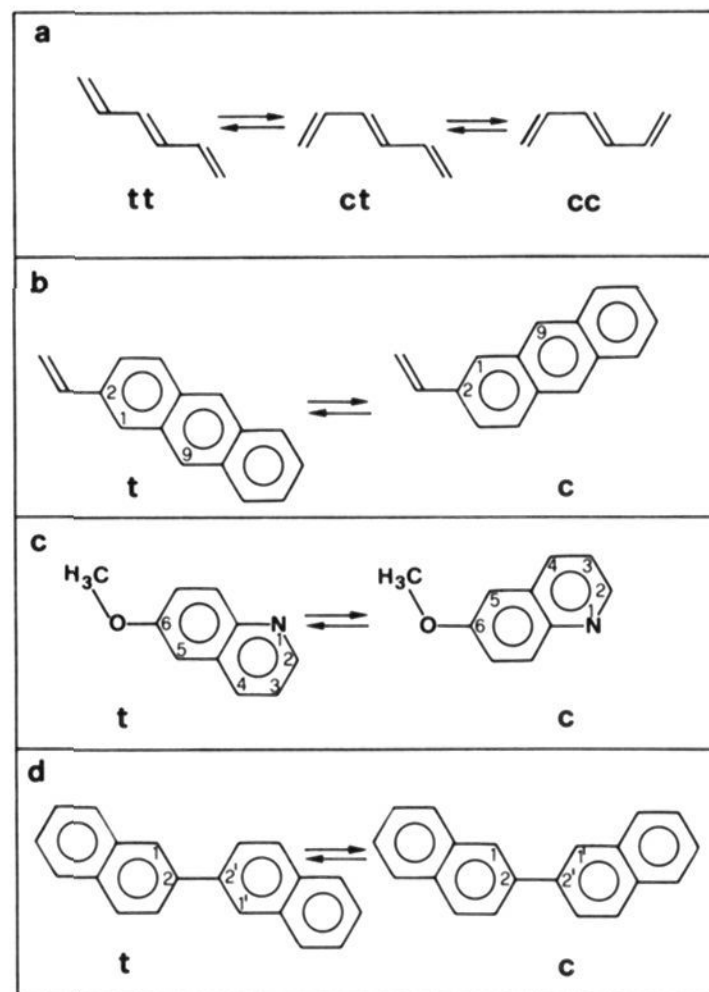


**Figure 1.** Rotational isomerism (rotamerism) in *trans*-1,3,5-hexatriene (a), 2-vinylanthracene (b), 6-methoxyquinoline (c), and 2,2'-binaphthyl (d). t and c stand for *s-trans* and *s-cis*.

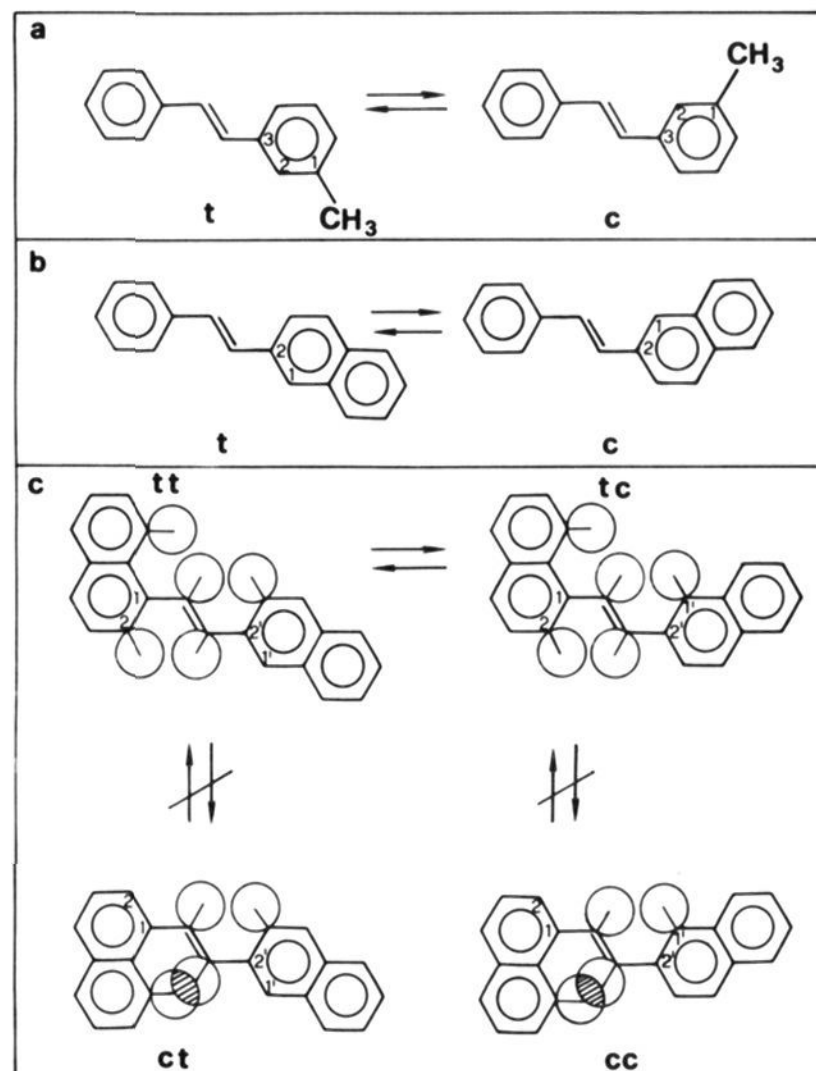


**Figure 2.** Rotamerism in some *trans*-1,2-diarylethylenes: 3-styryltoluene (a), 2-styrylnaphthalene (2-StN) (b), and di(1,2'-naphthyl)ethylene (1,2'-DNE) (c). van der Waals spheres of the hydrogen atoms responsible for steric strain are sketched for 1,2'-DNE. The heavily strained ct (*s-cis*, *s-trans*) and cc (*s-cis*, *s-cis*) forms are expected to be present with negligible fractions in solutions of 1,2'-DNE at room temperature.

the substitution positions at the aryl groups and Ar,Ar' are the radical abbreviations to be specified case by case

(e.g., N = naphthyl, Ph = phenanthryl, A = anthryl).

The conformations of DAE rotamers are determined by the interplay of two factors: the resonance stabilization of the delocalized  $\pi$ -electron system, favoring the coplanarity of the whole molecule, and the steric repulsions between the ethylenic hydrogens and the ortho hydrogens (or substituent groups) of the aryl chromophore(s), which tend to twist the molecule out of the plane.

In several cases, simple structural reasoning suggests that the distinct rotamers are nearly isoenergetic (quasi coplanar) with relatively small barriers between them (Figure 2, parts a and b). Consequently, these DAEs should exist in fluid solutions at room temperature as equilibrium mixtures of the expected rotamers in comparable amounts. In other cases (e.g., 1,2'-dinaphthylethylenes) (Figure 2c), the coplanar forms of one or more rotamers are strongly sterically hindered. Of course, these species are forced to assume markedly nonplanar configurations and their destabilization can become so important that the conformational equilibrium is completely shifted toward the rotamer(s) with a less-strained coplanar form.

Preferential conformations of stilbene-like molecules in solution were first discussed in the literature for some *trans*-styrylpyridines (*n*-StPs), on the basis of the study of electric dipole moments,<sup>9</sup> and for the same and other related compounds, on the basis of considerations of steric interactions<sup>10</sup> and of NMR chemical shifts.<sup>11-13</sup> The assumption of the existence of rotamers was demonstrated to be quite reasonable but no direct experimental evidence was given. Only later, was fluorimetric analysis of the rotamer mixture reported to be a powerful method for obtaining information on the distinct properties of the mixture components.

Until 10 years ago, the fluorescence of *trans*-stilbene-like molecules was described as a single emission. The corresponding *cis* isomers are generally nonfluorescent, at least in fluid solutions at not too low temperatures. The only indirect sign of the existence of different conformations in solution came from the intramolecular photocyclization of these *cis* compounds<sup>14</sup> (for *cis*-stilbene, e.g., this photoreaction gives an intermediate dihydrophenanthrene which then converts to the final stable phenanthrene in the presence of a hydrogen acceptor) which led to different isomeric photoproducts when they contained asymmetrical chromophores.<sup>15</sup> This behavior, however, does not give any information about the real stability of the rotamers nor about their relative abundance. In fact, the photocyclization quantum yield depends mainly on the electronic properties which determine the different reactivity of the distinct positions where the new bond has to be formed (electron density, free valence index, etc. at the reaction center).<sup>14,16</sup>

The existence of a dynamic equilibrium between distinct yet quasi-isoenergetic rotamers of *trans*-DAEs was first suggested by Hammond et al.<sup>17</sup> who discussed the fluorescence properties of 2-StN. Using this hypothesis, Fischer and Fischer<sup>18</sup> explained some anomalies in the fluorescence behavior of the same and related molecules, also on the basis of preliminary fluorescence decay measurements by Haas<sup>19</sup> indicating nonexponential behavior. In the late 1970s a series of more or less rigorous studies of the phenomenon began

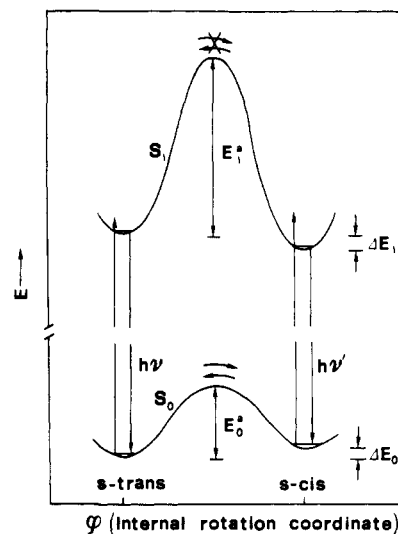


**Figure 3.** Schematic potential energy curves for the interconversion between rotamers of *trans*-1,2-diarylethylenes in the ground and first singlet-excited states. Typical values of  $E_0^*$  and  $\Delta E_0$ , as deduced by quantum mechanical calculations and experimental observations, are about 4–5 and 0.5–1 kcal mol<sup>-1</sup>, respectively.  $\Delta E_1$  is generally negative (thus implying  $h\nu' < h\nu$ ), and  $E_1^*$  values consistent with noninterconverting exciting rotamers should be  $\geq 2E_0^*$ .

to be reported from several laboratories based on different fluorimetric behavior of the distinct rotamers. These first papers triggered research on this subject in other laboratories. Great advances have thus been made in the last several years in our ability to treat rotamer systems and to separate their photophysical and photochemical properties.

To date, a great many fluorescence studies (both steady state and time resolved) have been reported for the 2-naphthyl analogues of stilbene and a variety of other stilbene-like compounds and their aza analogues where two or more distinct rotamers are expected to be present at equilibrium with comparable abundances. The principles of the independence of fluorescence upon excitation wavelength ( $\lambda_{\text{exc}}$ ) and that of mirror symmetry between absorption and emission spectra were found to be violated in these systems. In keeping with the early working hypothesis of Hammond<sup>17</sup> and the Fischers<sup>18</sup> and with the studies of Cherkasov<sup>3</sup> on 2-vinylnanthracene, all following papers ascribed the observed fluorescence anomalies ( $\lambda_{\text{exc}}$  dependence of fluorescence spectra and quantum yields, emission wavelength,  $\lambda_{\text{em}}$ , dependence of the fluorescence excitation spectra and multiexponential decay) to the existence of such almost coplanar (which implies a sufficiently high energy barrier to  $t \leftrightarrow c$  isomerization) and almost isoenergetic rotamers.

After Haas and the Fischers,<sup>20</sup> all of the observed anomalies in the emission spectra and decay kinetics of DAEs were rationalized by assuming that singlet excited rotamers do not interconvert during their short lifetime. This basic theoretical scheme, which relies on the expected enhancement of the double bond character of the aryl-ethylene bonds upon  $\pi \rightarrow \pi^*$  excitation, only extends the so-called principle of nonequilibration of excited rotamers (NEER) to DAEs. This was first proposed by Havinga and co-workers<sup>2</sup> to explain the photochemical behavior of hexatriene derivatives. The NEER hypothesis is illustrated in Figure 3 with the aid of schematic potential energy curves of the ground and

lowest singlet-excited states. We will return to this important assumption on several occasions. Its validity depends on the nature of the lowest singlet excited state and should in principle be verified case by case.

In the present article we first describe the methods of investigation which allowed rotamerism of DAEs to be brought to light and analyzed quantitatively. As stated above, steady-state and time-resolved emission spectroscopy played the leading role, but other methods, including the quantum mechanical approach, also contributed significantly. In the second part of the article we provide a survey of the main cases of rotamerism observed in solutions of DAEs since 1977, when Sheck et al.<sup>21</sup> began the systematic study of the phenomenon.

## II. Methods of Investigation

To prove the existence of distinct rotamers in a DAE solution, they should differ in some physical property, e.g. in spectral behavior. However, the techniques which can be selected must have a response time which is short enough to avoid interconversion between rotamers during the experiment. Therefore, electronic excitation, characterized by very short transition times ( $10^{-15}$  s), obviously offers the most powerful technique for studying rotamerism.<sup>22</sup>

### A. Techniques Based on Emission Spectroscopy

The use of these techniques is obviously limited to compounds characterized by an intense enough fluorescence emission in the temperature range being investigated. Since the *cis* geometrical isomers do not generally fluoresce (except at very low temperature), the fluorimetric studies of rotamerism in DAEs are practically confined to the substantially emitting *trans* isomers. The success of this technique for detecting ground-state rotamers relies on the validity of the NEER assumption,<sup>2</sup> which requires an excited-state interconversion barrier which is markedly higher than that of the ground state (see Figure 3) combined with a short lifetime in the fluorescent state. It must be remembered that the  $S_1$  lifetime is controlled by the rate of the nonradiative processes in competition with fluorescence, mainly the  $S_1 \rightarrow T_n$  intersystem crossing (ISC) and the rotation around the ethylenic double bond toward the perpendicular form (*trans*  $\rightarrow$  *perp*), the intermediate in the *trans*  $\rightarrow$  *cis* photoisomerization (singlet mechanism).<sup>23</sup> When the activation energy of the *trans*  $\rightarrow$  *perp* rotation is too high (generally  $\geq 8$ – $10$  kcal mol<sup>-1</sup>), the nonradiative decay occurs predominantly through ISC, generally followed by isomerization in the triplet manifold (triplet mechanism).<sup>24</sup> Since, in principle, different rotamers may be characterized by different kinetic parameters of the competitive decay processes, the composition of the conformer mixture may affect the overall quantum yield of the *trans*  $\rightarrow$  *cis* photoisomerization. Other possible photoreactions of these compounds (e.g. dimerization of the *trans* isomers, isomerization and cyclization of the *cis* isomers) may be influenced as well.

#### 1. Excitation Wavelength Effect

Slight differences in the optical absorption and emission spectra of *trans* DAEs make selective excita-

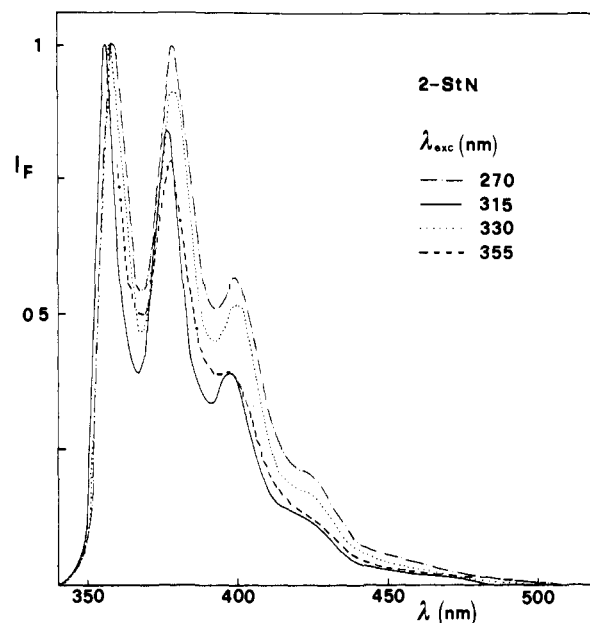


**Figure 4.** Effect of  $\lambda_{exc}$  on the fluorescence spectrum of 2-StN in MCH at room temperature (unpublished results related to refs 24 and 25).

tion possible since, at any absorbed  $\lambda_{exc}$ , the amount of light absorbed and emitted by each rotamer will be different. In fact, the methodology that initiated the in-depth investigations on rotamerism of DAEs is that based on the  $\lambda_{exc}$  effect on the fluorescence behavior of the rotamer mixture in solution.<sup>20,21</sup> The fluorescence spectrum in the first cases which were studied in depth (the naphthyl analogues of stilbene) was found to be strongly dependent on  $\lambda_{exc}$  (Figure 4) and temperature.<sup>20,21,25</sup> Moreover, the excitation spectrum changed with the analysis wavelength ( $\lambda_{em}$ ) and differed from the absorption spectrum. After having excluded impurity effects, the authors explained their data by assuming the existence of two or more conformers which differed in their electronic distributions and steric strain in the coplanar forms. Since individual conformers may differ in their absorption and emission spectra, their selective excitation is thus possible: irradiation at the tail of the absorption spectrum results in preferred excitation of one conformer while irradiation at shorter wavelengths leads to a fluorescence spectrum which is a superposition of emissions from two or more fluorescing species. Of course, these observations can be more or less affected by temperature changes: lowering the temperature should shift the rotamer equilibrium toward the more stable form, in addition to sharpening the spectra, thereby decreasing the band overlap. In some favorable cases, the absorption spectra of the rotamers are sufficiently shifted. When the absorption edges are almost coincident, as happens with 2-StN, the situation is more complicated. At any  $\lambda_{exc}$ , the spectral and photophysical properties of the solution are the weighted sum of those of the pure components. In this case, more complex analysis methods must be used<sup>25</sup> (see section II.A.5).

The  $\lambda_{exc}$  effect on the emission spectrum is almost always accompanied by changes in the fluorescence quantum yield,  $\phi$ , which, in turn, reflect different radiative ( $k_F$ ) and/or radiationless ( $k_{t \rightarrow c}$  or  $k_{ISC}$ ) rate parameters of the rotamers. As will be seen, it is not always easy to discriminate between the relative im-

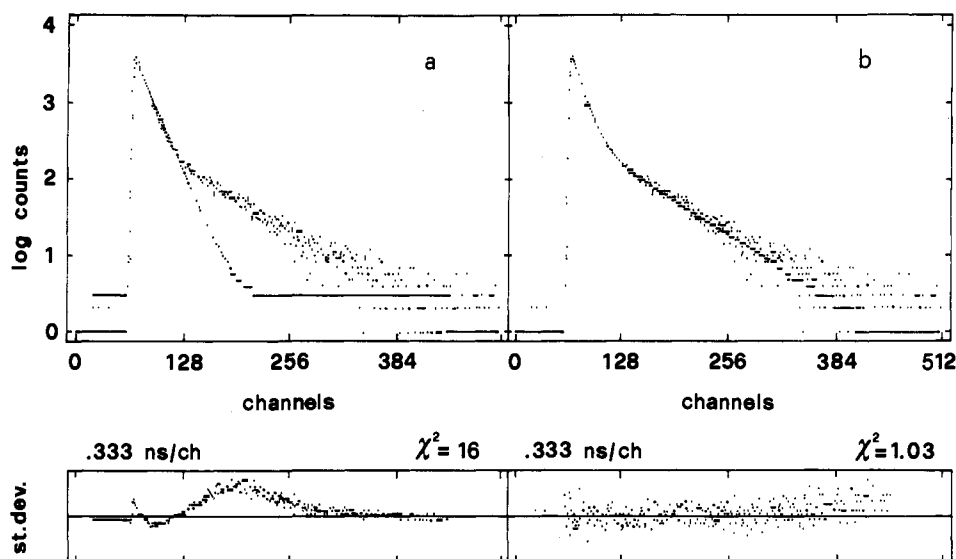


**Figure 5.** Fluorescence decay of 2-StN in MCH at room temperature ( $\lambda_{\text{exc}} = 355$  nm,  $\lambda_{\text{em}} = 395$  nm): (a) best fit for a monoexponential decay function (nonrandom residuals  $\chi^2 = 16$ ); (b) best fit for a biexponential decay function (random residuals,  $\chi^2 = 1.03$ ) (unpublished results related to refs 24 and 25).

portance of these competitive processes.

Narrow slits and low temperatures have generally been used to measure the spectra in order to obtain better resolution. However, large slits, even as wide as 20 nm, were sometimes used to reduce photosensitive excitation thus providing more informative spectra of the mixture.<sup>20,22,26,27</sup> In particular, excitation over a very broad range of  $\lambda_{\text{exc}}$  should yield an emission spectrum in which the contributions of the rotamers give a rough indication of the rotamer composition in the ground state, in solution. By careful variation of  $\lambda_{\text{exc}}$ , the emission spectra of three almost pure rotamers could be measured in suitable cases (see, e.g., ref 22 and section III.A.1.b).

## 2. Lifetime Measurements

In 1978 the methodology of selective excitation advanced when the usefulness of a kinetic study of the bi(multi)exponential decay response function of the rotamer fluorescence was demonstrated.<sup>20</sup> The technique most generally used was based on the time-correlated single photon counting which included nonlinear least-squares iterative reconvolution analysis (Figure 5). For short lifetimes, picosecond single-pulse laser-streak camera apparatuses have occasionally been used.<sup>28</sup> Provided the NEER hypothesis is valid, the emission decay curves of a rotamer mixture can be expressed by the sum of at least two exponentials:

$$I_t = I_0[A_A \exp(-t/\tau_A) + A_B \exp(-t/\tau_B)] \quad (1)$$

where  $\tau_A$  and  $\tau_B$  are the fluorescence lifetimes of the two rotamers. From the deconvolution treatment one can obtain the separate lifetimes and the preexponential factors whose ratio (which gives the relative contribution of the two species to the emission intensity and in some cases can provide a rough estimation of the mixture composition) changes with  $\lambda_{\text{exc}}$ . Both the lifetimes ( $\tau_i$ ) and preexponential factors ( $A_i$ ) are independent parameters which are changed by the least-square deconvolution procedure to give the best fit between experimental and calculated curves. Actually, only the  $A_i$  values were found to vary with  $\lambda_{\text{exc}}$  and  $\lambda_{\text{em}}$  while the  $\tau_i$  values were practically constant in the  $\lambda$  intervals

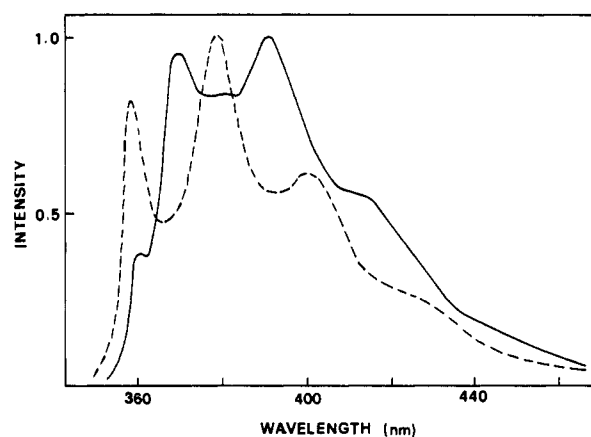


**Figure 6.** Time-resolved emission spectra for 2,2'-DNE excited at 297 nm: —, early-gated spectrum with time delay  $\Delta t = 0$  and gate width  $\delta t = 3$  ns; ---, late-gated spectrum with  $\Delta t = 30$  ns. The spectra were normalized to their maxima to emphasize differences between them (reprinted from ref 28; copyright 1980 Elsevier Sequoia).

explored at any temperature.<sup>20</sup> Whenever the rotamers differ in their decay rates, emission spectra and quantum yields, a combined examination of the fluorescence spectra and decay curves provides information on the relative abundances of the two species and on their distinct photophysical properties.

The correlation between fluorescence spectra and decay curves was treated more rigorously by Birks et al.<sup>25</sup> A detailed description of this analysis method for mixtures of rotamers of comparable fluorescence quantum yield ( $\phi$ ) and different  $\tau$  is reported in section II.A.5.

## 3. Time-Resolved Spectroscopy

Differences in rotamer lifetimes allowed the time-resolved fluorescence technique to be successfully used for these studies.<sup>28</sup> The peaks observed in the late-gated spectrum should reflect the spectral characteristics of the longer lived rotamer while those observed in the early-gated spectrum can support the existence of at least two discrete rotamers and confirm the indications given by the selective excitation (Figure 6).

The phase-resolved fluorescence spectroscopy, based on different combinations of  $\lambda_{\text{exc}}$  with detector phase angle, proved to be useful in the study of multicomponent systems since it improved accuracy by combining selectivity of fluorescence lifetimes with wavelength selectivity.<sup>29</sup>

#### 4. Frozen-In Nonequilibrium Mixtures of Rotamers

In searching for factors which affect the rotameric composition (change of solvent, incorporation into stretched films, aggregation in poor solvents, etc.) Alfimov et al.<sup>30</sup> and Castel and Fischer<sup>26</sup> independently found an elegant method to freeze-in nonequilibrium trans rotamer mixtures by low-temperature irradiation of the corresponding cis isomers. In fact, on cooling solutions containing trans rotamers, one would expect that thermal equilibrium among the rotamers would be established in favor of the more stable species until sufficiently high viscosities are reached that inhibit further equilibration. Therefore, at low temperatures, when the spectra are sharper and more suitable to show the contribution of different rotamers, the mixture is enriched in the most stable modification with small contributions from the other less stable species. To change this situation, recalling that, on cooling,  $\phi_{t \rightarrow c}$  drops much more sharply than  $\phi_{c \rightarrow t}$ ,<sup>23</sup> it is possible to photochemically prepare the trans isomer from the corresponding cis at low temperatures, at viscosities where thermal equilibration between rotamers no longer exists. The rotamer composition is thus governed by its equilibrium value in the cis form, which may differ from that of the trans form and which may favor the detection of a particular species. Comparison of these spectra with those obtained after heating the solution to higher temperatures (to get equilibration) and re-freezing proved to be a useful tool to evidence the contribution of the different modifications to the spectra of the mixture. More clearly defined spectra were obtained by Castel and Fischer,<sup>26</sup> possibly by virtue of using low concentrations which assured complete cis  $\rightarrow$  trans photoconversion, absence of association, and negligible reabsorption of emitted light (see also section III.A.1.b). Unlike the results of Alfimov et al.,<sup>30</sup> differences between the rotamer composition before and after heating/recooling were obtained only in those compounds where two or more isoenergetic rotamers are expected. Moreover, the kinetics of the thermal equilibration between the rotamers could be followed at several temperatures, both in emission and in absorption.<sup>26</sup> It is worth stressing that the freeze-unfreeze method is the only one which makes it possible to compare, under identical conditions, the emission spectra of two rotamer mixtures of widely differing composition. The same holds for the absorption spectra, thus enabling a direct experimental correlation between the absorption and emission spectra of the rotamers.<sup>26</sup> Moreover, the method can be applied to nonfluorescent compounds.

In principle, the freezing-in of nonequilibrium compositions could be a general phenomenon when a mixture of conformers postulated in solution is transferred to an organized system, e.g. by crystallization or incorporation into a host crystal. In section III some examples will be given where rigid matrices led to an enrichment of the mixture in a specific conformer which

was preferentially frozen-in.<sup>22</sup> A typical case is offered by the use of the Shpolskii matrix technique (see section II.A.7).

#### 5. Quantitative Methods of Fluorescence Analysis

Two methods, based on the fluorescence emission properties of the mixture, proved useful in obtaining separately the distinct properties of the rotamers from those of the mixture: (i) a "kinetic fluorescence analysis" (KFA), based on the deconvolution of fluorescence decay curves obtained at different  $\lambda_{\text{exc}}$  by monitoring at selected (possibly isoemissive)  $\lambda_{\text{em}}$ ,<sup>25,31,32</sup> and (ii) a *statistical* method, based on the "principal component analysis" (PCA), which requires the experimental determination of the "emission-excitation" matrix, obtained from a set of fluorescence spectra as a function of  $\lambda_{\text{exc}}$  or other external parameters.<sup>33-39</sup> The latter method, in combination with the self-modeling (SM) technique,<sup>40</sup> offers some advantages with respect to the kinetic method but gives more limited information. Its main utility lies in the fact that it tells us the number of fluorescent components without any preliminary assumption and allows the emission spectra of the mixture to be deconvoluted in a relatively easier way. Moreover, the method is applicable to systems with more than two components, when the KFA method does not practically work. The PCA-SM method is, however, not applicable when the spectra are completely overlapped (for exceptions, see below, section II.A.5.b) nor does it yield information about the kinetic parameters of the pure components. In the few cases where both KFA and PCA-SM methods were applied in parallel (see, e.g., the case of 3-StPh in section III.A.2), it is clear that they are complementary, and, in combination, offer the best approach to a complete knowledge of the fluorescence behavior of the distinct rotamers. However, before entering into the subject, it must be emphasized that the delicacy of these elegant quantitative analysis methods may give results which must be taken with caution. In fact, they require a large number of fluorescence measurements (spectra, quantum yields, and, in the case of the KFA, decay curves), generally in deaerated solutions, for compounds which photoreact. When the photoisomerization quantum yield is higher than 5-10%, the deaerated solution must be changed frequently. The situation becomes even more complex when measurements are made as a function of temperature since not only the fluorescence and photoisomerization quantum yields but also the equilibrium composition are influenced by temperature. In such situation, it could be quite difficult to distinguish between the two effects and to avoid unacceptable errors. Both methods, KFA and PCA-SM, are described in detail below.

a. *The Kinetic Method.* The KFA method<sup>25</sup> is limited in practice, but not in principle, to two-component systems. Suppose we have a solution containing two noninterconverting emitting species whose absorption edges almost coincide. In this case the individual properties cannot be isolated directly but need to be deduced from observations on the mixture. This can be achieved by the following procedure. Let us take a mixture of two rotamers of similar  $\phi$  and different  $\tau$ . The properties of the two fluorescent species are indicated by subscripts A and B ( $\tau_A < \tau_B$ ) and those of

the mixture by barred symbols. The total molar concentration is  $\bar{c} = c_A + c_B$ . The absorption spectrum of the mixture is

$$\bar{\epsilon}(\lambda_{\text{exc}}) = \sum \epsilon_i(\lambda_{\text{exc}}) c_i / \bar{c} \quad (2)$$

where  $i = A, B$ . The fractions of excited molecules of each species at  $\lambda_{\text{exc}}$  are

$$f_i(\lambda_{\text{exc}}) = [\epsilon_i(\lambda_{\text{exc}}) c_i] / [\bar{\epsilon}(\lambda_{\text{exc}}) \bar{c}] \quad (3)$$

being obviously  $f_A = 1 - f_B$ . The fluorescence quantum yield is

$$\bar{\phi}(\lambda_{\text{exc}}) = \sum f_i(\lambda_{\text{exc}}) \phi_i \quad (4)$$

and the fluorescence intensity is

$$\bar{F}(\lambda_{\text{exc}}, \lambda_{\text{em}}) = \sum f_i(\lambda_{\text{exc}}) F_i(\lambda_{\text{em}}) \quad (5)$$

The fluorescence response function (see eq 1) at  $\lambda_{\text{em}}$  following excitation at  $\lambda_{\text{exc}}$  is

$$\bar{i}(t)(\lambda_{\text{exc}}, \lambda_{\text{em}}) = \sum f_i(\lambda_{\text{exc}}) F_i(\lambda_{\text{em}}) k_i \exp(-k_i t) \quad (6)$$

Determination of  $\tau_A = 1/k_A$  and  $\tau_B = 1/k_B$  involves observations of  $\bar{i}(t)$  and deconvolution analysis to evaluate  $k_i$  and the ratio of the intensities of the fast and slow components

$$\alpha(\lambda_{\text{exc}}, \lambda_{\text{em}}) = \frac{A_A}{A_B} = \frac{f_A(\lambda_{\text{exc}}) F_A(\lambda_{\text{em}}) k_A}{f_B(\lambda_{\text{exc}}) F_B(\lambda_{\text{em}}) k_B} \quad (7)$$

The spectra observed at different  $\lambda_{\text{exc}}$  must be normalized to the same absorbed quanta in order to make the ratio of spectral area to the fluorescence quantum yield constant, independent of  $\lambda_{\text{exc}}$ . The analysis is simplified if the overlapping emission spectra of similar quantum efficiencies have one or more isoemissive wavelengths,  $\lambda_{\text{em}}'$ , at which  $\bar{F}(\lambda_{\text{em}}')$  is independent of  $\lambda_{\text{exc}}$ . This occurs when  $\bar{F} = F_A = F_B$ . An isoemissive  $\lambda_{\text{em}}'$  is preferably chosen for the observation of  $\bar{i}(t)$  in flatter regions of the spectrum when  $\delta F / \delta \lambda_{\text{em}}$  is small. Once  $\bar{i}(t)$  at  $\lambda_{\text{em}}'$  over the full range of  $\lambda_{\text{exc}}$  has been observed, the  $k_A$ ,  $k_B$  and  $\alpha(\lambda_{\text{exc}})$  values are determined as well as the derived parameter

$$\beta(\lambda_{\text{exc}}) = \alpha(\lambda_{\text{exc}}) k_B / k_A = (f_A / f_B)(\lambda_{\text{exc}}) \quad (8)$$

Hence, the parameters

$$f_A(\lambda_{\text{exc}}) = [\beta(\lambda_{\text{exc}})] / [1 + \beta(\lambda_{\text{exc}})] \quad (9a)$$

$$f_B(\lambda_{\text{exc}}) = 1 / [1 + \beta(\lambda_{\text{exc}})] \quad (9b)$$

are evaluated. They enable the absorption and fluorescence properties of the two species to be determined. The relative absorption spectra  $\epsilon_i(\lambda_{\text{exc}}) c_i / \bar{c}$  are then obtained by using eq 3. In order to evaluate the individual fluorescence quantum yields of the two species by using eq 4, the two most conveniently chosen excitation wavelengths,  $\lambda_x$  and  $\lambda_y$ , are those where the A and B rotamers, respectively, prevalently contribute to the fluorescence emission of the mixture. By eq 4 and the equation  $f_A = 1 - f_B$ , the fluorescence quantum yields of the two species can be obtained:

$$\phi_A = \frac{\bar{\phi}(\lambda_x) f_B(\lambda_y) - \bar{\phi}(\lambda_y) f_B(\lambda_x)}{f_B(\lambda_y) - f_B(\lambda_x)} \quad (10a)$$

$$\phi_B = \frac{\bar{\phi}(\lambda_y) f_A(\lambda_x) - \bar{\phi}(\lambda_x) f_A(\lambda_y)}{f_A(\lambda_x) - f_A(\lambda_y)} \quad (10b)$$

Analogous relations can be obtained for the fluorescence spectra by using eq 5. In this way, all the fluorescence

parameters of the two species can be obtained. It is to be noted that the emission spectra of the rotamers can also be directly obtained by measurements of the decay as a function of  $\lambda_{\text{em}}$  and using eqs 5 and 7 at a fixed  $\lambda_{\text{exc}}$  (see an application in section III.A.1.a).

From the 0-0 absorption band of the first electronic transition (known by the relative spectra,  $(\epsilon_i)_{00} c_i / \bar{c}$ ), if the Franck-Condon envelopes of the first band are similar in shape, it is to be expected from the radiative lifetime relation that

$$(\epsilon_A)_{00} / (\epsilon_B)_{00} = (k_F)_A / (k_F)_B \quad (11)$$

where the term on the right is the ratio of the radiative rate parameters. The relative abundance of the two species is thus obtained by the relation

$$\frac{c_A}{c_B} = \frac{(\epsilon_A)_{00} c_A (k_F)_B}{(\epsilon_B)_{00} c_B (k_F)_A} \quad (12)$$

If the conformers are in thermal equilibrium in the ground state and one neglects the entropy term, the abundance ratio leads to the enthalpy difference,  $\Delta H$ , between the two species. The  $\Delta H$  value can also be obtained by plots of  $\log \beta(\lambda_{\text{exc}})$  measured at  $\lambda_{\text{em}}'$  against  $1/T$ . Plots of  $\log \alpha(\lambda_{\text{exc}})$  vs  $1/T$  can be used in the temperature region where the fluorescence lifetime remains constant,  $\alpha$  being thus proportional to  $c_A / c_B$ .

In cases where  $\phi_A$  and  $\phi_B$  are dissimilar,<sup>32</sup> there is no isoemissive wavelength  $\lambda_{\text{em}}'$  and  $\bar{i}(t)(\lambda_{\text{exc}}, \lambda_{\text{em}})$  is observed at some other value of  $\lambda_{\text{em}}$ . The parameter  $\beta(\lambda_{\text{exc}})$  of eq 8 is then replaced by

$$\gamma(\lambda_{\text{exc}}, \lambda_{\text{em}}) = \alpha(\lambda_{\text{exc}}, \lambda_{\text{em}}) k_B / k_A = \frac{(f_A / f_B)(\lambda_{\text{exc}}) (F_A / F_B)(\lambda_{\text{em}})}{\quad} \quad (13)$$

From eqs 5 and 13, one obtains for the A species

$$f_A(\lambda_{\text{exc}}) F_A(\lambda_{\text{em}}'') = \gamma(\lambda_{\text{exc}}) [\bar{F}(\lambda_{\text{exc}}, \lambda_{\text{em}}'') - f_A(\lambda_{\text{exc}}) F_A(\lambda_{\text{em}}'')] \quad (14)$$

where  $\lambda_{\text{em}}''$  is the wavelength at which  $\bar{i}(t)$  is measured. Equation 14 can be rewritten in the following way

$$f_A(\lambda_{\text{exc}}) F_A(\lambda_{\text{em}}'') = \frac{\gamma(\lambda_{\text{exc}}) \bar{F}(\lambda_{\text{exc}}, \lambda_{\text{em}}'')}{1 + \gamma(\lambda_{\text{exc}})} = \sigma_A(\lambda_{\text{exc}}) \quad (15a)$$

By an analogous procedure one obtains for the B species

$$f_B(\lambda_{\text{exc}}) F_B(\lambda_{\text{em}}'') = \frac{\bar{F}(\lambda_{\text{exc}}, \lambda_{\text{em}}'')}{1 + \gamma(\lambda_{\text{exc}})} \quad (15b)$$

It is clear that, at the fixed  $\lambda_{\text{em}}''$ ,  $\gamma$  and  $\sigma$  are functions of  $\lambda_{\text{exc}}$  only. The parameters  $F_i$ 's can be thus calculated by the relations

$$F_A(\lambda_{\text{em}}'') = \frac{\sigma_A(\lambda_x) \sigma_B(\lambda_y) - \sigma_A(\lambda_y) \sigma_B(\lambda_x)}{\sigma_B(\lambda_y) - \sigma_B(\lambda_x)} \quad (16a)$$

$$F_B(\lambda_{\text{em}}'') = \frac{\sigma_A(\lambda_x) \sigma_B(\lambda_y) - \sigma_A(\lambda_y) \sigma_B(\lambda_x)}{\sigma_A(\lambda_x) - \sigma_A(\lambda_y)} \quad (16b)$$

where  $\lambda_x$  and  $\lambda_y$  are any two values of  $\lambda_{\text{exc}}$  but preferably those at which  $\sigma_i(\lambda_{\text{exc}})$  has maximum and minimum values, respectively. Substitution of the  $\bar{F}(\lambda_{\text{em}}'')$  values in eqs 15a and 15b gives the  $f_i(\lambda_{\text{exc}})$  values and the analysis can then proceed as in the case where isoemissive points are present.

An obvious comment on the results obtainable with the KFA method is that the derived quantities for the

distinct rotamers (quantum yields, rate parameters, equilibrium data) are generally subject to a higher uncertainty than the directly measured rotamer lifetimes.

In cases where  $\tau_A \approx \tau_B$  (but  $\phi_A \neq \phi_B$ ), the fluorescence response function can no longer be used to distinguish the species and differential quenching is negligible. Relations 2, 3, 4, 5, and 10 are still valid and they may assist the analysis (for the sake of simplicity, details are not reported). In conclusion, in all cases it appears possible to determine the fluorescence and absorption properties of the two fluorescent species from observations of the solution mixture except when the photophysical properties,  $\tau_i$  and  $\phi_i$ , are practically the same and there is complete overlap of the two absorption spectra.

b. *The Statistical Method.* Principal component analysis (PCA) is a mathematical method based on the statistical treatment of data pertaining to multicomponent systems. The method has recently been applied to deconvolute the fluorescence properties of a two- or three-component mixture of rotational isomers into those of the distinct pure components.<sup>33-39</sup> Once again, the nonequilibration of the excited-state species is implicitly assumed. However, being this method is mainly concerned with the resolution of spectral components, the validity of the NEER hypothesis is not as compulsory as in the case of the KFA method. Sets of fluorescence spectra obtained by varying an external parameter  $R$  ( $\lambda_{exc}$ , temperature or quencher concentration,  $[Q]$ ), are used to build a  $m \times n$  data matrix such that each of the  $m$  row vectors corresponds to an experimental spectrum  $S(R)$  read at  $n$  different  $\lambda_{em}$ 's [ $S = \sum \bar{F}(\lambda_{em})$ ] and  $n$  different column vectors correspond to changes in fluorescence intensity measured by systematically varying the experimental conditions that determine the relative contribution of the pure spectra. On the basis of the number of the significant eigenvectors derived, the matrix experimentally obtained represents a two-component or multicomponent system. In the case of three components, the experimental spectrum can be represented as a linear combination of three eigenvectors  $V$ 's

$$S(R) = \alpha(R)V_\alpha + \beta(R)V_\beta + \gamma(R)V_\gamma \quad (17)$$

where the Greek letters represent the  $R$ th set of combination coefficients. Taking  $\lambda_{exc}$  as the changeable external parameter, the columns of the matrix represent the excitation spectra of the mixture observed at different  $\lambda_{em}$ 's. By the constraint that all experimental fluorescence spectra are normalized to unit area

$$\alpha V_\alpha + \beta V_\beta + \gamma V_\gamma = 1 \quad (18)$$

the three  $V$  values define a normalization plane in the  $\alpha, \beta, \gamma$  space. All the  $\lambda_{exc}$ -dependent sets  $\alpha, \beta, \gamma$  which generate the  $S(\lambda_{exc})$  spectra, must be confined within a triangle in the normalization plane. The A, B, C corners of the triangle correspond to the coefficients of the pure-component spectra while its sides correspond to the combination of coefficients of two-component mixtures. The emission spectra of the three pure components ( $i = A, B, C$ ) will then be given by the expression

$$S_i = \alpha_i V_\alpha + \beta_i V_\beta + \gamma_i V_\gamma \quad (19)$$

For a two-component system, the  $V_\gamma$  eigenvector does not appear in eq 17, and eq 18 defines a normalization

line in the  $\alpha, \beta$  plane on which the  $\alpha(\lambda_{exc}), \beta(\lambda_{exc})$  pairs fit.

The success of the method consists in evaluating the number of the real components (given by the number of the significant eigenvectors) and the coefficients of the pure components. Several procedures are described in the literature to reduce the ambiguity regions in determining the above parameters,<sup>33-39</sup> however their details are not within the scope of the present review article.

The coefficients of the pure components can be estimated by the PCA-SM method,<sup>40</sup> based on the following requirements:

$$(i) \quad S(\lambda_{exc}) = \alpha(\lambda_{exc})V_\alpha + \beta(\lambda_{exc})V_\beta + \gamma(\lambda_{exc})V_\gamma \geq 0 \quad (20)$$

$$(ii) \quad S(\lambda_{exc}) = x_A(\lambda_{exc})S_A + x_B(\lambda_{exc})S_B + x_C(\lambda_{exc})S_C \quad (21)$$

which means that the experimental spectra of the mixture can also be expressed as a linear combination of those of the pure components. Consequently, the  $x_i(\lambda_{exc})$  values, the fractional contributions of the pure spectra to the observed ones, have to be  $\geq 0$  and their sum has to be unity.

(iii) The experimental spectra of the mixture have to be normalized to unity-area.

These requirements of the SM technique provide some uncertainty bands which should contain the pure-component coefficients.

For two-component systems, if at least two  $\lambda_{em}$ 's (or  $\lambda_{em}$  regions) exist where only one component emits (generally at the onset and tail parts of the spectra):

$$(i) \quad F_A(\lambda_{em}) = 0 \quad F_B(\lambda_{em}) > 0 \quad (22a)$$

$$(ii) \quad F_A(\lambda_{em}') > 0 \quad F_B(\lambda_{em}') = 0 \quad (22b)$$

then the pure-component coefficients are generated by the end points of the line in the  $\alpha, \beta$  plane (two components) or by the corners of the triangle obtained by projection of the coefficient triplets in the  $\alpha, \beta$  plane (three components).<sup>35-39</sup> From these coefficients and those generated by the mixture spectra, one can derive the  $x_i(\lambda_{exc})$  values:

$$x_B(\lambda_{exc}) = [\alpha(\lambda_{exc}) - \alpha_A] / [\alpha_B - \alpha_A] \quad (23a)$$

$$x_A(\lambda_{exc}) = [\alpha_B - \alpha(\lambda_{exc})] / [\alpha_B - \alpha_A] \quad (23b)$$

The use of unit-area normalized spectra leads to the derivation of pure-component spectra that are also normalized [ $S_i = 1$ ]. Therefore,

$$N(\lambda_{exc})S(\lambda_{exc}) = x_A(\lambda_{exc})S_A + x_B(\lambda_{exc})S_B = 1 \quad (24)$$

where  $N(\lambda_{exc})$  is the normalization factor. Equation 24 reduces to

$$S(\lambda_{exc}) = \frac{x_A(\lambda_{exc})}{N(\lambda_{exc})} + \frac{x_B(\lambda_{exc})}{N(\lambda_{exc})} \quad (25)$$

where the distribution of the two terms on the right reflects the shape of the absorption spectrum of the corresponding rotamer.

The fluorescence quantum yield of the mixture can be expressed by eq 4, where  $f_i(\lambda_{exc})$  represents the fraction of quanta absorbed by each species. Since  $\bar{\phi}(\lambda_{exc})$  is proportional to the area of the emission



spectrum  $S(\lambda_{\text{exc}})$ , it is possible to relate the contribution of A and B to the emission with the corresponding fractions of excited molecules belonging to each species:

$$\frac{x_i(\lambda_{\text{exc}})/N(\lambda_{\text{exc}})}{S(\lambda_{\text{exc}})} \bar{\phi}(\lambda_{\text{exc}}) = f_i(\lambda_{\text{exc}}) \phi_i \quad (26)$$

Being  $f_A + f_B = 1$ , if it is possible to measure  $\phi_i$  of one species by selective photoexcitation,  $f_i(\lambda_{\text{exc}})$  can be derived by eq 26 and then the relative absorption spectra and the relative abundances of the two emitting species can be obtained, as described for the KFA method.

At the beginning of this section, it was noted that generally the PCA-SM method is not applicable when the emission spectra of the mixture components are completely overlapped. This is only true when one is limited to relying on the criteria expressed in eq 22 for the determination of pure component coefficients.<sup>40</sup> Actually, other chemical relationships can be exploited to obtain, with more delicate procedures, the coefficients even when overlap is complete. Examples are reported in ref 36b for the use of the Stern-Volmer (SV) relationship and in ref 37 for the use of the van't Hoff relationship.

## 6. Differential Quenching

If the fluorescence lifetime of two rotamers differs significantly (for an exception, see below, section III. A.1.b), then the longer lived species, denoted as B, is more strongly quenched (by a factor of about  $\tau_B/\tau_A$ ) than the shorter lived species (A) when a fluorescence quencher is added to the solution. The use of differential quenching, e.g. by high oxygen concentrations, combined with selective excitation, can help to obtain the quasispectrum of the shorter lived component.<sup>20,25</sup> In fact, preferential quenching of the fluorescence, expressed in reversible spectral changes caused by oxygen, provided the first indication that the rotamers may differ not only in their spectra but also in their fluorescence decay rates.

The quenching rate parameters of the two species can be obtained from fluorescence lifetime measurements

$$k_{Qi} = (\tau_i - \tau_{Qi})/\tau_i\tau_{Qi}[Q] \quad (27)$$

or fluorescence quantum yield measurements

$$k_{Qi} = (\phi_i - \phi_{Qi})/\phi_{Qi}\tau_i[Q] \quad (28)$$

where  $i = A, B$ . For strong quenchers, such as  $O_2$ , it is to be expected that  $k_{Qi}$  has the diffusional value for both rotamers. The Stern-Volmer coefficients of fluorescence quenching ( $K_{SV} = k_{Q\tau}$ ) for the distinct species are easily obtainable from eqs 27 and 28. The corresponding coefficient of the mixture is more complicated<sup>25</sup> being given by

$$K_{SV}(\lambda_{\text{exc}}) = [\bar{\phi}(\lambda_{\text{exc}}) - \bar{\phi}_Q(\lambda_{\text{exc}})]/\bar{\phi}_Q(\lambda_{\text{exc}})[Q] = \frac{k_Q[f_A(\lambda_{\text{exc}})\phi_A\tau_A + f_B(\lambda_{\text{exc}})\phi_B\tau_B + k_Q[Q]\bar{\phi}(\lambda_{\text{exc}})\tau_A\tau_B][\bar{\phi}(\lambda_{\text{exc}}) + k_Q[Q][f_A(\lambda_{\text{exc}})\phi_A\tau_B + f_B(\lambda_{\text{exc}})\phi_B\tau_A]]^{-1}}{\quad} \quad (29)$$

where the barred symbol refers to the mixture. The values obtained by direct quenching measurements can

be interestingly compared with those calculated from the experimental  $\bar{\phi}$  values and from the parameters ( $f_i, \phi_i, \tau_i$ ) obtained from the analysis described in the previous chapter (II.A.5) by assuming the same  $k_Q$  value for both rotamers.

Due to differential quenching, the quenched fluorescence spectrum has a different intensity distribution than that without a quencher and the relative contribution of species A is increased since  $F_{QA}/F_{QB}(\lambda_{\text{em}}) > F_A/F_B(\lambda_{\text{em}})$ . With a proper choice of  $\lambda_{\text{exc}}$  and the use of a high concentration of a strong quencher, it is possible in suitable cases to almost completely suppress the emission of the longer-lived species,  $F_{QB}(\lambda_{\text{em}})$ , and thus observe  $F_{QA}(\lambda_{\text{em}})$  which is proportional to  $F_A(\lambda_{\text{em}})$ .

## 7. Emission from "Dilute Cold Gases"

The use of spectroscopic techniques, in which the samples consist of essentially isolated molecules at very low temperature, may contribute greatly to our knowledge of individual properties of DAE rotamers. In fact, in principle, with the high resolutions achievable under such conditions, the pure fluorescence and absorption spectra of the distinct rotamers can be detected and the structure assigned for each observed species.

The electronic spectra of various compounds dissolved in appropriate *n*-alkane frozen matrices (Shpolskii matrices) exhibit quasi line band systems which reflect approximate dilute-cold-gas conditions of the solute molecules.<sup>41</sup> Most of the available high-resolution data on large molecules, e.g. linear polyenes,<sup>42</sup> come from Shpolskii-type spectra at the liquid helium temperature.

In 1981, Muszkat and Wismontski-Knittel<sup>43,44</sup> observed quasi line fluorescence and fluorescence-excitation spectra of 2-StN, 2,2'-DNE, and their aza analogues in *n*-hexane matrices at 5 K. Evidence was obtained for the presence of at least two modifications of the guest molecules in the frozen host matrices, but quasi line spectra were obtained only for one modification, assigned as the most extended (t for 2-StN and tt for 2,2'-DNE) planar configuration. Very recently, Lamotte et al.,<sup>45</sup> using an improved high-resolution apparatus, observed new quasi line systems in the Shpolskii absorption spectrum of 2-StN (and its aza analogues) and, by selective narrow-band fluorescence excitation (fluorescence monitoring) at the respective vibronic lines, were able to resolve the fluorescence (fluorescence excitation) spectra of both t (B) and c (A) rotamers.

These findings and the relevant structural assignments given in ref 45 will be discussed later (see section III.A.1). Here, we deem it useful to address a problem which is crucial in any measurement aiming at the observation of distinct rotamers at low temperature. Briefly, at 5 K a thermally equilibrated mixture of two unstrained quasicoplanar rotamers ( $\Delta H \approx 0.5$  kcal mol<sup>-1</sup>) (see later) contains an absolutely negligible quantity of the less stable species. When the Shpolskii-matrix technique is used, this difficulty might be overcome by cooling the *n*-alkane solutions rapidly so as to freeze-in the room temperature composition or the composition at some intermediate temperature. However, Lamotte et al.<sup>45</sup> have shown that the mixture composition in Shpolskii matrices is not dependent on the rate of the cooling process, but is determined by the

*n*-alkane chain length. In particular, for 2-StN in *n*-hexane at 5 K, the composition is much richer in the less stable conformer ( $[A]/[B] \approx 1$ ) than is the room temperature equilibrium composition ( $[A]/[B] \approx 0.3$ ).<sup>31</sup> On the contrary, no evidence was found for the presence of the A species in frozen *n*-decane matrices.<sup>45</sup> Thus, the possibility of observing distinct rotamers of a DAE molecule in Shpolskii spectra is limited by the need of finding a Shpolskii solvent which gives an appropriate nonequilibrium mixture in the frozen matrix.

The electronic spectroscopy of jet-cooled samples is an even more suitable technique to probe the structure of large molecules under isolated-molecule conditions. A relevant example is provided by recent studies of the electronic spectrum of jet-cooled *trans*-stilbene,<sup>46,47</sup> where the analysis of the dispersed fluorescence and fluorescence-excitation spectra in the low-frequency region led the authors to conclude that isolated *trans*-stilbene has a planar, although very flexible, geometry ( $C_{2h}$ ) which is at variance with the nonplanar propeller-like geometry ( $C_2$ ) suggested by a previous gas-phase electron diffraction study.<sup>48</sup> However, in spite of its great potential usefulness, the applicability of this technique to probe the structure of different rotamers in DAEs is not straightforward in view of the basic problem concerning the concentration ratios of rotamers in jet-cooled samples. In fact, as far as we know, no jet-cooled spectroscopic studies of rotamerism in either DAEs or analogous systems have been reported to date.

## B. Other Experimental Techniques

### 1. Direct Detection Techniques

The detection of ground-state rotamers by emission spectroscopic techniques has an indirect character and can provide quantitative results on the condition that excited-state rotamers do not appreciably interconvert during their lifetime (NEER assumption). Thus, techniques devised for directly detecting rotameric equilibria in the ground state can be very useful either to confirm the results from emission spectroscopy or as alternative investigation tools in cases where the fluorescence quantum yield of one or more of the existing rotamers is exceedingly low. A considerable variety of physical methods is now available for studying rotational isomerism in molecules. We will only describe the two most relevant spectroscopic techniques, although valuable information might also be obtained by applying other spectroscopic (e.g., absorption spectroscopy at variable temperatures) and relaxation (dielectric, acoustic) methods.

a. *Magnetic Resonance Spectroscopy.* Since the various nuclei of distinct rotamers are in slightly different magnetic environments, application of NMR spectroscopy may provide valuable information on the properties of each single species.<sup>49</sup> On the other hand, detecting separate NMR spectra of the distinct rotamers requires that their lifetimes be long compared to the inherent time scale of the nuclear transition. This condition is hardly realizable when dealing with rotamers of DAEs because, due to the moderate rotational barriers (about 5 kcal mol<sup>-1</sup>, see section II.C), they interconvert at a frequency on the order of 10<sup>9</sup> s<sup>-1</sup> at room temperature. Thus, low-temperature measurements should be made. <sup>1</sup>H NMR spectra of 3,3'-dimethyl-

stilbene (where three quasi-isoenergetic rotamers can be envisaged) were measured by Fischer<sup>27</sup> down to 193 K. No indication of peak splitting was found: this suggests that the interconversion frequency is probably still too high at 193 K (neglecting viscosity effects, such frequency is  $\sim 10^7$  s<sup>-1</sup>). Of course, one could go down to  $\leq 100$  K by taking care of avoiding thermal equilibration, e.g. by fast sample cooling, in order that detectable quantities of the less stable species would still be present under those conditions. However, some valuable information can, in principle, be obtained from the statistically averaged values of the nuclear spin-spin coupling constants ( $J$ ) (or the chemical shifts ( $\delta$ )) observed at higher temperatures. In fact, the ( $J$ ) ( $\delta$ ) values are expected to vary with temperature changes as a consequence of a variation in the rotamer populations. Therefore, studies on temperature dependence of ( $J$ ) ( $\delta$ ) can lead to the evaluation of the free-energy differences ( $\Delta G$ ), as well as of the rotamers' individual  $J(\delta)$  values. Finally, an analysis of the change in line shape over the temperature interval where the transition from a single averaged spectrum to the separate spectra occurs, may allow the evaluation of the free energy of activation ( $\Delta G^\ddagger$ ) for the rotamer interconversion, although some difficulties may arise due to the nondegeneracy of the interconverting species. However, no application of these classic NMR techniques to DAEs capable of rotamerism has been reported in the literature, except for the above cited preliminary investigation on 3,3'-dimethylstilbene.<sup>27</sup>

The inherent time scale of electron-nuclear double resonance (ENDOR) spectroscopy, where the nuclear resonances are indirectly detected via their influence on the EPR lines,<sup>50</sup> is several orders of magnitude shorter than that of NMR spectroscopy. Hence, ENDOR measurements offer the possibility of studying rotamerism in the presence of rotational barriers as low as those of DAEs. Of course, this technique is applicable only to radical ions of DAEs and, therefore, the results will be qualitatively transferable to neutral DAEs so long as thermodynamic and kinetic parameters do not substantially change on switching from neutral to radical ionic forms. As an example, the ENDOR spectrum of 3,3'-dimethylstilbene anion radical at 183 K was interpreted by Higuchi et al.<sup>51</sup> as showing that the molecule exists as a mixture of rotamers whose sequence of stability is probably  $cc > ct > tt$  (for notation see Figure 2). Proper quantum mechanical calculations might be carried out in an attempt to determine if this conclusion is valid for the neutral compound as well.

b. *Vibrational Spectroscopy.* Another classic technique for studying rotamerism of molecules is vibrational (infrared and Raman) spectroscopy which, unlike NMR spectroscopy, is free from time-scale-related limitations (infrared transitions requiring times of about 10<sup>-13</sup> s). There are two main applications of vibrational spectroscopy to the problem of rotational isomerism concerning: (i) the determination of the enthalpy differences ( $\Delta H$ ) between rotamers<sup>52a</sup> and (ii) the measurement of the energy barriers hindering rotamer interconversion.<sup>52b</sup> The second application, which is based on the study of the torsional frequencies in the far infrared gas-phase spectrum, is impracticable for molecules as large as DAEs mainly because of their very

low vapor pressures at ordinary temperatures. Since the first application is also feasible for compounds in the pure liquid or liquid solution states, it can be considered for detecting rotameric equilibria in DAEs.

Assuming that a DAE exists as a mixture of two rotamers, A and B, one expects its vibrational spectrum to be a superposition of the two individual spectra whose relative intensities change as temperature is varied as a consequence of the change in composition of the equilibrium mixture. Thus, the first step of the whole procedure will be to find a region in the spectrum that exhibits a clear temperature dependence. The vibrational bands in this region must then be assigned by using one of the several methods available to unambiguously identify the bands of the same vibrational mode belonging to the distinct A and B species. Finally, the integrated intensities of the single bands ( $I_A$ ,  $I_B$ ) must be determined at different temperatures so as to derive  $\Delta H$  from the slope of a plot of  $\ln(I_A/I_B)$  vs  $1/T$ , according to the equation:

$$\ln(I_A/I_B) = \ln K_{eq} + \ln(\alpha_A/\alpha_B) = -\Delta H/RT + \Delta S/R + \ln(\alpha_A/\alpha_B) \quad (30)$$

where  $\alpha_A$  and  $\alpha_B$  are the integrated absorption or scattering coefficients depending upon the technique (infrared or Raman) used.

Scoptoni et al.<sup>53</sup> recently applied this procedure to the prototypical case of 2-StN in various solvents. The results of this study, which fully confirmed evidence derived from fluorescence analysis, will be described later (section III.A.1.a). Now, we simply want to point out a methodological aspect which is particular to these systems. Briefly, the vibrational spectrum in the low frequency region ( $\leq 400 \text{ cm}^{-1}$ ), where bands originating from modes of the whole molecule are expected to appear, is generally considered to be the most suitable for detecting rotameric equilibria. Actually, the low frequency solution spectrum of 2-StN showed only weak, broad bands which were unusable for reliable measurements. After extensive investigation, the dependence of the relative intensities on temperature was clearly observed in a pair of close Raman bands at 1630 and 1625  $\text{cm}^{-1}$ , which, when compared with Raman spectra of selected compounds, were attributed to the ethylene C=C stretching mode of the two rotamers (t and c forms of Figure 2b). The entire procedure for the analysis of the conformational equilibrium in 2-StN was performed by detailed measurements on this band pair in *n*-hexane solution. This can be taken as useful indication for applying the Raman technique to the study of rotameric equilibria in other DAEs. The success of this application will depend on some limiting factors related to the large molecular dimensions of DAEs: poor solubility, a limited temperature range over which solutions exist, and the degree to which the band pairs of interest overlap and merge with other strong bands.

## 2. Conventional and Laser Flash Photolysis

Both laser (nanosecond)<sup>54-56</sup> and conventional (microsecond)<sup>57,58</sup> flash photolysis techniques can be useful in the study of conformational equilibria. Since rotamers often display slightly different singlet-state absorption and emission properties, they may also have different triplet-state behavior. Their  $T_1 \rightarrow T_n$  absorption can be monitored after flash or pulsed-laser

excitation of the molecule followed by fast ISC. The properties of the lowest triplet state (spectrum, quantum yield, lifetime) can thus be obtained for the different rotamers by the usual methods. As will be shown in section III, the triplet-triplet absorption has been used in several cases,<sup>57</sup> combined with the freeze-unfreeze technique, to get information on these properties.

Selective quenching of the transients assigned to different rotamers with different triplet lifetimes, where observed, can also be investigated by this technique. A particularly interesting use of flash photolysis is the study of rotamer interconversion in specific cases where a particularly long triplet lifetime allows equilibration between the different species, against the NEER principle (see section III.A.4).

An obvious extension of the use of flash photolysis is to study the transient absorption of the radical ions of the rotamers produced by photoinduced interaction with electron donors or acceptors.

When the transient lifetime is in the micro- or millisecond range, conventional flash photolysis and cells with longer light paths can be applied. It has been noted<sup>58</sup> that this technique may have some advantages over laser flash photolysis. At times, better spectra are obtained because it may avoid complications due to singlet transitions (both  $S_1 \rightarrow S_n$  absorption and  $S_1 \rightarrow S_0$  emission) and/or to high transient concentrations. On the other hand, experiments on the picosecond time scale, using mode-locked lasers as exciting flashes, have been sometimes carried out on DAE rotamers to gather information on fast processes involving particularly short-lived excited states.

## C. Quantum Mechanical Calculation Techniques

Two types of questions, to which quantum mechanical calculations should give answers, arise from an analysis of the large body of experimental evidence for the existence of conformeric equilibria in solutions of DAEs.

The questions of the first type concern rotamers in the ground state and can be expressed as follows:

(1) What are the expected energy differences ( $\Delta E_0$  in Figure 3) between rotameric species?

(2) How high are the intramolecular energy barriers ( $E_0^{\ddagger}$  in Figure 3) which impede interconversion between different rotamers?

Of course, reliable answers to these questions would enable one to predict both the composition of the equilibrium mixtures and the rates at which the ground-state rotamers may interconvert in fluid media. This type of information, in turn, indicates the characteristics which an experimental technique must have in order to be used for the direct measurement of rotameric equilibria in DAEs (see discussion in section II.B.1).

The questions of the second type, arising in the context of investigation techniques involving electronic excitation (e.g. emission spectroscopy), can be formulated as follows:

(1) What are the expected differences between the  $S_0-S_1$  energy separations of the postulated rotamers?

(2) Should one expect significantly different emission lifetimes and quantum yields for distinct rotamers?

(3) What are the estimated energy barriers between electronically excited rotamers?

As is evident, the answers to these questions would provide the necessary theoretical support to the reported emission spectroscopy evidence for the occurrence of rotameric equilibria in DAEs and help to establish the conditions when the basic NEER assumption may break down.

The search for a calculation method capable of correctly handling the above stated questions is not trivial. The large dimensions of the molecules under consideration do not lend themselves to the use of ab initio techniques. In fact, all of the reported theoretical studies on rotamerism in DAEs were based on semiempirical MO methods. However, the current semiempirical techniques, either formally limited to  $\pi$  electrons (PPP-type) or extended to all valence electrons (CNDO, INDO, MINDO, MNDO, etc.),<sup>59</sup> are more or less incapable of giving correct answers to the above mentioned questions taken together. For instance, PPP-type procedures simulating  $\sigma$  electrons via empirical potentials,<sup>60,61</sup> can correctly locate the rotamers as well as reliably predict their ( $\pi \rightarrow \pi^*$ ) transition properties, but they decidedly overestimate barriers to rotamer interconversion because they neglect  $\sigma$ - $\pi$  mixing which occurs in nonplanar geometries. In contrast, all-valence-electron techniques overestimate  $\sigma$ - $\pi$  (hyperconjugative) interactions, the defect size being related to the neglected portion of differential overlap. As a consequence, they unreasonably favor highly twisted structures. Thus, strictly speaking, the current all-valence-electron techniques may give reliable relative energies and geometries of the envisaged "planar" rotamers in the ground state, but they cannot provide any correct information on the activation energies of the rotamer interconversion processes in either the ground or excited states. On the other hand, the well-known CNDO/S<sup>62</sup> and INDO/S<sup>63</sup> schemes, although appropriate for predicting the ( $\pi \rightarrow \pi^*$  and  $n \rightarrow \pi^*$ ) transition properties, give results which are worse than those of the original CNDO-INDO schemes as far as the relative energies of the distinct rotamers and the internal rotation potentials are concerned. As previously pointed out,<sup>64</sup> these failures of CNDO-INDO/S methods are related to overall imbalances between attractive and repulsive interactions caused by one-sided reparametrization of two-electron ( $\gamma_{AB}$ ) and resonance ( $\beta_{\mu\nu}$ ) integrals. In conclusion, the current semiempirical MO methods can give rather limited answers to the questions which arise when studying the rotamerism of DAEs. In fact, very few theoretical papers devoted to this specific subject have used these methods. We can cite four representative articles by Marconi, Orlandi, et al.<sup>31,65-67</sup> dealing with styrylpyridines (StPs), dipyrindylethylenes (DPEs),<sup>65,66</sup> styrylnaphthalenes (StNs)<sup>31</sup> and styrylanthracenes (StAs),<sup>67</sup> where the MNDO or the Warshel's QCFF/PI<sup>60</sup> methods were adopted to evaluate relative stabilities and dipole moments of the planar rotameric forms in the ground state,<sup>66,67</sup> while INDO/S,<sup>65,66</sup> CNDO/S<sup>31,67</sup> or QCFF/PI<sup>67</sup> methods were used to calculate the transition properties of the different rotamers.

In 1982 Momicchioli et al.<sup>68</sup> proposed a new INDO-type procedure characterized by the use of a basis of hybridized  $\sigma$  and  $\pi$  atomic orbitals which allows  $\sigma$ - $\sigma$ ,  $\pi$ - $\pi$ , and  $\sigma$ - $\pi$  core interactions to be correctly balanced by introducing three specific screening constants ( $k_{\sigma\sigma}$ ,

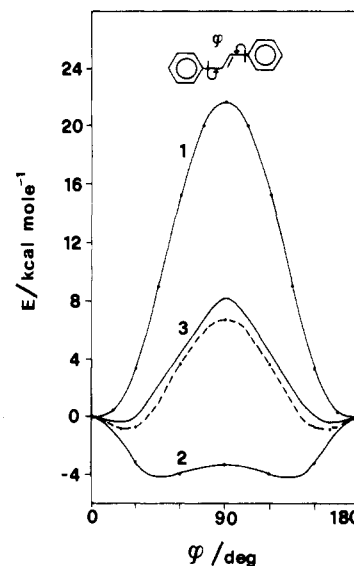


**Figure 7.** Ground-state potential energy curves for the symmetrical rotation of *trans*-stilbene around the exocyclic C-C "single" bonds: (1) PPP (from ref 61); (2) standard INDO; (3) ab initio (from ref 69); (---) C-INDO (from ref 68). A rigid rotor model was adopted in all cases. Idealized geometries were also used, with the only exception of calculation 3 where the C—C=C bond angle was given a value (127°) optimized for the planar conformation (reprinted from ref 64; copyright 1983 Elsevier (Amsterdam)).

$k_{\pi\pi}$ , and  $k_{\sigma\pi}$ ). As a result of these changes, the new INDO-based procedure (later named C-INDO) can reproduce fairly well the results of ab initio SCF calculations as far as the ground-state internal rotation potentials of conjugated molecules are concerned, thus representing a real improvement with respect to previous semiempirical methods. This is clearly shown in Figure 7, where the symmetrical twisting of the two exocyclic C-C "single" bonds of *trans*-stilbene is taken as a fitting example in connection with the phenomenon of rotamerism in DAEs.

In 1983, further modifications (i.e. a "spectroscopic" parametrization of electron repulsion integrals combined with a new core-core repulsion formula) were introduced into the C-INDO scheme. A new method was obtained (CS-INDO)<sup>64</sup> which is capable of preserving the quality of the C-INDO predictions as far as the ground-state properties are concerned, and of handling the properties of the lowest excited states of conjugated molecules at an equally satisfactory level of accuracy. Thus, in principle, the CS-INDO method appears to be a suitable theoretical device for testing the assumptions in current interpretations of experimental data on rotamerism of DAEs. As an example, the applicability of the NEER hypothesis to the rotamers of DAEs can be soundly appraised with the aid of Figure 8, where the (CS-INDO SCI) excited-state potential energy curves for the twisting of a phenyl ring in *trans*-stilbene are reported together with that of the ground state. Figure 8 shows that in the state  $S_1$ , giving rise to the intense  ${}^1A$ - ${}^1B$  "conjugation" band, the energy barrier hindering internal rotation is much higher than that of the ground state, this being due to significant bond order enhancement of the C-C "single" bonds upon  ${}^1A$ - ${}^1B$  (essentially HOMO-LUMO) excitation.

On the other hand, the  $S_2$  and  $S_3$  excited states, having essentially benzenic character, may have rotational barriers as low as that of the ground state (e.g.,

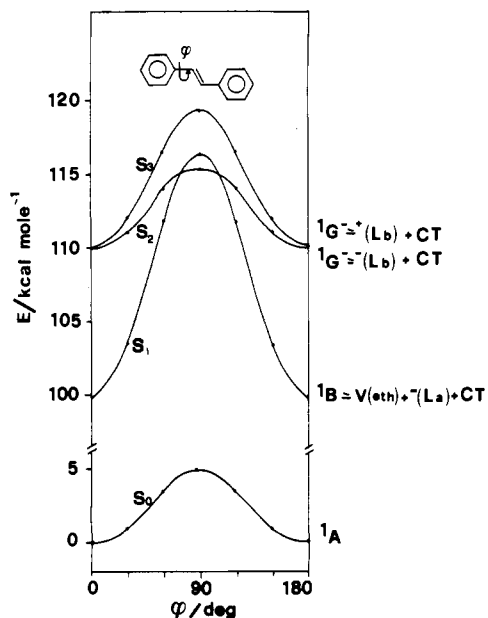


**Figure 8.** CS-INDO SCI potential energy curves describing the internal rotation of one phenyl group of *trans*-stilbene in the ground and three lowest excited singlet states. The C—C=C bond angle was taken equal to 128°, the other structural parameters being given standard values. The Platt's notation of the states and their interpretation in terms of "local" and charge transfer excitations are given on the right (unpublished results related to ref 70).

$S_2$ ). Thus, the results of Figure 8 point out that the NEER assumption will be valid whenever the excited state involved has a markedly delocalized character. If the excitation is essentially localized on an aryl group, as may happen for  $S_1$  and  $T_1$  states of DAEs containing polycyclic aromatic groups,<sup>24</sup> the NEER hypothesis may be maintained only if the excited-state lifetime is short enough to prevent any rotamer interconversion (see section III.A.4).

C-INDO and CS-INDO have been applied to the study of the thermodynamic and kinetic aspects of rotamerism in the ground and lowest ( $S_1$ ,  $T_1$ ) excited states in a variety of DAEs: StN, DNEs,<sup>71</sup> StPhs,<sup>72</sup> StAs.<sup>70,73</sup> The C-INDO and CS-INDO techniques have also been used to study rotamerism in *m*- and *p*-terphenyl<sup>74</sup> and 2,2'-binaphthyl,<sup>8</sup> as well as to investigate conformational and internal rotation properties in the ground and lowest excited states of various conjugated systems.<sup>75,76</sup>

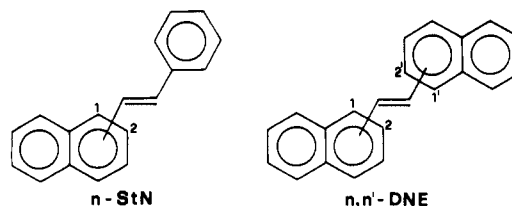
### III. Survey of Studies on Rotamerism of Various DAE Compounds

#### A. Hydrocarbon Compounds

##### 1. Naphthyl Derivatives

As stated above, rotamerism of the naphthyl analogues of *trans*-stilbene, *n*-styrylnaphthalenes (*n*-StNs), and 1,2-di(*n,n'*-naphthyl)ethylenes (*n,n'*-DNEs), has been the most widely investigated in numerous laboratories to obtain the properties of the individual components of the rotamer mixture.<sup>20-22,24a,25,28,30,31,34-36</sup>

In contrast with the first detailed report of Sheck, Alfimov, et al.,<sup>21</sup> the more quantitative study by Haas and the Fischers<sup>20</sup> stressed the primary role of the steric interactions, showing that in certain DAEs the fluorescence behavior can be explained by the confor-



meric equilibrium being shifted toward the rotamer(s) with relatively unstrained coplanar form(s) (e.g., species *tt* and *tc* in 1,2'-DNE, see Figure 2c). For this reason, subsequently confirmed by theory, conformeric equilibria were observed in 2-StN and 2,2'-DNE, while only one species was evident in solutions of 1-StN and 1,1'-DNE.<sup>20</sup> For 1,2'-DNE, two species were indicated by the  $\lambda_{exc}$  effect even though a monoexponential decay was observed.<sup>20</sup> As to the conformers of the 2-naphthyl derivatives, all authors agree that at least two fluorescent species are present in solution, one A, the short-lived component, characterized by an emission spectrum shifted to the red (L, long wavelength absorbing species, in Fischer's notation<sup>20</sup>), and B, the longer lived and short-wavelength absorbing species (S in Fischer's notation). The main evidence that the two conformers are short- (A) and long-lived (B), respectively, comes from the fact that, under appropriately chosen experimental conditions, the fluorescence spectrum of the mixture can be moved toward the spectrum of either A or B, and the decay curve shows a prevalence of the fast or slow decay component, respectively.

Next, we shall focus our attention on the most extensively investigated 2-naphthyl derivatives, although reference to properties of 1-naphthyl derivatives will be made for purposes of comparison.

a. *2-Styrylnaphthalene*. *trans*-2-StN is certainly the DAE for which the most abundant documentation exists in the literature. It has generally been considered to be a suitable prototype system for analyzing the rotamer phenomenon in DAEs. Also, some controversy on the interpretation of its fluorimetric behavior motivated deeper investigations (see later).

The first studies on this compound, concerning the effects of  $\lambda_{exc}$  and temperature on the emission spectra<sup>20,21,28</sup> emphasized the presence of two species in solution (Figure 2b) and led to an approximate description of their equilibrium and individual spectral properties. Further experimental and theoretical studies provided quantitative evaluation of the spectroscopic and photophysical properties of the two components, the composition of the mixture and the structural assignment. Figures 4 and 5 show, as an example, the  $\lambda_{exc}$  effect on the spectra and the nonexponentiality of the decay. Figure 9 shows the temperature effect on the spectra.

A relevant observation, repeated in different solvents and confirmed by different laboratories, concerns the markedly different  $S_1$  lifetime of the two rotamers (Table I). The difference in fluorescence lifetimes of the A and B rotamers ( $\tau_B/\tau_A \approx 6$ ) was first explained by a difference in the photoisomerization rate<sup>20,28</sup> rather than by difference in the natural emission lifetimes which was proven in later investigations.<sup>31,77</sup>

The oxygen effect on 2-StN, which selectively quenches the longer-lived rotamer, was explored by Fischer.<sup>20,78</sup> He found that the oxygen effect was much less than had been expected on the basis of the dif-

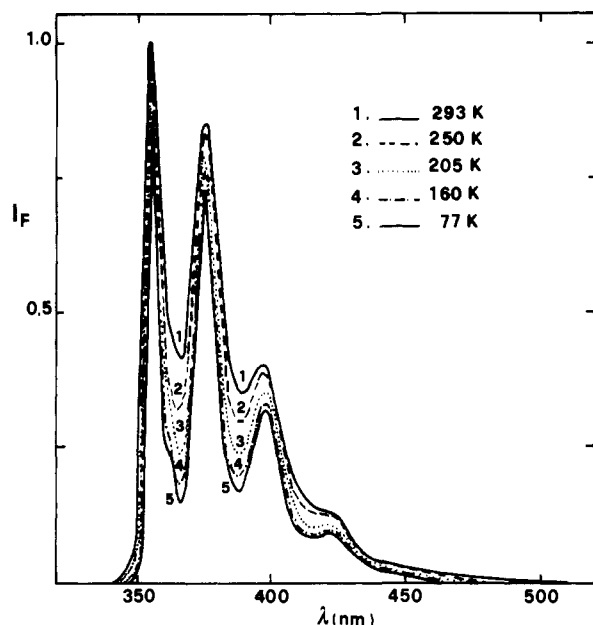


**Figure 9.** Corrected fluorescence emission spectra of *trans*-2-StN in 3-MP as a function of temperature at  $\lambda_{\text{exc}} = 315$  nm (curve 5 refers to the almost pure B spectrum) (reprinted from ref 77; copyright 1986 Elsevier (Amsterdam)).

**TABLE I.** Fluorescence Lifetimes (ns) of the Rotamers of *trans*-2-StN in Various Solvents at Room Temperature

solvent	$\tau_A$	$\tau_B$	ref
MCH	3.7	22	20
CH	3.1	23	28
<i>n</i> -hexane	5.2	27.6	31
3-MP	5	26.2	77
ethanol	3.5	19.9	31

**TABLE II.** Temperature Effect on the Fluorescence Decay Parameters for *trans*-2-StN in MCH ( $\lambda_{\text{exc}} = 355$  nm, isoemissive  $\lambda_{\text{em}} = 395$  nm) as Derived by the KFA Method (from ref 77)

$T$ , K	$\tau_A$ , ns	$\tau_B$ , ns	$\alpha(\lambda_{\text{exc}})$	$\beta(\lambda_{\text{exc}})$	$f_A(\lambda_{\text{exc}})$	$f_B(\lambda_{\text{exc}})$
293	3.73	22.7	8.18	1.34	0.57	0.43
190	2.85	21.0	5.63	0.76	0.43	0.57
150	2.62	19.8	3.57	0.47	0.32	0.68
127	2.72	18.5	2.53	0.37	0.27	0.73
77	2.33	17.7	0.86	0.11	0.10	0.90

ference in emission spectra and lifetimes of the two rotamers. However, a more quantitative analysis,<sup>31,77</sup> showed the spectral difference to be rather smaller than that reported in refs 20 and 78. The modest oxygen effect was treated by Saltiel and Eaker<sup>34</sup> with the statistical PCA method (see section II.A.5.b). A strange interpretation was given based on the existence of four fluorescence lifetimes (two for each rotamer, involving two nearby located singlet excited states). Later,<sup>77,79</sup> it was recognized that this result was incorrect and was caused by the use of excitation-emission input matrices of too small dimensions.

The behavior of 2-StN was more fully explained using the KFA method (see section II.A.5.a).<sup>25,31,77</sup> Table II shows the fluorescence decay parameters for the two rotamers of 2-StN in methylcyclohexane (MCH) at different temperatures and the  $\lambda_{\text{exc}}$ -dependent  $\alpha$ ,  $\beta$  and  $f_i$  parameters as derived from eqs 7-9. A decrease in temperature caused a decrease in the fraction of excited A molecules (which is proportional to the A concentration, see eq 3) and a corresponding increase in the concentration of B which thus appears to be the more

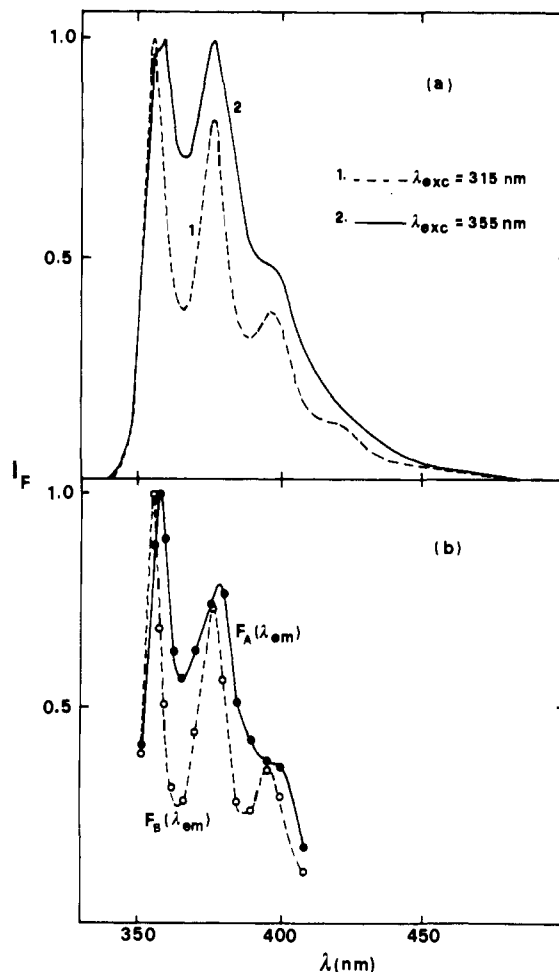


**Figure 10.** (a) Corrected fluorescence emission spectra of *trans*-2-StN in 3-MP at 293 K; curve 1 in absence of oxygen and curve 2 with 1 atm oxygen. (b) Limiting spectra of conformers A and B as obtained by the decay analysis at  $\lambda_{\text{exc}} = 335$  nm (reprinted from ref 77; copyright 1986 Elsevier (Amsterdam)).

stable species. The quasipure emission spectrum of B (Figure 9, curve 5) was then obtained by lowering the temperature until the equilibrium is shifted toward the more stable B species and using a  $\lambda_{\text{exc}}$ , 315 nm for example, where the fraction of excited molecules belonging to B is favorable.<sup>77</sup> At these low temperatures, the excitation spectrum no longer depends on  $\lambda_{\text{em}}$ , thus showing that the absorption spectrum is essentially due to a single species and the corresponding emission decay is practically monoexponential (e.g., in 3-methylpentane (3-MP) at 77 K,  $\tau \approx \tau_B = 20.5$  ns). On the other hand, exciting with 355-nm light at room temperature, where the fraction of excited A molecules, absorbing at longer wavelengths, becomes substantial (Table II), the spectrum starts to show the features of the A modification. This is much more true if one operates in the presence of 1 atm of oxygen since the preferential quenching of B shifts the composition of the mixture of excited molecules even more toward A (see Figure 10a). The spectrum of A alone could not be obtained by direct measurements. In fact, 2-StN is one of the few compounds for which no almost-pure emission spectrum of the bathochromic rotamer could be directly obtained by long  $\lambda_{\text{exc}}$  at either room or low temperatures<sup>78</sup> due to the small shift between the rotamer spectra.<sup>77</sup>

The peculiar fact that the large difference in the rotamer lifetimes is accompanied by a small difference

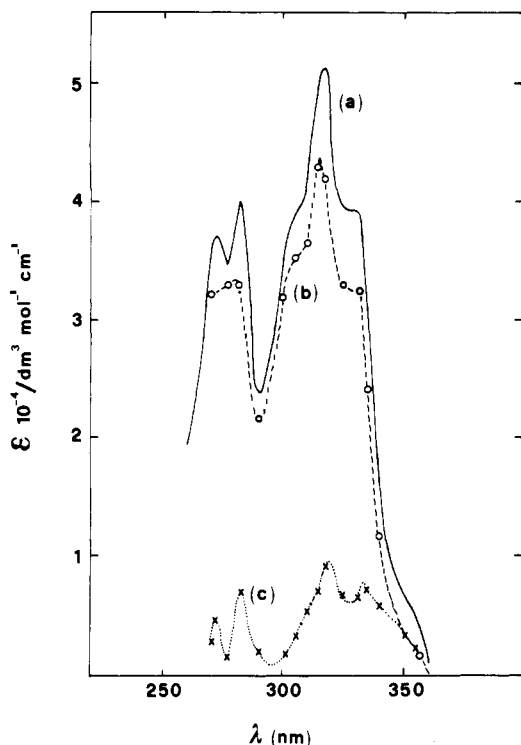


**Figure 11.** Spectra of 2-StN in ethanol: (a) absorption spectrum  $\epsilon$  ( $\lambda_{exc}$ ), (b) relative absorption spectrum of conformer B, and (c) relative absorption spectrum of conformer A. Spectra b and c are derived from the KFA analysis (adapted from ref 31).

in their emission spectrum was interestingly confirmed by the changes in the ratio of the preexponential factors with  $\lambda_{em}$ . The distinct  $F_i(\lambda_{em})$  values were calculated by eq 5 with use of the  $f_i(\lambda_{exc})$  values at 335 nm and the experimental emission spectrum of the mixture,  $\sum F_i(\lambda_{em})$ , at the same  $\lambda_{exc}$ . Figure 10b shows the normalized emission spectra of the two rotamers thus obtained, in reasonable agreement with those recently reported by Saliel and Sun.<sup>79</sup> They indicate a very small shift of  $\sim 3$  nm between the maxima (instead of  $\sim 8$  nm as reported in refs 20, 34, and 78) and less spectral resolution for rotamer A. The slight change (decrease) in lifetime observed at rather low temperatures ( $<150$  K), shown in Table II, is not peculiar to 2-StN; it is reported for several other stilbene-like compounds and their aza analogues in MCH and 3-MP, particularly when  $\tau$  was measured in a rigid matrix. The reason for this behavior is probably due to a solvent-induced (dispersive forces<sup>80</sup> and/or viscosity<sup>72</sup>) reduction of the  $S_1$ -( $^1L_b$ )- $S_2$ ( $^1L_a$ ) energy gap with decreasing temperature. This, in turn, involves a gain of  $^1L_a$  character by the almost forbidden  $^1L_b$  state and then an increase in the probability of the radiative transition.

An example of the relative absorption spectra of 2-StN(A) and 2-StN(B) as derived from the KFA method is shown in Figure 11. The relative concentrations of the rotamers were derived by using eqs 11 and 12. The  $\Delta H$  between the two species was then evaluated as described in section II.A.5.a. Practically the same  $\Delta H$  value and derived relative abundances were obtained by plots of the parameter  $\beta = A_A\tau_A/A_B\tau_B = f_A/f_B$  against  $1/T$  (Figure 12). The necessary  $\beta$  values were obtained from fluorescence decay measurements in a temperature region where  $\phi$  and  $\tau$  remain constant (meaning that photoisomerization no longer occurs by the singlet mechanism, firstly proposed by Saliel for

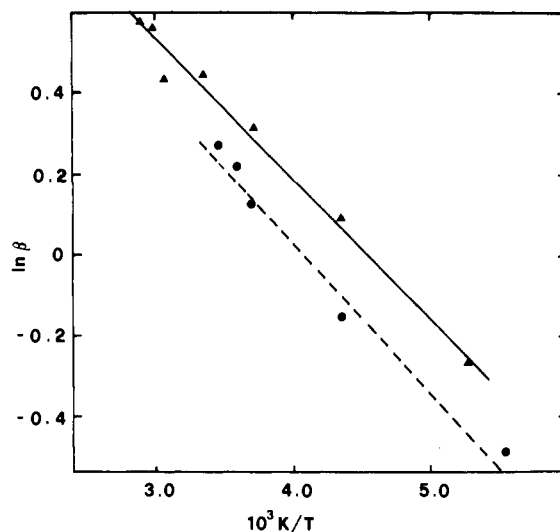


**Figure 12.** Plot of  $\ln \beta$  ( $\lambda_{exc}$ ) against  $1/T$  for 2-StN in (---) ethanol and (—) MCH ( $\lambda_{exc} = 355$  nm) (reprinted from ref 31; copyright 1984 Royal Society of Chemistry).

**TABLE III. Photophysical Parameters and Relative Abundances of the Two Rotamers of *trans*-2-StN at 293 K and Their Enthalpy Difference in Two Solvents (from ref 31)**

solvent parameters	n-hexane		ethanol	
	A	B	A	B
$\phi$	0.83	0.50	0.37	0.60
$\tau$ , ns	5.2	27.6	3.5	19.9
$k_F$ , $10^7$ s <sup>-1</sup>	16.0	1.8	11.0	3.0
relative abundance, %	24	76	20	80
$\Delta H$ , cal mol <sup>-1</sup>	680		720	

the room temperature process<sup>23b,c</sup>). The main results obtained by kinetic analysis of 2-StN are summarized in Table III. The two different lifetimes do not reflect different emission quantum yields but do show rate constants for radiative decay differing by about 1 order of magnitude. This behavior then should be related to an intrinsically different nature of the first excited singlet state of the two rotamers as will be discussed below.

The effect of temperature on  $\tau$  and  $\phi$  in the upper  $T$  region allowed the activation energy for the *trans*  $\rightarrow$  *perp* internal rotation in the singlet manifold (leading to *trans*  $\rightarrow$  *cis* isomerization) to be evaluated. Figure 13 shows a nice example of such an effect in two solvents.

In principle, the two rotamers may also display a different photoreactivity. The mechanism for *trans*  $\rightarrow$  *cis* photoisomerization of StNs proved to be predominantly an activated singlet pathway above room temperature where both  $\phi$  and  $\tau$  decrease and  $\phi_{t \rightarrow c}$  increases with an increase in temperature. The high frequency factors ( $\geq 10^{13}$  s<sup>-1</sup>) found in the study of the temperature effect on  $\phi$  and  $\tau$  above room temperature, led to the exclusion of a spin-forbidden process as the rate-determining step. Only below room temperature, when  $\phi$  and  $\tau$  remain practically constant, could a triplet mechanism become operative.<sup>31,81</sup> A similar activation energy for the *trans*  $\rightarrow$  *perp* rotation of the two rotamers in the singlet manifold was reported from the Arrhenius plots of Figure 13 both in MCH (10.5 and 10.3 kcal mol<sup>-1</sup> for A and B, respectively) and in ethanol (8.1 and 8.2 kcal mol<sup>-1</sup> for A and B, respectively).<sup>31</sup> These barriers, however, are probably overestimated on the

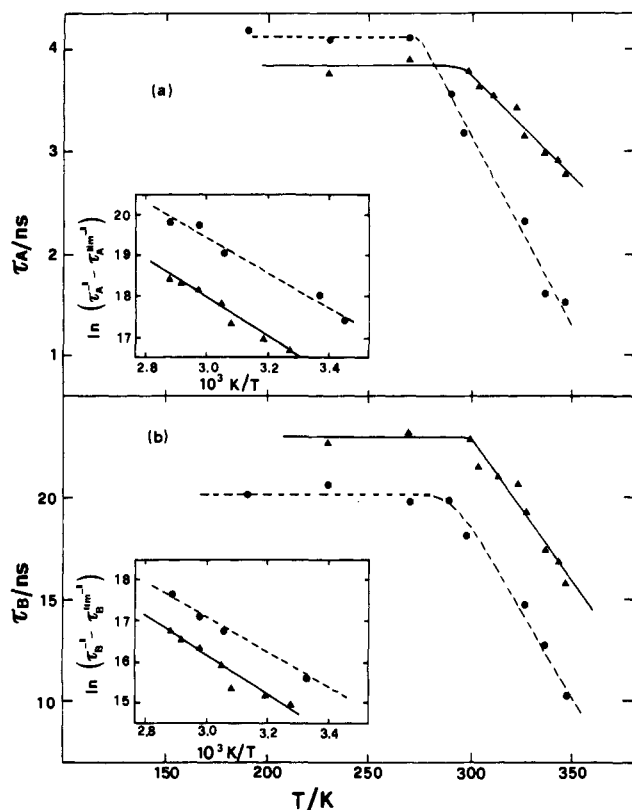
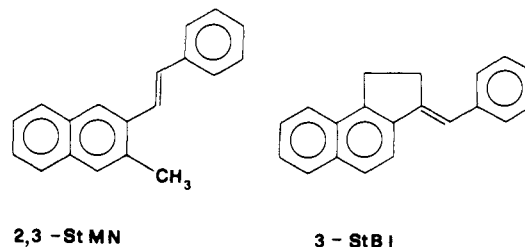


**Figure 13.** Plots of fluorescence lifetimes against  $T$  for (a) 2-StN-A and (b) 2-StN-B in (—) cyclohexane and (---) ethanol. The insets show the corresponding Arrhenius plots (adapted from ref 31).

basis of further experimental<sup>81</sup> and theoretical<sup>82</sup> considerations. Nevertheless, a higher frequency factor was reported for the A rotamer, which could indicate a higher rate for rotation to the perp configuration for the shorter lived rotamer ( $k_{t \rightarrow p} = 3 \times 10^6$  and  $1 \times 10^6$  s<sup>-1</sup> for A and B, respectively, in *n*-hexane at 293 K). However, differences in the frequency factors could also depend on experimental uncertainty in evaluating both the intersections of the Arrhenius plots and the limiting value of  $\tau$  at low temperatures where the activated isomerization is inhibited. In any case, even if some differences in the radiationless deactivation rate parameters ( $k_{t \rightarrow p}$  and  $k_{ISC}$ ) of the two rotamers may be operative (see also a slight  $\lambda_{exc}$  dependence of  $\phi_{t \rightarrow c}$ ), the main difference in  $\tau$  is certainly due to the radiative rate parameters which differ by almost 1 order of magnitude.<sup>31,77</sup> The short-lived rotamer of 2-StN was also studied by picosecond absorption spectroscopy.<sup>83</sup> A transient peaking at 510 nm with a lifetime of 2 ns, assigned to the  $S_1 \rightarrow S_n$  transition of the A rotamer, was observed in *n*-hexane at 298 K at 10-ps delay after excitation with a 352 nm, 6-ps pulse. The increase in lifetime of the rotamers in linear alkanes, due to viscosity-induced slowing in the rate of twisting around the double bond, was taken as evidence of a prevailing singlet mechanism for the *trans*  $\rightarrow$  *cis* photoisomerization.

An interesting approach was used by Saltiel and Eaker to assign the structure of the rotamers of 2-StN.<sup>34</sup> The authors synthesized two conformationally restricted analogues, namely *trans* 2-styryl-3-methylnaphthalene (2,3-StMN) and 3-styrylidenebenz[*e*]indane (3-StBI), which should closely represent the



proposed 2-StN conformers in terms of electronic structure, properties, etc. The fluorescence spectra of the analogous compounds have maxima at  $\lambda_{em}$  which closely match those of the distinct rotamers. This indicates that the short wavelength component B is StBI-like (t) while the long-wavelength component A is StMN-like (c). This assignment is also in agreement with subsequent results of independent theoretical and experimental approaches.

Muszkat and Wismonska-Knittel<sup>43</sup> provided very accurate information on the rotamer structures of 2-StN derived from Shpolskii-type emission and absorption spectra at the liquid helium temperature (see section II.A.7). Very recently, Lamotte, Muszkat, et al.<sup>45</sup> reported similar results obtained using improved experimental conditions. Only the results of ref 45 will be illustrated since they include and exceed those of ref 43. The main achievement of ref 45 was that it demonstrated that the well-resolved absorption spectrum obtained for 2-StN in a *n*-hexane Shpolskii matrix at 5 K (Figure 14, II on the left) is the superposition of two quasi line spectra attributable to the two possible rotamers. In practice, both broad-band excitation at 337 nm and narrow-band excitation at the vibronic lines denoted  $B_{0,0}$  and  $B_{0,v}$  yielded a quasi line fluorescence spectrum (Figure 14, III on the right) similar to that previously reported<sup>43</sup> and assigned to the most extended and stable *s-trans* conformer (B). On the other hand, selective excitation centered on the  $A_{0,v}$  line resulted in a completely different fluorescence spectrum (Figure 14, I on the right) which, by comparison with the quasi line spectrum obtained for a conformationally restricted analogue 2,3-StMN (Figure 14, II on the right), was assigned to the *s-cis* conformer (A). The two excitation spectra (Figure 14, I and III on the left) obtained by observing fluorescence in the regions of selected vibronic bands confirmed the existence of two distinct species and allowed the bands belonging to either A or B species to be distinguished in the absorption spectrum of the mixture (Figure 14, II on the left). Moreover, from the analysis of the difference in the vibronic structure of the two individual fluorescence spectra, the authors could infer that the  $S_1$  state of the A rotamer has a marked stilbenic character, while the  $S_1$  state of B appears to be sensibly localized on the naphthalenic moiety (this being further confirmed by the similarities between the quasi line absorption spectra of 2-StN(B) and 2-methylnaphthalene). The fact that at least one of the two rotamers of 2-StN had an  $S_1$  state of naphthalenic character was indicated by the low-resolution absorption spectrum in a glassy matrix,<sup>24a</sup> which showed a long-wavelength band attributed to the naphthalene moiety.<sup>84</sup> These findings strongly support previous conclusions from kinetic fluorescence analysis.<sup>25,31,77</sup> They indicate that the long  $\tau$  of B (the short-wavelength absorbing species) and the short  $\tau$  of



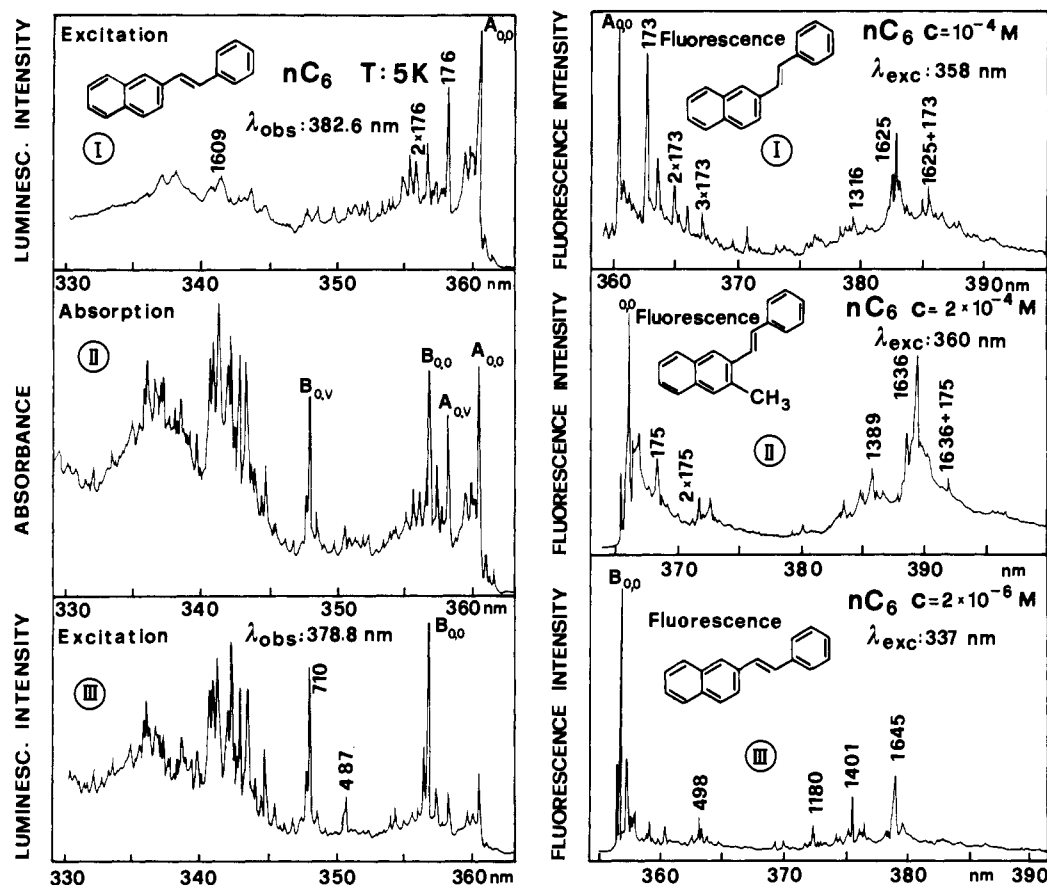


**Figure 14.** Left: (II) absorption spectrum of 2-StN in *n*-hexane at 5 K; (I and III) fluorescence excitation spectra of 2-StN monitored at selected fluorescence vibronic lines ( $\Delta\lambda_{em} < 0.4$  nm) of the distinct rotamers. Right: (I and III) the two selectively excited fluorescence spectra ( $\Delta\lambda_{exc} < 0.4$  nm) obtained from a *n*-hexane solution of 2-StN at 5 K; (II) fluorescence spectrum of *trans*-2-styryl-3-methyl-naphthalene (2,3-StMN) in *n*-hexane at 5 K (adapted from Figures 1 and 2 of ref 45).

A (the long-wavelength absorbing species) reflect a marked difference in the radiative rate constants originating in the different nature of their singlet excited states. Direct evidence for an assignment of the shorter fluorescence lifetime to the rotamer A was obtained by time-resolved quasi line fluorescence experiments. Somewhat less convincing is, in our opinion, the attribution of a markedly nonplanar structure to the rotamer A, in contrast to a completely planar structure of B. The fact that the observations are entirely specific to the host *n*-alkane matrix (the spectra of both A and B species were observed in frozen *n*-hexane while only the B spectrum was evidenced in *n*-decane matrices) is no proof in this respect. Also, the absence of progressions in the  $C_{eth}$ -aryl torsional modes<sup>43</sup> in the quasi line spectra of both A and B rotamers in frozen *n*-hexane does not agree with a marked difference in coplanarity. As a matter of fact, quantum mechanical calculations of the electronic spectra<sup>31</sup> and ground-state potential energy curves<sup>71</sup> showed that the photophysical and thermodynamic properties of 2-StN rotamers are well accounted for without resorting to nonplanarity of the *s-cis* species (see later).

Selective quenching of the rotamers of 2-StN by electron donors and acceptors was mainly investigated by Wismontski-Knittel et al.<sup>54</sup> who used charge-transfer (CT) interactions with several amines and paraquat dication. The fluorescence of 2-StN was normally quenched by the partners and an exciplex emission spectrum appeared at relatively high [Q] showing broad and structureless shape with a maximum red-shifted

relative to 2-StN alone. Non-linear, complex Stern-Volmer relationships<sup>25,54,77</sup> were obtained which permitted the extrapolation of quenching constants at relatively low [Q] values. As expected, these systems exhibited a clear dependence of exciplex emission maxima and lifetimes and of quenching constants on  $\lambda_{exc}$  and/or  $\lambda_{em}$ . Exciplex lifetimes of 20–30 ns were measured by nanosecond kinetic spectrofluorimetry following laser pulse excitation in the presence of amines. From these data, bimolecular quenching rate constants in the range  $1-2 \times 10^{10} M^{-1} s^{-1}$  were obtained. In polar solvents the singlet quenching of 2-StN by amines resulted in the formation of the corresponding radical anion. With paraquat as the quencher as well as through direct biphotonic photoionization, the radical cation was also formed. The  $\lambda_{exc}$  effect on these transients was quite small and slightly informative.<sup>54</sup>

Despite the large amount of experimental data on the behavior of the first singlet-excited state of 2-StN, relatively little attention has been given to the behavior of the lowest triplet state. Due to the well-known lack of phosphorescence in 2-StN and related DAEs, the triplet state can be studied in absorption by flash techniques. Laser flash photolytic observations by Görner et al.<sup>85</sup> and Wismontski-Knittel and Das<sup>56</sup> of T-T transients of 2-StN with distinct lifetimes ( $\sim 140$  and  $\sim 70$  ns) and absorption maxima (400 and 500 nm) were tentatively interpreted as conformeric in origin.<sup>85</sup> It should be noted, however, that these laser measurements can be distorted by the contribution of the tailing of the strong fluorescence in the 400 nm region and of

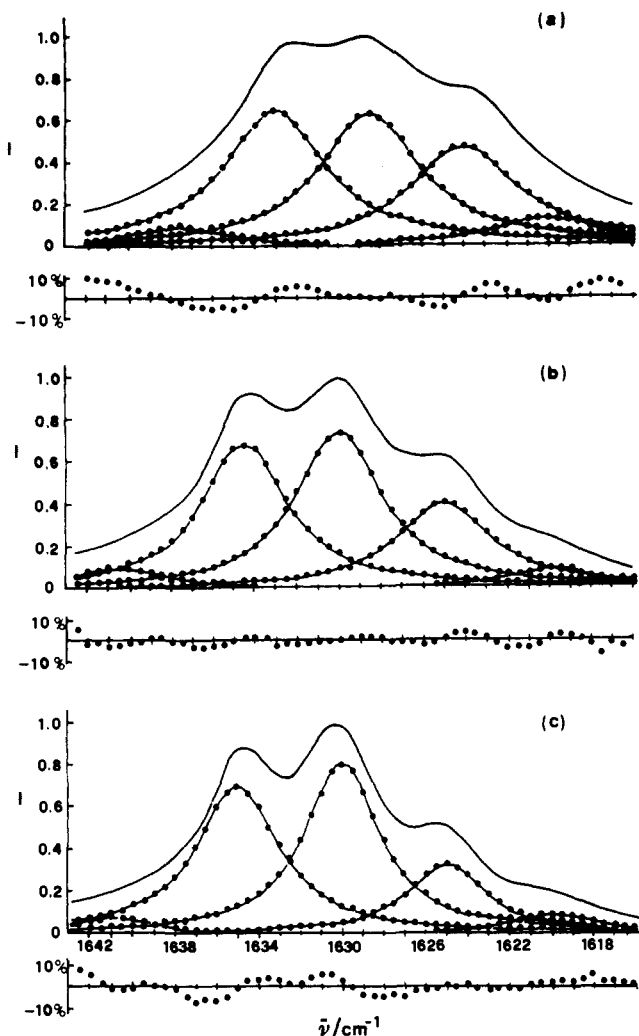


**Figure 15.** Upper curves: Raman spectra of 2-StN in *n*-hexane at 323 (a), 263 (b), and 210 K (c). Dotted lines: resolved spectra obtained by using five Lorentzian-type component bands (i.e. the 1634, 1630, and 1625  $\text{cm}^{-1}$  bands cited in the text and two very weak bands, ca. 1640 and 1620  $\text{cm}^{-1}$ , attributable to combination tones). The relative deviations between the observed and resolved spectra are reported at the bottom of each diagram (reprinted from ref 53; copyright 1988 Royal Society of Chemistry).

the  $S_1 \rightarrow S_n$  absorption in the 500 nm region.<sup>56</sup> This aspect was further investigated by Fischer with conventional flash photolysis<sup>57</sup> at low temperatures, using the freezing method described in section II.A.4. He observed that the spectra at 113 K had two main peak groups, although emission indicated the predominant presence of the longer lived rotamer B. He thus concluded that the two sets of peaks could not be assigned to different rotamers.

As to the direct study of the rotamerism in the ground state, clear-cut evidence for the existence of two distinct quasi-isoenergetic species in 2-StN solutions was provided by using classic vibrational-spectroscopy methods.<sup>53</sup> As pointed out in section II.B.1.b, the analysis of the rotameric equilibrium was based on a pair of close Raman bands, at 1630 and 1625  $\text{cm}^{-1}$ , whose relative intensities were found to be strongly temperature dependent. These bands appear to be largely overlapping and both merged with another strong band at 1634  $\text{cm}^{-1}$ . By referring to the vibrational assignment of naphthalene and styrene, and by comparison with the 1650–1600- $\text{cm}^{-1}$  Raman spectra of

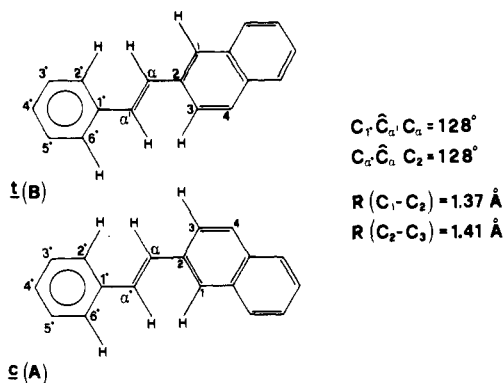


**Figure 16.** Molecular models of *s-trans*- and *s-cis*-2-StN and relevant, nonstandard, structural parameters adopted for the C-INDO calculations of ref 71.

related compounds (2-methylnaphthalene, 2-ethylnaphthalene, and 2-acetylnaphthalene), the 1634- $\text{cm}^{-1}$  band was attributed to the higher energy stretching fundamental of the naphthalene ring, while the 1630- and 1625- $\text{cm}^{-1}$  pair was attributed to the C=C stretching mode of the two rotamers of 2-StN. In order to determine the enthalpy difference between the rotamers, the Raman spectra of the 1650–1600- $\text{cm}^{-1}$  region were recorded at five temperatures. Figure 15 shows, as a representative selection, the spectra obtained at 323, 263, and 210 K (upper curves) and suggests that of the bands at 1630 and 1625  $\text{cm}^{-1}$ , the former (whose relative intensity increases with decreasing temperature) must be attributed to the C=C stretching of the more stable isomer (B) and the latter to the less stable one (A) (the reversed notation was adopted in ref 53). By graphical resolution of the recorded spectra (Figure 15), the integrated intensities of the bands at 1630 (B) and 1625 (A)  $\text{cm}^{-1}$  were derived and a plot of  $\ln(I_A/I_B)$  vs  $1/T$  yielded  $\Delta H = 0.71 \pm 0.07 \text{ kcal mol}^{-1}$  by a least-squares fit (eq 30). As is evident, this value is in excellent agreement with those obtained for 2-StN by the KFA method (Table III). A parallel Raman investigation of 1-StN showed no doubling of the C=C stretching band (appearing at 1633  $\text{cm}^{-1}$ ), thus confirming that, because of steric strain of one of the rotamers, 1-StN exists practically in a single form.

Finally, we will survey the results of quantum-mechanical calculations on the rotamerism of 2-StN. By reference to the general considerations of section II.C, we can say that the reported theoretical studies answer exhaustively the basic questions concerning the ground-state rotamers,<sup>71</sup> while they give partial, yet significant, elucidations about the excited-state properties.<sup>31</sup>

In ref 71, the C-INDO method<sup>68</sup> was used to set up detailed ground-state potential energy curves for the rotamer interconversion in 2-StN and, for the sake of comparison, 1-StN. The choice of the structural parameters appeared to be crucial, especially in the case of 2-StN. First of all, a thorough preanalysis of the internal rotation in styrene, where both experimental<sup>86</sup> and theoretical *ab initio*<sup>87</sup> results were available for comparison, indicated that the  $\angle C_{\alpha'}-C_{\alpha}-C_2$  and  $\angle C_1-C_{\alpha}-C_{\alpha'}$  bond angles have values larger than 120° at all conformations, owing to the  $C_{\alpha'}\cdots C_2$  and  $C_{\alpha'}\cdots C_1$  nonbonded repulsions (Figure 16). A fixed value of 128°, as derived from the C-INDO studies on styrene and experimentally found for gas-phase stilbene,<sup>48</sup> was

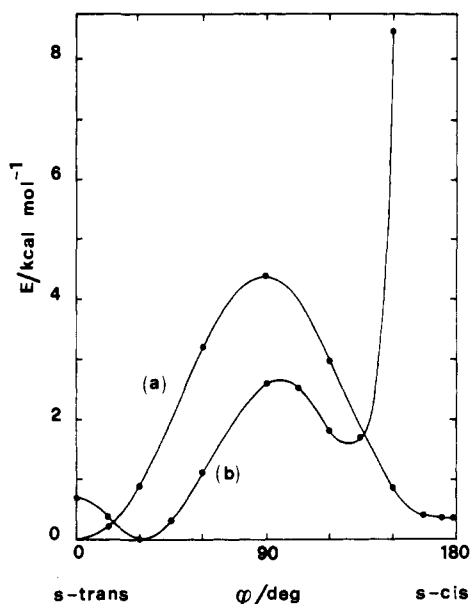


**Figure 17.** C-INDO ground-state potential energy curves for internal rotation of 2-StN (a) and 1-StN (b) about the essential single bond connecting the naphthyl group to the ethylenic bridge. In both cases the styryl group was assumed to be planar (adapted from Figures 5 and 6 of ref 71).

adopted for both the cited bond angles in the calculation of the torsional potential of 2-StN. As first pointed out by Muszkat and Wisniewski-Knittel,<sup>43</sup> another basic structural property is the nonequivalence of the  $C_1-C_2$  and  $C_2-C_3$  bond lengths in the naphthyl group, which reflects the characteristic double-bond "localization" in naphthalene (Figure 16). This factor was accounted for in ref 71 by using the naphthalene experimental geometry<sup>88</sup> for the naphthyl group. All other structural parameters were given standard values. C-INDO calculations based on the above assumptions yielded the potential energy curves represented in Figure 17a. The two rotamers of 2-StN were found to correspond to the t(B) and c(A) planar conformations, the A species being 0.34 kcal mol<sup>-1</sup> less stable than the B species. It is to be pointed out that the planarity of the rotamers, which is in keeping with the observed planarity of styrene<sup>86</sup> and stilbene,<sup>46,47</sup> is the outcome of the deformation of the  $\angle C_\alpha-C_\alpha-C_2$  bond angle which weakens the nearest  $H_{\alpha\cdots H_3}$  and  $H_{\alpha\cdots H_1}$  nonbonded repulsions coming into play near  $\phi = 0^\circ$  and  $180^\circ$ , respectively (Figure 16). The previously assumed nonplanarity of the rotamer A<sup>43,45</sup> is simply reflected in a relative flatness of the  $180^\circ$  minimum. The slight, yet significant, relative instability of the rotamer A is almost entirely induced by the nonequivalence of the  $C_1-C_2$  and  $C_2-C_3$  bond lengths causing the  $H_{\alpha\cdots H_1}$  distance (at  $\phi = 180^\circ$ ) to be shorter than the  $H_{\alpha\cdots H_3}$  one (at  $\phi = 0^\circ$ ). As a matter of fact, an energy difference of just 0.12 kcal mol<sup>-1</sup> was obtained using an idealized geometry (regular hexagons with  $R_{C-C} = 1.397 \text{ \AA}$ ) for the naphthyl group.<sup>71</sup> The calculated  $\Delta E(A-B)$  is about half of the experimentally determined  $\Delta H$ ,<sup>31,53</sup> but the theoretical predictions can be considered satisfactory in view of the quasidegeneracy of the rotamers. The energy barrier separating the two rotamers was predicted to be ca. 4 kcal mol<sup>-1</sup> (precisely,  $E(B \rightarrow A) = 4.38$ ,  $E(A \rightarrow B) = 4.04$  kcal mol<sup>-1</sup>). With such an intramolecular barrier, and considering the relatively small extra volume (over the van der Waals volume occupied

**TABLE IV.** Energies, Oscillator Strengths, Radiative  $S_1$  Rate Constants, and Composition for the Two Lowest Excited Singlet States of *trans*-StNs, as Obtained by CNDO/S Calculations (from ref 31)

state	$E$ , eV	$f$	$k_F^a$ $10^7 \text{ s}^{-1}$	composition <sup>b</sup>
1-StN, $\varphi = 0^\circ$ (s-trans)				
$S_1$	3.68	1.021	26.6	0.97 (9 $\rightarrow$ 10) ethylenic
$S_2$	3.91	0.021		0.74 (9 $\rightarrow$ 12) + 0.55 (7 $\rightarrow$ 10) naphthalenic
2-StN, $\varphi = 180^\circ$ (rotamer A)				
$S_1$	3.79	0.471	13.0	0.55 (9 $\rightarrow$ 10) + 0.60 (9 $\rightarrow$ 11) mixed
$S_2$	3.80	0.574		0.79 (9 $\rightarrow$ 10) + 0.31 (9 $\rightarrow$ 11) mixed
2-StN, $\varphi = 0^\circ$ (rotamer B)				
$S_1$	3.79	0.072	2.0	0.70 (9 $\rightarrow$ 11) + 0.50 (8 $\rightarrow$ 10) naphthalenic
$S_2$	3.91	1.311		0.95 (9 $\rightarrow$ 10) ethylenic

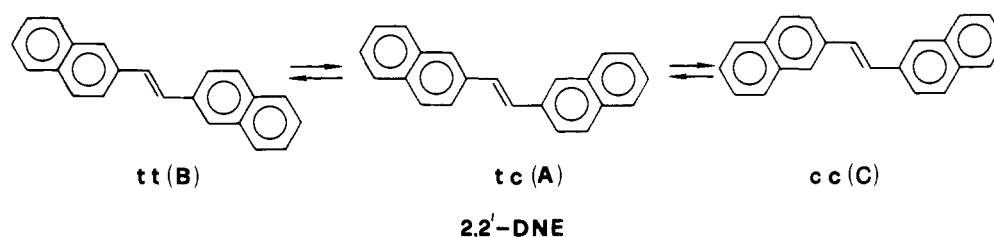
<sup>a</sup> Obtained by the formula<sup>89,95</sup>  $k_F = f\nu^2 k_F^{St} / (f\nu^2)^{St}$ , where  $f$  and  $\nu$  are the calculated oscillator strength and frequency of  $S_1$  and the superscript refers to stilbene. <sup>b</sup> The numbering of the orbitals involved in the transitions ( $i \rightarrow j$ ) refers to the  $\pi$  MO subset.

by the molecule) swept out by 2-StN during internal rotation, the rotamers are expected to interconvert very rapidly in a rather large range of the medium viscosity.

The parallel C-INDO study carried out for 1-StN yielded the potential energy curve of Figure 17b. Calculations were performed taking  $\angle C_1-C_\alpha-C_\alpha = 128^\circ$ ,  $\angle C_\alpha-C_\alpha-C_1 = 126^\circ$  (the latter value being optimized for 1-vinylnaphthalene) and the idealized geometry for the naphthalene moiety (the use of nonequalized bond lengths being immaterial in this case). The stable conformation (B) of 1-StN was predicted to lie at  $\phi \simeq 30^\circ$ . A second energy minimum (A) was found to exist at  $\phi \simeq 130^\circ$ , about 1.6 kcal mol<sup>-1</sup> above the stable form, while the planar c( $180^\circ$ ) form appeared to be completely hindered because of exceedingly high steric interactions. From the calculated  $\Delta E(A-B)$  the fractions of the A and B species came out to be 0.06 and 0.94 at 293 K. In other words, the rotamer B appeared to be largely predominant and this explains why the reported experimental studies on 1-StN in solution have not revealed the existence of more than one species.<sup>20,31,53</sup>

A theoretical study on the properties of the excited states of 1- and 2-StN was performed, again in 1984, by Bartocci et al.<sup>31</sup> using the CNDO/S method.<sup>62</sup> Calculations were carried out for the more stable species of 1-StN and the two rotamers of 2-StN, assuming planar conformations for all species and using bond lengths deduced from some available X-ray crystallographic data.<sup>43</sup> The most relevant results are collected in Table IV. According to the nature of the predominant electron configuration in the CI wave functions, the excited states were classified as naphthalenic, ethylenic, and mixed ("delocalized" would be a more proper notation than "ethylenic" in view of the real shape of the involved HOMO and LUMO, see later). From this point of view, the excited-state ordering of 2-StN(B) is inverted with respect to that of 1-StN(t), the  $S_1$  state being ethylenic (essentially HOMO  $\rightarrow$  LUMO) in 1-StN(t) and naphthalenic (corresponding to the  $^1L_b$  state of naphthalene) in 2-StN(B). This is due to the HO and LU orbitals being much more delocalized (i.e. the HOMO  $\rightarrow$  LUMO transition is much more stilbenic)

## SCHEME I



in 1-StN(t) than in 2-StN(B), even if the phenomenon should be less marked when assuming a more realistic nonplanar conformation for 1-StN (Figure 17). As a consequence, the  $S_0 \rightarrow S_1$  oscillator strength (and hence the radiative  $S_1$  rate constant) of 2-StN(B) was found to be 1 order of magnitude smaller than that of 1-StN(t). The rotamer A of 2-StN came out in an intermediate situation. In practice, the B(t) to A(c) conversion is accompanied by a slight relative energy lowering of the [HOMO, LUMO] configuration, probably attributable to the passage from a trans to a cis conformation of the  $C_\alpha = C_\alpha$  and  $C_2 = C_1$  "double bonds" (see Figure 16),<sup>90</sup> which enhances its interaction with the naphthalenic configurations and yields two almost degenerate states of mixed character with averaged oscillator strengths. The point to be emphasized is that the resulting  $S_1$  radiative rate constant is much higher than that of the rotamer B; comparison between Tables IV and III shows that the calculated values of  $k_F$  are in good agreement with those derived from experiments.<sup>31</sup> In conclusion, the CNDO/S calculations clearly show, in keeping with kinetic fluorescence analyses<sup>25,31,77</sup> and emission spectroscopy in Shpolskii matrices,<sup>45</sup> that the markedly different fluorescence lifetimes of the two rotamers of 2-StN derive from the different nature of their fluorescent states. It is to be noted, however, that the calculated photophysical properties of the rotamer A were determined, to some extent, by its assumed planarity. In other words, the results of ref 31 are consistent with the rotamer A being planar or quasi-planar, in keeping with the C-INDO prediction (Figure 17). The CNDO/S calculations, however, were not able to reproduce the observed red shift of the absorption spectrum of A with respect to that of B.<sup>45</sup> Moreover, the problem of the energy barriers hindering rotamer interconversion in the lowest excited singlet state remains open. From unpublished CS-INDO calculations on 2-StN,<sup>82</sup> such a barrier was found to be ca. 11 kcal mol<sup>-1</sup>, i.e. about twice that of the ground state. Thus the validity of the NEER assumption is maintained because the interconversion of the excited rotamers is expected to occur in the microsecond time scale at room temperature, while the observed  $S_1$  lifetimes are about 3 orders of magnitude shorter (Tables I and II). This theoretical prediction clearly supports the conclusions drawn by emission spectroscopy which were based on the assumption that the excited rotamers of 2-StN decay independently with different lifetimes.

b. *trans-1,2-Di(2-naphthyl)ethylene*. This compound (2,2'-DNE) has also been extensively investigated in various laboratories. Its particular interest lies in the fact that three quasi-coplanar, almost isoenergetic rotamers can be a priori envisaged (Scheme I). Therefore, it represents a challenge to verify the basic as-

sumptions generally accepted in the interpretation of the DAE rotamerism. The first observations,<sup>20,21</sup> however, were unable to identify the third rotamer and were therefore discussed in terms of a two-component system. The difference in the  $S_1$  lifetime between the two rotamers was found to be smaller ( $\tau_B/\tau_A = 7.4/2.2 \approx 3.3$  in MCH at room temperature) than in the case of 2-StN ( $\tau_B/\tau_A > 5$ ) but the  $\lambda_{exc}$  effect on the spectra was more pronounced, the shift being almost 10 nm.<sup>20</sup> The shift becomes even more pronounced at low temperatures where sharper spectra were obtained. It is interesting to note the technique that was sometimes used to prevent precipitation on cooling because of its very low solubility. A solution of *cis*-2,2'-DNE was cooled to  $-185^\circ\text{C}$  and converted into *trans* by 366-nm irradiation. Under these conditions no aggregation or crystallization takes place because of the combined effect of high viscosity and low temperature.<sup>20</sup> Contributions of 24 and 76% of the A and B species, respectively, was roughly determined from the preexponential factors (eq 1) of the decay curves.

Also 2,2'-DNE was investigated with the Shpolskii matrix technique.<sup>43,44</sup> The quasi line electronic spectra obtained in *n*-hexane and *n*-pentane matrices at 5 K were analyzed with reference to the spectrum of stilbene. A highly resolved spectrum was obtained for only one of the three expected rotamers and assigned to the most extended planar conformer (tt). The available crystallographic and spectral information indicated that the two other less extended conformers (tc and cc) depart significantly from planarity.<sup>43,44</sup> It is to be noted that this compound was not revisited with the improved instrumental facilities more recently used with success by the same authors for related molecules.<sup>45</sup>

Details on the spectral properties of the conformers of 2,2'-DNE were obtained by Ghiggino using time-resolved fluorescence techniques.<sup>28</sup> The spectra observed (coincident with the excitation pulse and at a 30-ns delay after excitation) are shown in Figure 6. Comparison of the time-resolved spectra with the spectrum of the mixture provided an insight into the spectral and temporal characteristics of the rotamers, in substantial agreement with Fischer's results.<sup>20</sup> Even with the high temporal resolution of the picosecond laser apparatus used by Ghiggino, no evidence was obtained for any "grow-in" of the emitting species over time which confirms that no conformational changes occur during the lifetime of the excited state.<sup>28</sup> Even with this technique, only two species were identified for this DAE. Indication of more than two species was only argued on the basis of bad ( $>2$ )  $\chi^2$  values obtained for the fit of the biexponential decay and by differential quenching methodology which suggests the presence of three differently quenchable species.<sup>28</sup> The presence of three components received convincing confirmation from

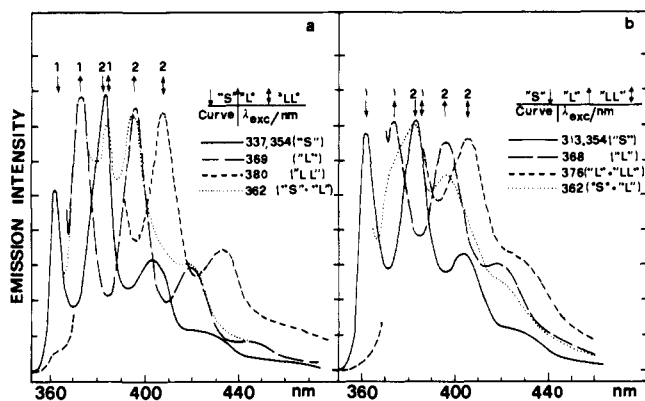


**Figure 18.** Emission spectra of *trans*-2,2'-DNE in ethanol, excited at the wavelengths indicated: (a) following *cis*  $\rightarrow$  *trans* photoconversion at 98 K; and (b) heated to 173 K (equilibrium mixture). The three modifications S, L, and LL are each characterized by a set of three peaks, as indicated by the arrows (adapted from ref 26).

further investigations by the Fischers who observed three sets of peaks shifted by about 10 nm between each other by selective excitation in fluid solution at room temperature<sup>91</sup> and at  $-100$  °C,<sup>22</sup> in an unstretched polyethylene film as well as in frozen-in nonequilibrium mixtures (see section II.A.4) obtained by low-temperature irradiation of the *cis* isomer in ethanol and in decalin.<sup>26</sup> In the latter case, Castel and Fischer succeeded in showing the spectra of the three expected rotamers of *trans*-2,2'-DNE formed by UV irradiation at 98 K (Figure 18). After heating to 173 K (to permit equilibration) and cooling again, the contribution of the species emitting at the longest wavelengths (LL in Fischer's notation) diminished to almost zero while that emitting at medium wavelengths (L) contributed much less than the previous values. Therefore, on cooling, a change of the emission spectrum in favor of the rotamer having the lower enthalpy, namely the hypsochromic S (B) species, was clearly observable after equilibration while the spectra before heating were more informative about the other two rotamers.<sup>26</sup>

Crystallization as a tool to freeze-in a distinct preferred modification was successfully used to crystallize-in the more elongated (tt) form of *trans*-2,2'-DNE (citation 9 in ref 27).

The KFA method was not applied to 2,2'-DNE. Saltiel et al., however, successfully used the PCA method to obtain the resolution of three-component spectra, by using, this time, large input matrices.<sup>35,36</sup> Changes in the spectral shape with  $\lambda_{\text{exc}}$  and  $[\text{O}_2]$  agreed with earlier reports. The method first led to a two-component solution which indicated a longer wavelength component A and a shorter wavelength component B (B and A, respectively, in Saltiel's notation). These components accounted for >99% of the total variance of all measured spectra.<sup>36a</sup> In pursuing a three-component solution it was assumed that the less resolved, longer wavelength component spectrum was a fluorescence combination of two species, A and C (named B and C, respectively, in ref 36b). The analysis was then extended to a matrix of experimental spectra of 2,2'-DNE and its conformationally restricted analogue, 3-methyl (MDNE, 2 nm blueshifted, two rotamers expected) and 3,3'-dimethyl (DMDNE, 9 nm blueshifted, one rotamer expected) derivatives. These substituted compounds were thus used as guides in the

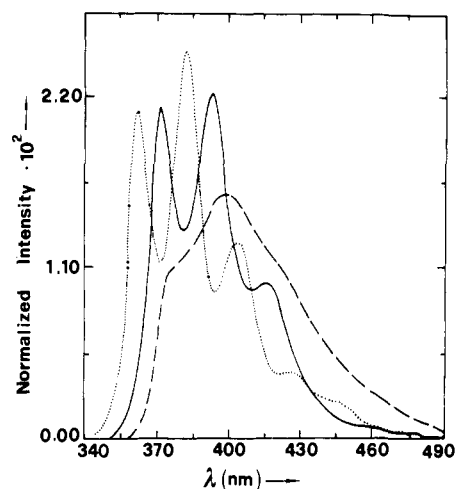


**Figure 19.** Pure component spectra for the 2,2'-DNE/ $\text{CCl}_4$  system: DNE-B (---), DNE-A (—) and DNE-C (- -) as derived from the PCA-SM method. Rotamer notation refers to Scheme I (reprinted from ref 36b; copyright 1988 American Chemical Society).

selection of pure component combination coefficients for the three rotamers of the unsubstituted 2,2'-DNE.<sup>36a</sup>

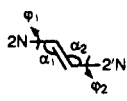
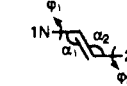
Improved solutions for pure component coefficients of A and C were later achieved without relying on the methyl derivative spectra.<sup>36b</sup> The PCA-SM method extended to three-component systems<sup>35</sup> was applied on a matrix of emission spectra in MCH obtained for  $\lambda_{\text{exc}} = 366$  nm (excitation at the onset of the absorption spectrum gives selectively the short-lived component<sup>20</sup>) and different concentrations of  $\text{CCl}_4$  (which differentially quenches the A and C fluorescence<sup>28</sup>). This procedure succeeded in resolving the experimental spectra into three different components.<sup>36b,79</sup> Spectral matrices for  $\text{O}_2$  and  $\text{CCl}_4$  quenching, treated separately, yielded nearly identical pure component fluorescence spectra. Those with  $\text{CCl}_4$  are shown in Figure 19. The choice of pure component spectra was refined by imposing the additional constraint that  $K_{\text{SV}}$  for each quencher be independent of  $\lambda_{\text{exc}}$ . The  $K_{\text{SV}}$  values obtained for each rotamer and the lifetimes of  $\sim 7.3$  ns for rotamer B and  $\sim 2.2$  ns for the other two rotamers<sup>20</sup> led to practically identical (diffusional)  $k_{\text{Q1}}$  values of rotamers A and C for the quenching by  $\text{O}_2$  but preferential quenching of A with respect to C in the case of  $\text{CCl}_4$ . The mechanism of quenching by  $\text{CCl}_4$  giving rise to this unusual behavior, remains to be explained.<sup>36b</sup>

Selective quenching by charge-transfer interactions with amines and paraquat dication was studied by Wismontski-Knittel et al.<sup>54</sup> with results similar to those already described for 2-StN.

As for the triplet behavior, laser flash excitation studies on 2,2'-DNE in benzene by Wismontski-Knittel and Das<sup>56</sup> showed T-T absorptions with  $\tau \approx 210$  ns at 400–450 and 500–600 nm, similar to 2-StN. However, in this case, the two-band systems did not show differences in the first-order rate constants from decay profiles monitored in the two different regions. It is to be noted that for this naphthyl derivative a minor short-lived component of transient decay with lifetime  $\sim 80$  ns became evident when monitoring at the low-energy tail of the bathochromic band. This component probably represents a minor conformer of 2,2'-DNE.

With this compound, too, Fischer studied the triplet behavior by conventional flash photolysis in alcoholic

**TABLE V. Conformational Angles and Relative Energies (kcal mol<sup>-1</sup>) of the Rotamers of 2,2'-DNE and 1,2'-DNE as Obtained by C-INDO Calculations (from ref 71) (Energies are Given Relative to the Most Stable Species (B))**

molecular schemes <sup>a</sup>	tt (B)	tc (A)	cc (C)	ct (D)
 $\alpha_1 = \alpha_2 = 128^\circ$	$\left. \begin{array}{l} \varphi_1 = 0^\circ \\ \varphi_2 = 0^\circ \end{array} \right\} 0.0$	$\left. \begin{array}{l} \varphi_1 = 0^\circ \\ \varphi_2 = 180^\circ \end{array} \right\} 0.33$	$\left. \begin{array}{l} \varphi_1 = 180^\circ \\ \varphi_2 = 180^\circ \end{array} \right\} 0.68$	$\left. \begin{array}{l} \varphi_1 = 180^\circ \\ \varphi_2 = 0^\circ \end{array} \right\} = \text{tc (A)}$
 $\alpha_1 = 126^\circ, \alpha_2 = 128^\circ$	$\left. \begin{array}{l} \varphi_1 = 30^\circ \\ \varphi_2 = 0^\circ \end{array} \right\} 0.0$	$\left. \begin{array}{l} \varphi_1 = 30^\circ \\ \varphi_2 = 180^\circ \end{array} \right\} 0.33$	$\left. \begin{array}{l} \varphi_1 = 130^\circ \\ \varphi_2 = 180^\circ \end{array} \right\} 1.81$	$\left. \begin{array}{l} \varphi_1 = 130^\circ \\ \varphi_2 = 0^\circ \end{array} \right\} 1.48$

<sup>a</sup> For more explicit schemes of 2,2'-DNE and 1,2'-DNE rotamers, see Scheme I and Figure 2C, respectively.

glasses at low temperatures applying the freezing-unfreezing method.<sup>57</sup> Thus, the T-T spectra were measured, first, immediately after cis  $\rightarrow$  trans photoconversion, and then, after slight heating and recooling. In the last case, the spectrum was simpler, reflecting the presence of the predominant hypsochromic B rotamer at the equilibrium. The first spectrum was more complex, probably due to the contribution of the shorter lived A rotamer. The differences between the two spectra ("before" and "after") increased markedly by using longer  $\lambda_{\text{exc}}$  ( $>350$  nm) because of the preferential excitation of the A rotamer under these conditions.

Results in accordance with the presence of three distinct species in solutions of 2,2'-DNE at ordinary temperatures, were obtained by a C-INDO analysis of the potential energy curves describing interconversion of the three rotamers (Scheme I).<sup>71</sup> The geometric parameters were given the same values as those adopted for the naphthalene and ethylene fragments in the previous calculations on 2-StN (see preceding section 1.a). The results concerning the preferred conformational angles and the relative energies of the rotamers are reported in Table V (first row). As could be expected from the structural similarities between 2,2'-DNE and 2-StN, the three rotamers were found to be planar, with the A and C species lying 0.33 and 0.68 kcal mol<sup>-1</sup> above the B species. This implies relative abundances of 0.53 (B), 0.30 (A), and 0.17 (C) at 293 K, and hence indicates that all three rotamers should be detectable at room temperature. In accordance with the above mentioned observation by Castle and Fischer<sup>26</sup> on frozen-in nonequilibrium mixtures, B, A, and C rotamers should be identified as the species emitting at the shortest (S), medium (L), and longest (LL) wavelengths, respectively (Figure 18). The energy barriers hindering B  $\rightarrow$  A and A  $\rightarrow$  C conversions were predicted to be 4.4 and 4.7 kcal mol<sup>-1</sup>, respectively.

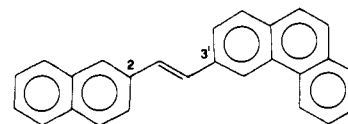
In ref 71, calculations were extended for comparison to 1,2'-DNE, where four species can, in principle, be expected (Figure 2c). The results are reported in the second row of Table 5. They show that the two rotamers, B and A, corresponding to the more stable conformations of the 1-naphthyl group ( $\varphi_1 = 30^\circ$ ), should be expected to be largely predominant at equilibrium, the markedly nonplanar C and D forms lying at too high relative energies. This description agrees with the observation of only two modifications in 1,2'-DNE solutions.<sup>20</sup>

No calculations of the electronic transitions and excited state torsional potentials have been reported for

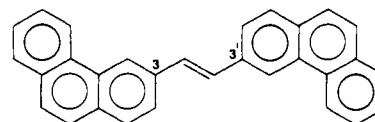
2,2'- and 1,2'-DNE, so no explicit theoretical predictions exist about the validity of the NEER assumption in these molecules. It seems reasonable, however, to extend the conclusions previously reached for 2-StN to these DAEs, considering that rotamerism of naphthyl groups is involved in both cases. Moreover, the application of the NEER scheme is fully justified by the picosecond fluorescence decay study of Ghiggino<sup>28</sup> (see above), where no initial formation phenomena attributable to rotamer interconversion were observed.

## 2. Phenanthryl Derivatives

An extensive emission spectroscopy study on rotamer systems of *trans*-DAEs containing the phenanthryl group, 1,2-(*n,n'*-naphthylphenanthryl)ethylene (*n,n'*-NPhE) and 1,2-(*n,n'*-diphenanthryl)ethylene (*n,n'*-DPHE), was first carried out by Fischer.<sup>27</sup> As observed in the naphthyl analogues, the emission spectra were found to vary with  $\lambda_{\text{exc}}$ , indicating the existence of two or even three species of each compound, with slightly shifted absorption and emission peaks. The temperature effect was explored in detail down to 95 K in different solvents but no quantitative analysis of the rotamer mixtures was reported. Contrary to the case of the naphthyl analogues, the emission quantum yield of the phenanthryl derivatives was found to be virtually independent of  $\lambda_{\text{exc}}$  in a wavelength range where the shape of the spectrum varies greatly with  $\lambda_{\text{exc}}$ . Oxygen did not affect the shape of the emission spectra, giving indirect evidence of a lifetime similarity of the various conformers. From the  $\lambda_{\text{exc}}$  effect on the spectra, a conformeric composition of  $\sim 30\%$  of the bathochromic species (L) was roughly estimated for 3,3'-DPHE in MCH/toluene at 173 K and for 2,3'-NPhE in decalin



2,3'-NPhE

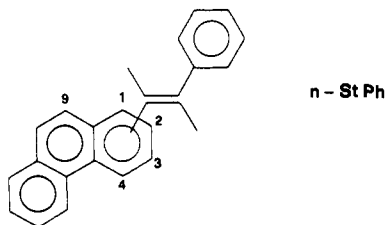


3,3'-DPHE

at 153 K. For the latter compound, in addition to the two usual rotamers, a third species was identified in nonpolar matrices at low temperatures by an emission spectrum shifted even more to the red.<sup>27</sup>

Due to the low solubility of these compounds in aliphatic hydrocarbons, some temperature effects observed on the spectra were explained by the intervention of aggregation phenomena. The latter might take place preferably in one conformeric species thus allowing almost complete conversion into one conformer. This effect was observed by chance with 3,3'-DPhE: on cooling solutions of this slightly soluble DAE in a nonpolar solvent mixture to 153 K, excitation first gave rise to a mixed emission spectrum; further slow cooling to 133 K resulted in a gradual transition to an almost pure spectrum of the red-shifted modification.<sup>22,27</sup> This compound was also studied by Ghiggino et al.<sup>28</sup> Double-exponential fits to the fluorescence decay gave two rather similar lifetimes (1.06 and 3.5 ns) which were in qualitative agreement with Fischer's observations.<sup>27</sup> However, slightly nonrandom weighted residual distributions and bad  $\chi^2$  values ( $>2$ ) indicated that more than two kinetically distinct emitting species were present. Also, parallel quenching experiments showed an efficiency which varied with  $\lambda_{\text{exc}}$ , indicating the existence of three differently quenchable entities.<sup>28</sup>

The merit of the cited studies on NPhEs and DPhEs<sup>27,28</sup> was, of course, that they provided the first evidence for the existence of more than one conformer in solutions of DAEs containing the phenanthryl group. On the other hand, more in-depth knowledge on the rotamerism of the phenanthryl group and a sharp comparison with the rotamerism of other aryl groups (e.g. naphthyl, anthryl) could only be derived from a systematic investigation on the simplest phenanthryl derivatives, i.e. *trans*-*n*-styrylphenanthrenes (*n*-StPhs).



A basic consideration for the studies based on emission spectroscopy, is that the electronic spectrum of the phenanthrene moiety is closer to the spectrum of naphthalene than to that of the corresponding linear acene, i.e. anthracene (Figure 20). In particular, the lowest excited singlet state is the almost forbidden  $^1L_b$  state in both naphthalene and phenanthrene, while it is the allowed  $^1L_a$  (essentially HOMO  $\rightarrow$  LUMO) state in anthracene. The correctness of this assignment is further supported by the fact that the radiative rate constants of anthracene, naphthalene, and phenanthrene, as derived from the measured fluorescence lifetimes and quantum yields, are  $\sim 7 \times 10^7$ ,  $3 \times 10^6$ , and  $2 \times 10^6$  s<sup>-1</sup>, respectively, in saturated hydrocarbon solvents.<sup>95</sup> This suggests that *n*-StN is more suitable than *n*-StA as a reference system for interpreting the fluorescence characteristics of *n*-StPh. Following this guideline, a rather complete photophysical and theoretical study of the rotamerism of *trans*-*n*-StPh was published in 1987 by Bartocci et al.<sup>72</sup> The observed fluorescence properties and simple structural consid-

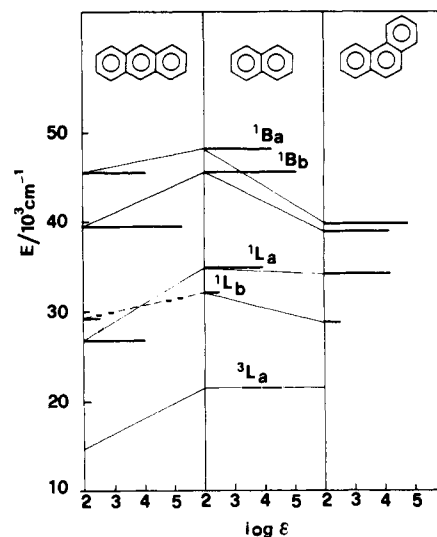


**Figure 20.** Correlation of the UV transitions of naphthalene with those of anthracene and phenanthrene, as derived by FEMO<sup>92</sup> and PPP<sup>93</sup> calculations. The general Platt's notation is used for the electronic states. Transition energies and absorption coefficients were taken from ref 94.

**TABLE VI. Kinetic Fluorescence Analysis of Rotamers of *trans*-3-StPh in *n*-Hexane at 293 K (from ref 39)**

$\lambda_{\text{exc}}$ , nm	$\phi$	$\tau_A$ , ns	$\tau_B$ , ns	$\alpha$ ( $\lambda_{\text{exc}}$ )	$\bar{F}$ ( $\lambda_{\text{exc}}, 372$ )	$f_A$ ( $\lambda_{\text{exc}}$ )
370	0.92	7.6	18.6	7.83	0.46	0.83
355	0.84	7.6	17.6	3.06	0.53	0.69
335	0.71	7.5	18.2	1.22	0.57	0.50
315	0.70 <sub>6</sub>	8.0	18.9	1.36	0.61	0.48

erations led to the classification of the five isomers ( $n = 1, 2, 3, 4, 9$ ) into three categories. The 2 and 3 isomers are the analogues of *trans*-2-StN: the nonbonded interactions are small in both coplanar forms obtained by rotation of the polycyclic group. Therefore, they are expected to possess two almost equivalent potential energy minima near 0° and 180° thus existing in solution as a mixture of rotamers of comparable abundance. The 1 and 9 isomers are the analogues of *trans*-1-StN: the steric interference between the aromatic and ethylenic hydrogens is strong in one of the two coplanar forms, thus the equilibrium being almost completely shifted toward the more stable rotamer. Finally, the 4 isomer is so crowded that only a single species, strongly deviating from coplanarity, is expected to exist in its solutions. The ground-state potential energy curves (obtained by the CS-INDO method) which describe the internal rotation around the essential single bond connecting the phenanthrenic and styrenic moieties (Figure 21) showed that the suggested classification matches the theoretical description.<sup>72</sup>

The presence of two distinct rotamers in solution, as shown by the dependence of the fluorescence spectra and decay curves on  $\lambda_{\text{exc}}$ , is then expected for the 2 and 3 isomers. However, it was detected only for the latter. For 2-StPh, as for the 1, 4, and 9 isomers, the fluorimetric behavior did not show any anomaly, being practically independent of  $\lambda_{\text{exc}}$ , and the emission decay profile was monoexponential in all the experimental conditions investigated. Therefore, the two almost planar and isoenergetic rotamers expected for 2-StPh would seem to have almost identical photophysical properties (spectra, quantum yield, decay rate parameters).<sup>72</sup> CS-INDO CI calculations qualitatively confirmed this interpretation, since they indicated that the

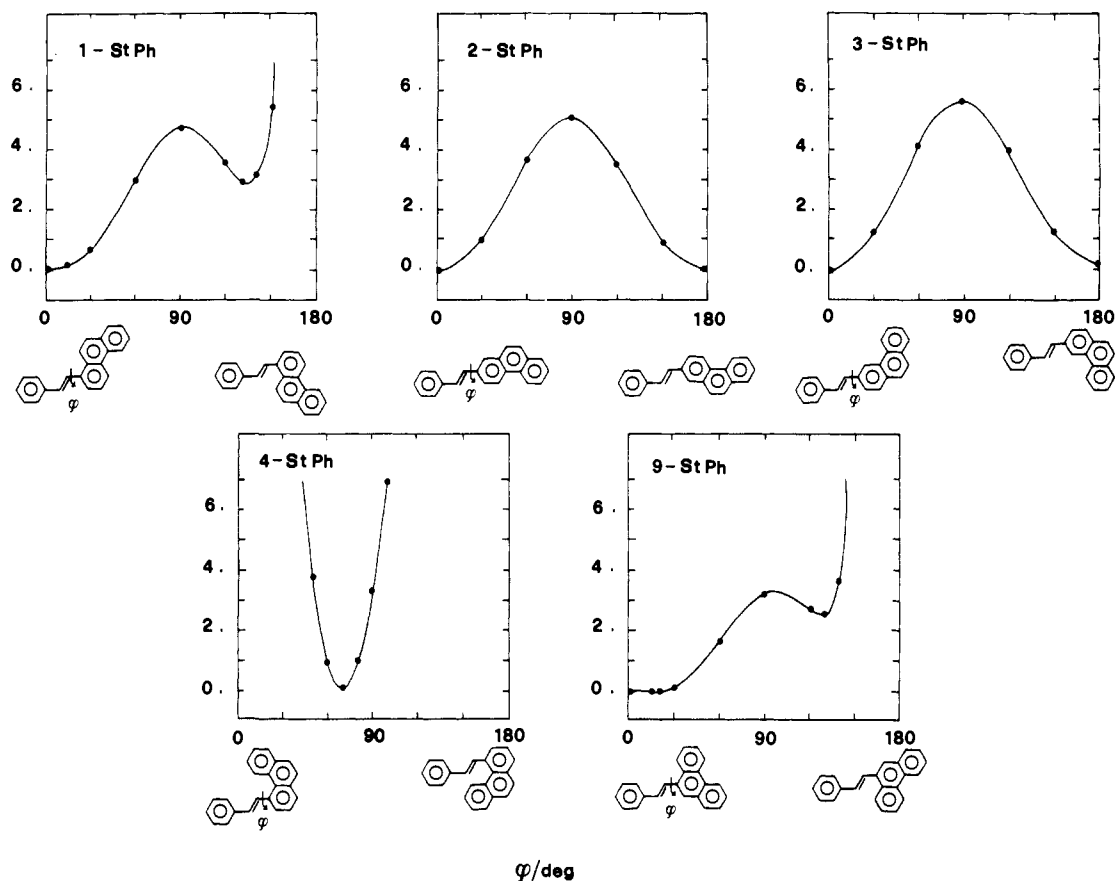


**Figure 21.** CS-INDO ground-state potential energy curves for internal rotation of *n*-StPh around the "single" bond connecting the phenanthryl group to the ethylenic bridge.<sup>72</sup> The experimental X-ray structure of phenanthrene<sup>96</sup> was given the phenanthryl group. The following values were given the bond angles at the ethylene carbon atoms: C=C—C (phenyl) = 128° (by analogy with styrene), C=C—C (phenanthryl) = 128° in 2- and 3-StPh (by analogy with 2-StN) and 126° in 1-, 4-, and 9-StPh (by analogy with 1-StN) (see ref 71 and section III.A.1). All other structural parameters were given standard values (adapted from ref 72).

**TABLE VII.** Photophysical Parameters of *trans*-3-StPh in *n*-Hexane at 293 K, Enthalpy Difference and Relative Conformer Concentrations as Obtained from the KFA Method (Values in Parentheses Were Obtained by the PCA-SM Method) (from ref 39)

parameters	3-StPh(A)	3-StPh(B)
$\phi$	0.94 (1.00)	0.45 (0.44 <sub>5</sub> )
$\tau$ , ns	7.7	18.3
$k_F$ , 10 <sup>7</sup> s <sup>-1</sup>	12.2	2.5
$\Delta H$ , cal mol <sup>-1</sup>	190 (200)	
relative abundance, %	42	58

$S_0 \rightarrow S_1$  transitions of the two rotamers of 2-StPh had almost identical properties (energy, oscillator strength).<sup>72</sup>

The KFA method was applied to the fluorescence of 3-StPh.<sup>72</sup> The  $\phi$  values of its two rotamers are rather different and there are no isoemissive points in their fluorescence spectra. Therefore, the KFA method was applied following the treatment described in section II.A.5.a for the special case of a rotamer mixture without isoemissive points. The results reported in ref 72 have recently been revised<sup>39</sup> using a new correct set of  $\phi$  values. The data collected in Tables VI and VII refer to these latest results. Table VI contains the experimental fluorescence parameters ( $\phi$  values for the rotamer mixture, lifetimes, ratios of the preexponential factors measured at  $\lambda_{em}'' = 372$  nm, and  $F$  intensities of the mixture measured at different  $\lambda_{exc}$  with the same number of absorbed quanta) and the derived fractions of excited A molecules,  $f_A(\lambda_{exc})$ . These data allowed the fluorescence quantum yields and the relative absorption

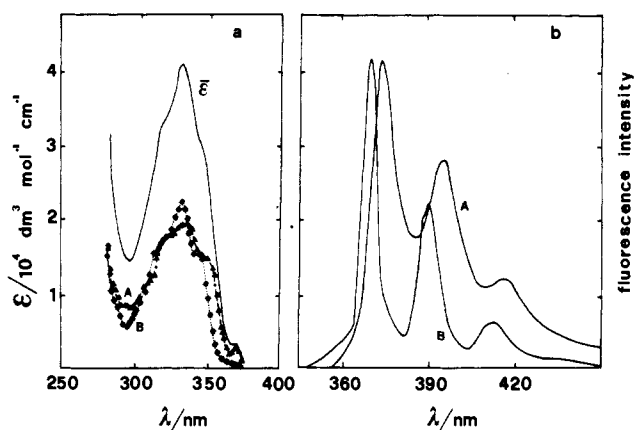


**Figure 22.** Absorption spectra of 3-StPh in *n*-hexane at 293 K: (a) spectrum of the rotamer mixture,  $\epsilon(\lambda_{exc})$ , and relative spectra,  $\epsilon_i(\lambda_{exc})c_i/c$ , of the two rotamers, as derived from the KFA analysis, and (b) fluorescence emission spectra of the two rotamers as derived from the PCA-SM analysis [unpublished results related to refs 38 and 39].

spectra of the two components (Figure 22a) to be calculated. The short-lived 3-StPh (A) species displays a slightly red-shifted absorption spectrum as also shown by the high fraction of excited A species ( $f_A = 0.83$ ) found when excited at the longest wavelength (see Table VI). From these spectra, one could estimate the relative abundance of the two conformers and the enthalpy difference between them. All of the parameters are shown in Table VII. In comparison to 2-StN, there is a larger difference in  $\phi$  and a smaller difference in



$\tau$ . Both of these factors lead to very different radiative rate constants, which is probably due to the differences in the nature of the fluorescent states. The data also indicate that the longer lived B rotamer is the more stable species (even if the relative abundances are not much different) and has the lower  $k_F$  value. The similar abundance of the two species is reflected in the very small  $\Delta H$  value (190 cal mol<sup>-1</sup>).

The statistical PCA-SM method was also applied to 3-StPh.<sup>39</sup> A 47 × 150 data matrix was used. Two significant eigenvectors were found which expressed 84.7% and 7.5% of the total variance of the measured spectra. The high value of unaccounted variance (7.8%) was attributed to the high noise caused by the narrow slits and filtered light needed to prevent *trans* → *cis* photoisomerization. The pairs of coefficients fell, as expected, into a line of the  $\alpha, \beta$  plane, thus defining the coefficients of the pure components. Figure 22b shows the emission spectra of the rotamers as obtained from a reduced form of eq 19 for two-component systems. The fractional contributions of each component was then obtained as a function of  $\lambda_{exc}$ . Their trend reproduces the shape of the excitation spectrum of each rotamer. Since  $\phi_A$  could be directly measured by selective excitation of the A rotamer which absorbs at longer wavelengths, the fraction of excited A molecules, the relative absorption spectra and the  $\phi_B$  value were then obtained through eqs 26, 3, and 4. The results of the statistical analysis (values in parentheses in Table VII) were in excellent agreement with those of the kinetic method.

The CS-INDO ground-state torsional potential curve (Figure 21) and the CS-INDO SCI  $S_0 \rightarrow S_1$  transition properties of 3-StPh<sup>72</sup> are in good agreement with the photophysical and thermodynamic parameters of Table VII. First of all, the calculated energy difference between the  $\phi = 180^\circ$  and  $0^\circ$  conformers ( $\sim 180$  cal mol<sup>-1</sup>) is almost coincident with the enthalpy difference derived by both the KFA and PCA-SM procedures (190–200 cal mol<sup>-1</sup>). According to this result the more abundant B component (58%), characterized by a longer fluorescence lifetime (18.3 ns) and a slightly blue-shifted spectrum, should be identified as the more stable ( $\phi = 0^\circ$ ) rotamer. This is qualitatively confirmed by the calculated values of  $\lambda$  and  $f$  for the  $S_0 \rightarrow S_1$  transition of the two rotamers ( $\phi = 0^\circ$ :  $\lambda = 329$  nm,  $f = 0.01$ .  $\phi = 180^\circ$ :  $\lambda = 330$  nm,  $f = 0.31$ ). It is to be noted that such an assignment was not possible in ref 72 where similar  $k_F$  values had been derived from the fluorescence analysis for the two rotamers, because a first incorrect set of  $\phi$  values was used.

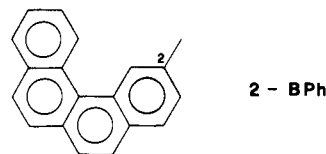
In conclusion, the photophysical and theoretical studies<sup>72,39</sup> on the whole indicate that the behavior of 3-StPh resembles that of 2-StN. This is in agreement with the initial considerations of this section (Figure 20). However, some small, yet significant, differences do exist. For instance, the enthalpy difference between the rotamers is sensibly lower in 3-StPh than in 2-StN ( $\sim 200$  instead of  $\sim 700$  cal mol<sup>-1</sup>). The theoretical explanation of this resides in the very close  $C_2-C_3$  and  $C_3-C_4$  phenanthrenic bond lengths (1.398 and 1.383 Å, respectively)<sup>96</sup> of 3-StPh, in contrast to the markedly different  $C_1-C_2$  and  $C_2-C_3$  naphthalenic bond lengths (1.37 and 1.41 Å)<sup>88</sup> of 2-StN. Unlike 2-StN, with this structural feature the two planar rotamers of 3-StPh

experience almost the same nearest nonbonded interactions, thus being quasi-degenerate. Similar considerations can be made for 2-StPh [ $R(C_1-C_2) = 1.381$  Å in phenanthrene],<sup>96</sup> where an even smaller energy difference ( $\sim 50$  cal mol<sup>-1</sup>) was theoretically predicted.<sup>72</sup> Another difference is that the radiative rate constant of the shorter lived component (A) is a little larger for 2-StN than for 3-StPh ( $\sim 16 \times 10^7$  and  $\sim 12 \times 10^7$  s<sup>-1</sup>, respectively, in *n*-hexane) (Tables III and VII). This feature is reflected in the calculated oscillator strengths for the  $S_0 \rightarrow S_1$  and  $S_0 \rightarrow S_2$  transitions of the less stable rotamer ( $\phi = 180^\circ$ ) which amount to 0.47 and 0.57, respectively, in 2-StN (Table IV)<sup>31</sup> and 0.31, 0.93 in 3-StPh.<sup>72</sup> Such  $f$  values indicate that the mixing between "localized" ( $^1L_b$ ) and "delocalized" (HOMO, LUMO) configurations, which is responsible for the shorter lifetime of the rotamer A, is less marked in 3-StPh than in 2-StN, this being traceable to the larger  $^1L_a-^1L_b$  energy gap in the unsubstituted parent chromophore (Figure 20).

An investigation on the rotamerism of the *cis* isomer of 3-StPh was also made, on the basis of the NMR spectrum and photocyclization product.<sup>97</sup> The results indicated a preference of the *s-trans* conformation in the rotamer mixture compared to the *s-cis*, contrary to some benzo analogues (see the following section).

### 3. Benzophenanthryl Derivatives

Compounds bearing the 2-benzo[*c*]phenanthryl (BPh) group, studied by Fischer,<sup>27</sup> showed some anal-



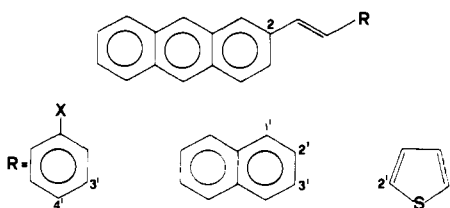
ogies with the phenanthryl derivatives but clear analysis of the component spectra was impossible. Generally, little variation in the emission spectrum with  $\lambda_{exc}$  was observed even when exciting up to the long wavelength edge of the absorption spectrum. The emission spectrum seemed to indicate an equilibrium containing predominantly the hypsochromic species. Only at low temperatures did more evident variations gradually develop but these could also be due to some sort of aggregation, as mentioned above. For 2-StBPh, the spectrum changed with  $\lambda_{exc}$  at reduced temperatures but clear assignment of peaks to distinct modifications was not possible. 2,2'-NBPhE showed slight dependence on  $\lambda_{exc}$ , except at the long wavelength edge of the absorption spectrum where the emission changed in favor of the long wavelength modification which was shifted by about 15 nm (the largest shift encountered hitherto). For the 3,2'-PhBPhE, the  $\lambda_{exc}$  effect was discernible even at room temperature; the spectra of the two observed components were only shifted by 2–3 nm. The behavior of 2,2'-DBPhE resembles that of 2,2'-NBPhE. Fischer<sup>27</sup> tentatively imputed this general insensitivity of the spectra to  $\lambda_{exc}$  in 2-BPh derivatives to the slight steric interference operative in one of two (or more) envisaged conformers. This might prevent its coplanarity, thus substantially shifting the equilibrium in favor of the other more stable conformer. Although this hypothesis cannot be ruled out a priori, another possible explanation is that, as a consequence

of a markedly benzophenanthrylic (implying a moderate barrier to rotamer interconversion) and quasiforbidden (implying rather a long lifetime)  $^1L_b$  character of the  $S_1$  state, thermal equilibration of the excited rotamers might take place contrary to the NEER assumption. The latter interpretation seems to be consistent with the appearance of a certain variation of the emission spectra with  $\lambda_{exc}$  at lower temperatures, where the interconversion process is sensibly slowed.<sup>27</sup>

An investigation<sup>97</sup> of the cis isomer of 2-StBPh and some benzo analogues of 3-StPh showed that in the series StPh, StBPh, dibenzo[*c,g*]triphenylene, and styrylhexahelicene, only 2-StBPh exists mainly as an *s*-cis (cis-syn) conformation notwithstanding its larger crowding in comparison with the *s*-trans (cis-anti) rotamer. This phenomenon, which is the basis of the formation of hexahelicene (which is enriched in one of its enantiomeric forms when 2-StBPh is irradiated in chiral solvents) was ascribed to van der Waals interaction between the aryl groups. The introduction of an additional benzo group at the ring of 2-StBPh and 3-StPh bearing the styryl substituent, which leads to styrylchrysene and styrylbenzo[*c*]chrysene, was found to shift the conformational equilibrium toward the more crowded *s*-cis rotamer, probably because of a smaller repulsion compared to the *s*-trans rotamer. The authors concluded that the occurrence of a helical overcrowded conformation in cis isomers of styryl-substituted aromatics depends on the presence of a favorable balance between attractive and repulsive forces in the overcrowded region. A favorable situation seems to be present in cis 2-StBPh whose preferred rotamer is spatially related to hexahelicene.<sup>97</sup>

#### 4. Anthryl Derivatives

The existence of distinct rotamers in DAEs containing the anthryl group was essentially demonstrated by emission spectroscopy studies. In all cases, the experimental observations were analyzed within the NEER assumption by analogy with the compounds described so far. For a number of 2-anthryl derivatives, the Fischers<sup>91</sup> first observed a variation in the emission spectra with  $\lambda_{exc}$  which was most pronounced when exciting in the tail of the absorption bands. In all cases the emission spectra could be described by a superposition of two sets of peaks, shifted 8–15 nm one from the other. Oxygen preferably quenched the short wavelength absorbing species, indicating that it has a longer fluorescence lifetime, as in StNs and StPhs. Several derivatives of 2-StA (para substituted at the phenyl ring with methyl, isopropyl, and methoxy groups) and their analogues (phenyl group replaced by naphthyl, thienyl) behaved like the parent hydrocarbon.



For the *p*-isopropyl-2-StA, the emission decay was found to be biexponential ( $\tau_A = 5.6$  ns,  $\tau_B = 17$  ns) and the contribution of the longer lived modification was estimated to be 80%.

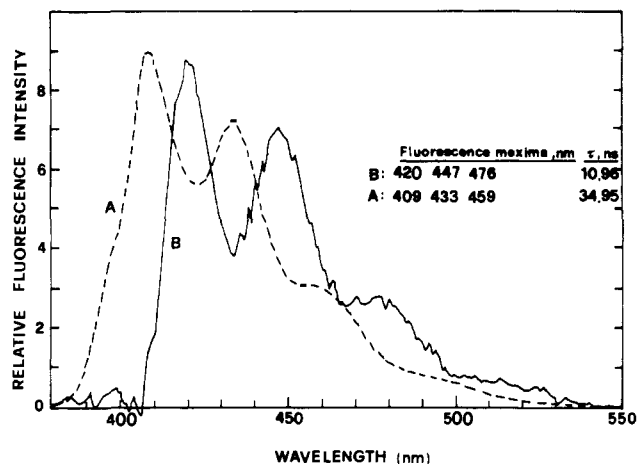


**Figure 23.** Fluorescence spectra for the rotamers of 2-StA in toluene ( $\lambda_{exc} = 370$  nm) as obtained by the "phase resolution spectroscopy" method of SLM (reprinted from ref 98; copyright 1984 American Chemical Society).

A subsequent paper by Wisniewski-Knittel, Das, and Fischer<sup>98</sup> on fluorescence lifetime and quenching in 2-StA and its 2'-naphthyl (2,2'-ANE) and 2'-thienyl (2,2'-ATE) analogues gave further insight into the subject. The good fit of the biexponential decay suggested that two fluorescing species were the predominant contributors in all these compounds, although four structurally distinct rotamers are possible for the naphthyl and thienyl derivatives. The authors suggested that some of these species are either very similar in terms of photophysical properties or have contributions too small to be revealed under low-resolution conditions. The KFA method, applied to derive the fractional absorbances,  $f_i$ 's, confirmed that the longer wavelength absorbing species was the short-lived rotamer A.<sup>98</sup> The authors succeeded in obtaining a good separation of the A and B spectra by applying the "phase resolution of spectra" technique<sup>29</sup> (Figure 23). Selective quenching by oxygen, ethyl iodide (EtI), and *N,N*'-dimethylaniline (DMA) was studied in various solvents. On the basis of the assumption that the quenching data obtained by using short  $\lambda_{exc}$  and  $\lambda_{em}$  values were related essentially with the longer lived B species, the bimolecular rate constants for quenching in benzene were found to be in the range  $(0.18\text{--}2.0) \times 10^8$   $M^{-1} s^{-1}$  with EtI,  $\approx 2 \times 10^{10}$   $M^{-1} s^{-1}$  with oxygen and  $(1.7\text{--}5.1) \times 10^9$   $M^{-1} s^{-1}$  with DMA. With the latter quencher, the rate parameter increased markedly in acetonitrile, as expected from the CT nature of the interactions. On the other hand, in nonpolar solvents the quenching by the charge donor DMA was accompanied by the formation of fluorescent exciplexes, whose spectra in turn showed  $\lambda_{exc}$  dependences similar to those of the acceptor partners. The quenching of the  $S_1$  state of 2-StA and its derivatives resulted in enhanced formation of triplets in nonpolar solvents and of radical ions in acetonitrile.<sup>98</sup>

The parent compound, 2-StA, was also investigated by Ghiggino et al.<sup>99</sup> On the basis of the relative wavelength shift of the two species, it was possible to monitor the extreme blue edge of the emission and isolate only the fluorescence of the longer lived species, while observations at other wavelengths should contain contributions from both species. By time-resolved spectroscopy, the emission spectrum of the two distinct

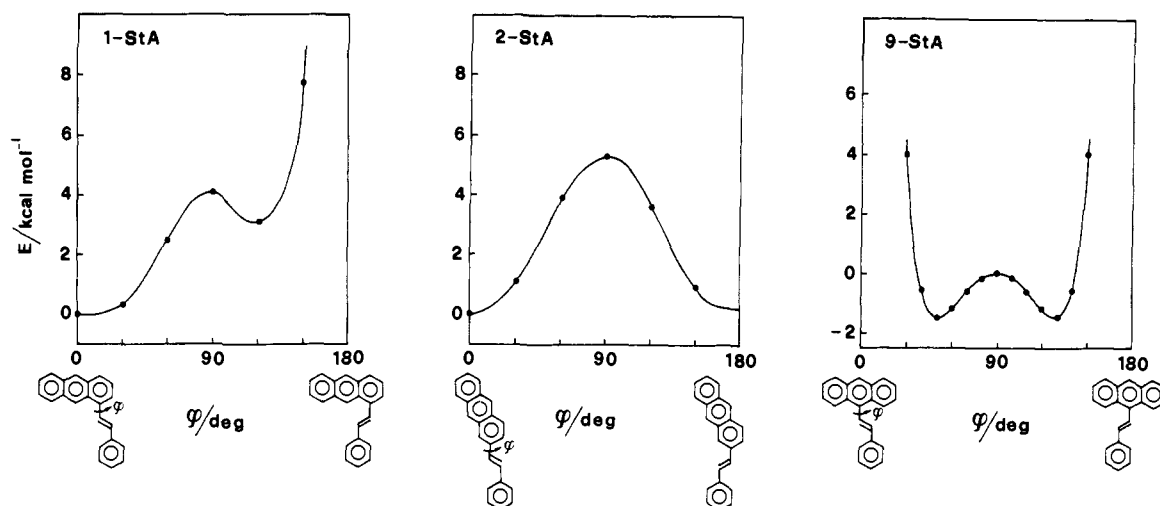


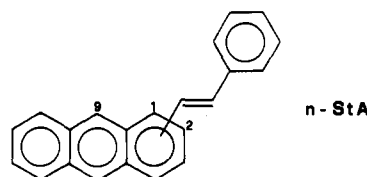
**Figure 24.** Ground-state potential energy curves for internal rotation of *n*-StAs around the anthryl-ethylene "single bond", as obtained by the CS-INDO method.<sup>73</sup> The experimental geometry of anthracene<sup>106</sup> was adopted for the anthryl group and the following values were given the bond angles at the ethylenic carbon atoms by analogy with *n*-StNs and *n*-StPhs: C=C—C (phenyl) = 128°, C=C—C (anthryl) = 128° in 2-StA and 126° in 1-StA and 9-StA (adapted from ref 73).

species was detected. The results obtained were in substantial agreement with both the earlier steady-state work of the Fischers<sup>91</sup> and the kinetic measurements of Wismontski-Knittel et al.<sup>98</sup> Both kinetic and PCA methods were used by Ghiggino et al.<sup>99</sup> to separate the spectral properties of the two rotamers. The difference in fluorescence decay times of the two species was attributed to a difference in their nonradiative decay rates, a conclusion subsequently revised on the basis of further experimental observations.<sup>73</sup> From the temperature effect on the spectra, which showed an enrichment in the B rotamer in cool media,  $\Delta H$  and the equilibrium constant for the rotamers were estimated.<sup>99</sup> The energy difference of 1.08  $\text{kcal mol}^{-1}$  was really too high to explain the existence of the two rotamers in comparable amounts and was revised by additional experimental and theoretical investigations (see below).

It is important to note that, from their detailed analysis of the fluorescence decay characteristics, Ghiggino et al.<sup>99</sup> concluded that, in accordance with the NEER hypothesis, no appreciable excited-state equilibration of the rotamers occurs in 2-StA under ordinary conditions. This behavior appears to be in contrast with that manifested by the parent compound 2-vinylanthracene (2-VA) and related alkenylantracenes in recent picosecond fluorescence studies by Barbara et al.<sup>100-102</sup> In fact, these authors observed fast rise/decay processes, following laser excitation, which were clear evidence that a thermally activated interconversion occurs between the *t* and *c* forms in the excited state. From a full kinetic description, including  $t \leftrightarrow c$  isomerization in  $S_1$ , and reasonable approximations for the torsional potential function, the activation energies of the forward (indicated as A  $\rightarrow$  B) and reverse (B  $\rightarrow$  A) excited-state conversions were estimated to be 5.3 and 6.9  $\text{kcal mol}^{-1}$ , respectively, for 2-VA.<sup>100</sup> More recently, Arai et al.<sup>103</sup> reported slightly different activation energies for the two excited-state conversions: 3.9 and >6  $\text{kcal mol}^{-1}$  for the  $t \rightarrow c$  and  $c \rightarrow t$  isomerizations, respectively, which suggests that the first process is the only operative one. Anyway, both sets of values are comparable with those expected for the  $t \leftrightarrow c$  isomerization of an arylethylene compound in the ground state (Figures 3 and 8) and hence they indicate—in keeping

with the shape of the absorption spectrum<sup>100</sup>—that the  $S_0 \rightarrow S_1$  transition of 2-VA is markedly localized on the anthracene moiety. Of course, the situation cannot be drastically different in 2-StA. However, as a consequence of the replacement of the vinyl group (of 2-VA) with a styryl group (in 2-StA), the excited-state torsional barriers should increase enough to freeze (at room temperature) both the forward and reverse conversion during the  $S_1$  lifetime, as was experimentally found.<sup>99</sup> In accordance with these considerations, recent CS-INDO SCI calculations<sup>70</sup> predicted the barriers hindering  $t \rightarrow c$  and  $c \rightarrow t$  isomerizations of 2-StA in  $S_1$  to be 7.2 and 8.2  $\text{kcal mol}^{-1}$ , respectively (the latter value had not been reported in ref 70). As will be shown, the behavior of the  $T_1$  state of 2-anthryl derivatives may be quite different, essentially because of their very long lifetimes.

Three papers by Bartocci, Mazzucato, et al.<sup>67,73,104</sup> on the behavior of the three isomeric *trans* *n*-StAs ( $n = 1,2,9$ ) were recently published. Contrary to the case



of other DAEs, fluorescence and ISC were found to be the predominant deactivation pathways of the  $S_1$  state (as first pointed out by Karatsu et al. for 2-anthryl-ethylenes<sup>105a</sup>) with a minor contribution of internal conversion, at least for 9-StA. As already reported for isomers 2 and 9,<sup>105</sup> the  $\phi_{t \rightarrow c}$  was practically undetectable for all StAs because of high barriers to isomerization in both the  $S_1$  and  $T_1$  states.<sup>67</sup> A direct  $^3\text{trans} \rightarrow ^1\text{trans}$  (ground) ISC seems to be the pathway for  $T_1$  deactivation. As a consequence, much longer triplet lifetimes were found for these StAs compared with stilbene and other stilbene-like molecules.

The rotameric behavior of the three isomeric *n*-StAs is well described by the  $S_0$  torsional potential-energy curves set up by the CS-INDO method (Figure 24).<sup>73</sup> As expected by symmetry, two equivalent minima, markedly nonplanar because of steric strain (52° and 128°), were found for 9-StA. For 1-StA, on the other

TABLE VIII. Kinetic Parameters and Fluorescence Quantum Yields of *trans-n*-StA in MCH (in toluene for 2-StA) at 293 K (from refs 67 and 73)

parameter	1-StA	2-StA(A)	2-StA(B)	9-StA
$\phi$	0.64	1.0	0.80	0.44
$\tau$ , ns	5.0	8.7	27.0	3.6
$k_F$ , $10^8$ s <sup>-1</sup>	1.3	1.15	0.3	1.2

hand, CS-INDO calculations predicted an absolute—rather flat—minimum at  $\phi = 0^\circ$  (t conformation) and a secondary minimum at  $\phi = 115^\circ$ – $120^\circ$ , with an energy difference of 3.1 kcal mol<sup>-1</sup> (corresponding to a negligible rotamer abundance of ca. 0.6% at room temperature). The potential energy curve for 2-StA indicated, in qualitative agreement with the experimental observations, two quasiisoenergetic ( $\Delta E = 0.2$  kcal mol<sup>-1</sup>) and coplanar rotamers, separated by a barrier of about 5 kcal mol<sup>-1</sup>, the more stable form being the more elongated one (t conformation). By comparison of these results with those of Figure 17, it would appear that the energy difference and the barrier between the rotamers of 2-StA are slightly smaller and larger, respectively, than in the naphthyl analogue. Actually, considering the structural similarities, such small differences are better attributed to incomplete equivalence of the theoretical approaches (C-INDO for 2-StN<sup>71</sup> and CS-INDO for 2-StA<sup>73</sup>) rather than to intrinsic characteristics of the two systems.

The KFA method was applied to the biexponential decay function of 2-StA, even though the scarce dependence of  $\bar{\phi}$  on  $\lambda_{exc}$  and of the  $\alpha$  parameter on temperature limited the extension of its application.<sup>73</sup> By an accurate choice of experimental conditions, the almost pure emission spectra and  $\phi$  values of the two rotamers were obtained. Thus,  $\phi_A$  was measured with  $\lambda_{exc} > 415$  nm, namely at the threshold of the absorption spectrum where the almost pure emission spectrum of A was observed. On the other hand,  $\phi_B$  was measured using  $\lambda_{exc} = 355$  nm at  $\sim 170$  K ( $\tau_B$  being practically independent of temperature) where the almost pure spectrum of B was observed. The results obtained are collected in Table VIII where the data for the 1 and 9 isomers are also included for comparison.

From these data, one can see that (a) the two rotamers are characterized by fairly different fluorescence lifetimes in agreement with the values previously reported by other authors; (b) both  $\phi$  values are very high implying that the  $S_1$  state decay is mainly radiative, this result being in contrast with the much lower value (0.24) reported by other laboratories<sup>99</sup> for  $\phi_A$  (the formation of some sort of aggregate, due to the use of too high concentrations, might be the origin of this result); (c) as a consequence of point b, the resulting  $k_F$  values are

rather different, with a much higher value for the short-lived A rotamer, as found in the case of 2-StN and 3-StPh. Moreover, the temperature effect on the spectra suggested a revision<sup>67,73</sup> also of the  $\Delta H$  between the conformers, which came out to be much smaller than that previously published,<sup>99</sup> closer to the value obtained by both CS-INDO<sup>73</sup> and QCFF/PI<sup>67</sup> theoretical calculations (0.2 and 0.3 kcal mol<sup>-1</sup>, respectively).

An identification of the B (short- $\lambda$  absorbing) and A (long- $\lambda$  absorbing) components as the t or c rotamers was attempted in ref 67 on the basis of CNDO/S SCI calculations of the  $S_0 \rightarrow S_n$  transitions (Table IX). The main point in Table IX is the inversion in the ordering of the first two excited singlet states on passing from one rotamer to the other: the  $S_0 \rightarrow S_1$  transition being intense ( $f = 0.46$ ), essentially HOMO  $\rightarrow$  LUMO in character, in the c ( $\phi = 180^\circ$ ) form and weak ( $f = 0.02$ ), with partial <sup>1</sup>L<sub>b</sub> anthracenic character, in the t ( $\phi = 0^\circ$ ) form. As a consequence, the less elongated rotamer (c), absorbing at slightly longer wavelengths, should have a radiative rate constant larger than that of the t rotamer, and hence should be identified as the A component in accordance with Table VIII. This assignment, however, should be accepted with a certain caution, considering that parallel QCFF/PI calculations<sup>67</sup> predicted the more intense, essentially HOMO  $\rightarrow$  LUMO, transition to be the first one in both t and c rotamers (Table IX), thus suggesting comparable radiative rate constants for the two components. Further theoretical effort appears to be necessary in order to eliminate this ambiguity in the identification of the observed conformers.

The fact that the photophysical behavior of 2-StA is a complex one was recently indicated by the observation of a third component (C) in the emission spectrum, revealed by a shoulder at 355 nm.<sup>73,104</sup> This partially hidden transition was only observable in particular experimental conditions ( $T > 200$  K,  $\lambda_{exc} < 410$  nm) and showed lifetime and excitation spectrum coincident with those of the longer lived B rotamer thus pointing out to a common origin. This transition was assigned to an emission from an upper excited state  $S_2$  thermally populated by the lower  $S_1$  state of B. The equilibrium between the two states became observable above 200 K. The energy gap between the two states was estimated from the ratio of the fluorescence quantum yields of  $S_2$  and  $S_1$  as a function of temperature, using the relationship

$$\frac{\phi_2}{\phi_1} \simeq \frac{I_{F2}}{I_{F1}} = \frac{k_{F2}}{k_{F1}} \tau_2 A e^{-\Delta E(S_2-S_1)/RT} \quad (31)$$

where 1 and 2 refer to the  $S_1$  and  $S_2$  states, respectively. The corresponding logarithmic plot is shown in Figure

TABLE IX. Energies, Oscillator Strengths, and Composition of the Two Lowest Lying Excited Singlet States of the Two Rotamers of *trans*-2-StA, as Obtained by CNDO/S Calculations (from ref 67) (Energies and Oscillator Strengths in Parentheses Were Computed<sup>67</sup> by the QCFF/PI Program of Warshel<sup>60b</sup>)

state	$E$ , eV	$f$	composition <sup>a</sup>
2-StA, $\phi = 0^\circ$ (s-trans)			
$S_1$	3.46 (3.63)	0.02 (0.10)	-0.62 (11 $\rightarrow$ 13) - 0.43 (11 $\rightarrow$ 14) + 0.18 (10 $\rightarrow$ 14)
$S_2$	3.50 (3.28)	0.54 (0.54)	-0.96 (11 $\rightarrow$ 12)
2-StA, $\phi = 180^\circ$ (s-cis)			
$S_1$	3.44 (3.51)	0.46 (0.32)	-0.96 (11 $\rightarrow$ 12)
$S_2$	3.46 (3.76)	0.02 (0.06)	-0.60 (11 $\rightarrow$ 13) + 0.44 (11 $\rightarrow$ 14) - 0.34 (9 $\rightarrow$ 12) + 0.18 (10 $\rightarrow$ 14)

<sup>a</sup> The numbering of the orbitals refers to the  $\pi$  MO subset.

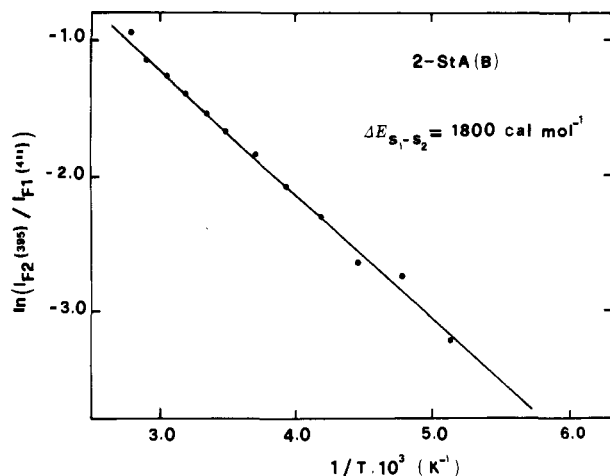


**Figure 25.** Plot of  $\ln [I_{F2} (395) / I_{F1} (411)]$  against  $1/T$  for *trans*-2-StA(B) in toluene. The full line is a computer least-squares fit to eq 31 (reprinted from ref 104; copyright 1990 Pergamon).

25; it led to  $\Delta E(S_2-S_1) = 1800 \text{ cal mol}^{-1}$ , a value very similar to those obtained by the same authors by analogous plots<sup>104</sup> (yet double that predicted by the CNDO/S SCI calculation of ref 67, see Table IX). The analysis of this "anomalous" emission, led to the extrapolation of the relative spectrum of the  $S_2 \rightarrow S_0$  radiative process and the derivation of some kinetic parameters based on the Siebrand theory of radiationless transitions.<sup>107</sup> The values of 1.25 ps for the  $S_2$  lifetime,  $1.1 \times 10^8 \text{ s}^{-1}$  for  $k_{F2}$  and  $8 \times 10^{11} \text{ s}^{-1}$  for  $k_{12}$ , the rate constant for the  $S_2 \rightarrow S_1$  internal conversion, were found. The fluorescence intensity of  $S_2$  ( $I_{B2}$ ) thermally repopulated from  $S_1$ , favored by the high ratio  $\tau_{B1}/\tau_{B2}$  and the small  $\Delta E(S_2-S_1)$ , is then due to the high values of  $k_{F2}(B)$  and  $\tau_{B1}$  (relative to  $k_{F1}(B)$  and  $\tau_{B2}$ ). The  $\tau_{B1}$  value was long enough to maintain the equilibrium between the two singlet states over the high temperature range.

No such "anomalous" emission was observed for the A rotamer of 2-StA, probably because of an unfavorable  $k_{F2}/k_{F1}$  ratio which leads to a fluorescence intensity of  $S_2$  below the detectability limit.

To conclude, we will survey those works where the rotamerism of DAEs with the 2-anthryl group as one of the substituents was studied by analyzing its effect on the spectral and kinetic behaviors of the triplet state ( $T_1$ ).<sup>55,58,70</sup> A rather extensive laser flash photolysis study was first carried out by Wisnionski-Knittel and Das<sup>55</sup> on three 2-anthryl derivatives, i.e. 2-StA, 2,2'-ANE, and 2,2'-ATE. In the visible region 400–700 nm, the triplet-triplet (T-T) absorption spectra of the three compounds were found to be characterized by two well-defined band systems, with maxima located at 450–465 and 620–640 nm (a finding soon afterward confirmed by Karatsu et al.,<sup>105a</sup> for 2-StA and 2,2'-ANE) and no appreciable variations were observed when exciting with laser pulses at 400 nm (i.e. at the long-wavelength edge of the ground-state absorption) rather than at 337.1 nm. The triplet lifetimes were found to be in the range 15–120  $\mu\text{s}$  (e.g., in benzene solution:  $\sim 115$ ,  $\sim 85$  and  $\sim 20 \mu\text{s}$  for 2-StA, 2,2'-ANE, and 2,2'-ATE, respectively), with no significant differences when the monitoring wavelength was changed from the short- $\lambda$  (450–465 nm) to the long- $\lambda$  (620–640 nm) maximum. Also, both the kinetics of the triplet for-

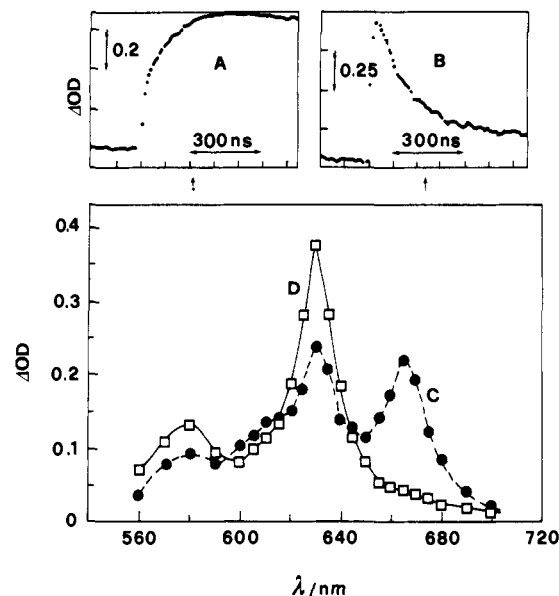


**Figure 26.** Experimental traces for the processes of transient formation at 630 nm (A) and of decay at 665 nm (B) and transient absorption spectra at 80 (C) and 600 ns (D) following the 337.1-nm laser flash, in a benzene solution of 2,2'-ATE ( $2 \times 10^{-5} \text{ M}$ ) and di-*tert*-butyl nitroxide (12 mM) (reprinted from ref 55; copyright 1984 American Chemical Society).

mation via exciplexes with DMA and that of the triplet decay in the presence of different quenchers, were found to be independent of the triplet monitoring wavelength. Finally, the authors noticed no difference between the T-T spectra measured in the presence of very different concentrations of DMA in an attempt to obtain different fractions of the rotameric triplets. These facts led Wisnionski-Knittel and Das to conclude that both T-T band systems belong to the same predominant rotamer and that, since the triplets are primarily anthracene-like, the other rotamer, probably formed in smaller concentration, behaves very similarly to the main one. We must note, however, that the above described behaviors, observed  $\sim 1 \mu\text{s}$  after the laser flash, may indicate that the triplet rotamers undergo thermal equilibration on a shorter time scale after their formation, which is contrary to the NEER hypothesis. That this really occurs, at least for 2,2'-ATE, was shown by the evolution of the T-T spectrum on the nanosecond time scale. In fact, a growth in the transient absorption at 625–640 nm and a concomitant decay at 660–680 nm was observed over  $\sim 500 \text{ ns}$ . This phenomenon is emphasized in Figure 26 which shows the results obtained enhancing the triplet formation by addition of di-*tert*-butyl nitroxide.<sup>55</sup> The authors themselves tentatively attributed the observed formation/decay process to interconversion of the triplet rotamers subsequent to their formation.

More recently, Krongauz et al.<sup>58</sup> readdressed this problem by extensive conventional (microsecond) flash-photolysis measurements on 2-StA and related compounds (including 2,2'-ATE and 2,1'-ANE) over a wide range of temperatures (between room temperature and  $-170 \text{ }^\circ\text{C}$ ). Interestingly, they found that all the compounds studied exhibited marked variations in the T-T absorption spectra with temperature. In particular, cooling was found to cause the disappearance of the peak at 625–640 nm and the appearance of a new peak at 660–680 nm, the main temperature effect taking

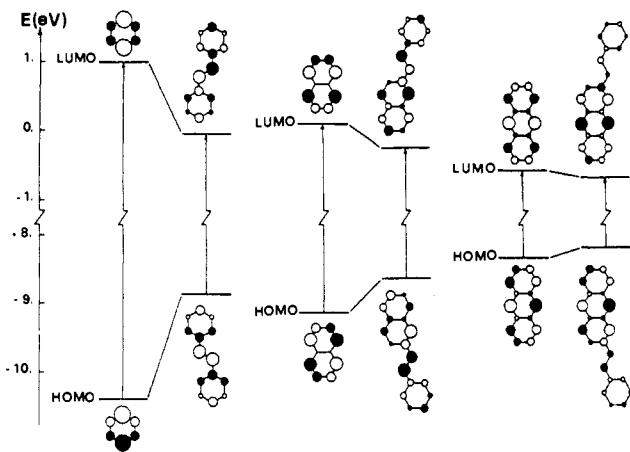


**Figure 27.** Correlation diagram of HOMOs and LUMOs of planar stilbene, 2-StN, and 2-StA with those of their parent aromatic hydrocarbons (benzene, naphthalene, and anthracene), as obtained by CS-INDO SCF calculations. The bond lengths and angles were given the same values as in the previously cited C-INDO and CS-INDO calculations (see captions of Figures 8 and 24 and section III.A.1.a). Areas of the circles are proportional to squares of the MO coefficients (reprinted from ref 70; copyright 1989 Elsevier Sequoia).

place from  $-60$  to  $-130$  °C. In this range of temperature various anomalies of the triplet decay behavior were observed, including dependence of the decay rate on the monitoring wavelength, growing-in, and fast initial decay of the absorbance for the 625–640-nm and the 660–680-nm peak, respectively. All these features, which appear to be consistent with the room temperature behavior observed by laser flash photolysis,<sup>55</sup> were interpreted in terms of a temperature-dependent equilibrium between the two rotameric triplets. No such anomalies were observed with 1-StA, where one rotamer predominates, and with 9-StA, where only one rotamer exists.

Further support to this interpretation has recently been given by a theoretical (CS-INDO CI) comparative study on the  $T_1$ -state properties of 2-StA, 2-StN, and stilbene.<sup>70</sup> Considering that the  $T_1$  state of DAEs is generally dominated by the [HOMO,LUMO] configuration, the characteristics of the HO and LU MOs were first analyzed. It was found (Figure 27) that in 2-StA the "frontier" MOs are markedly localized on the anthryl group and retain essentially the same form and energy as those of anthracene. On the contrary, the HO and LU MOs of stilbene and (to a lesser extent) 2-StN are markedly delocalized and deviate substantially from those of the parent aromatic hydrocarbon. According to these arguments, the  $T_1$  state of 2-StA is expected to be primarily anthracene-like and, as a consequence, the energy barriers hindering  $t \leftrightarrow c$  isomerization in  $T_1$  should not be very different from those of  $S_0$ . Of course, the opposite is expected to occur in stilbene and 2-StN in view of the "olefinic-like" character of their triplet states. In agreement with these predictions, the calculated potential energy curves describing the rotamer interconversion in the  $T_1$  state (Figure 28a) were found to exhibit barriers of 11–13 kcal mol<sup>-1</sup> in stilbene and 2-StN, and about 6 kcal mol<sup>-1</sup> in 2-StA, the ground-state barrier being about 5 kcal mol<sup>-1</sup> in all cases. With such barriers, the rate constants for interconversion of triplet rotamers are expected to be  $10^3$ – $10^4$  s<sup>-1</sup> in 2-StN and  $10^7$ – $10^8$  s<sup>-1</sup> in 2-StA (at room temperature), with associated lifetimes of 1–0.1 ms and 100–10 ns, respectively.

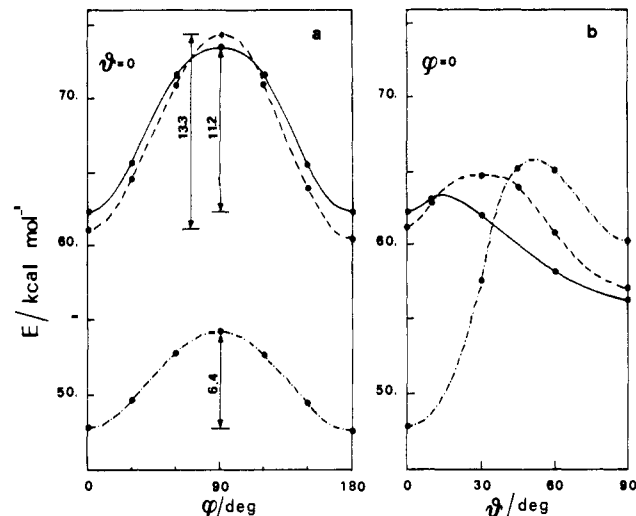
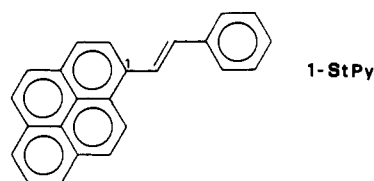


**Figure 28.** CS-INDO SCI potential energy curves for the  $T_1$  states of stilbene (—), 2-StN (---), and 2-StA (— · — · —): (a) rotation around the aryl-ethylene "single" bond. (b) torsion (trans  $\rightarrow$  perp) around the ethylenic double bond. Energies are given relative to the planar ( $\phi = 0^\circ$ ) ground states (reprinted from ref 70; copyright 1989 Elsevier Sequoia).

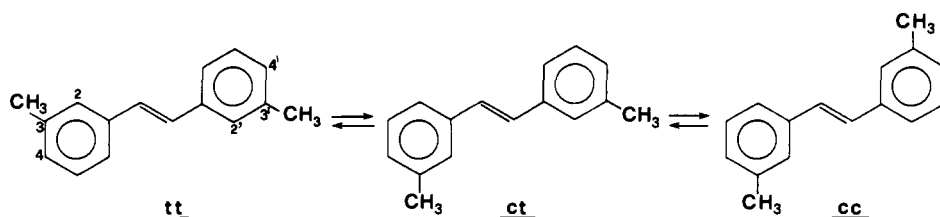
As the observed triplet lifetimes (in low viscosity solutions) amount to some 100 ns in 2-StN<sup>85</sup> ( $\sim 60$  ns in stilbene)<sup>108</sup> and  $\sim 0.1$  ms in 2-StA,<sup>55,58,105a</sup> it was concluded that the NEER hypothesis can be maintained in the  $T_1$  state of 2-StN but, most likely, it breaks down in the  $T_1$  state of 2-StA, in accordance with the working hypothesis of refs 55 and 58. In the  $S_1$  state of 2-StA, on the other hand, a slightly higher barrier and the short lifetime are combined so that the validity of the NEER assumption is maintained (see above). The comparatively very long triplet lifetime of 2-StA and other 2-anthryl ethylenes, which is an important concurrent factor in relation to the rotamer equilibration, was explained in ref 70 in terms of the potential energy curves describing the torsion (trans  $\rightarrow$  perp) about the ethylenic double bond (Figure 28b). It was found that in the  $T_1$  state of stilbene and 2-StN the activation energy for the trans  $\rightarrow$  perp torsion is much lower than that for the rotamer interconversion (1–4 against 11–13 kcal mol<sup>-1</sup>). Thus, after their formation, the distinct triplet rotamers of 2-StN will undergo independent fast relaxation toward the perp absolute minimum and subsequent  ${}^3\text{perp} \rightarrow {}^1\text{perp} \rightarrow \alpha^1\text{trans} + (1 - \alpha)^1\text{cis}$  decay. On the contrary, in the  $T_1$  state of 2-StA the barrier for the trans  $\rightarrow$  perp torsion was found to be rather high (17–18 kcal mol<sup>-1</sup>) with respect to that hindering rotamer interconversion ( $\sim 6$  kcal mol<sup>-1</sup>). According to these findings, the 2-StA triplet is expected to decay predominantly via slow  ${}^3\text{trans} \rightarrow {}^1\text{trans}$  ISC, thus living long enough to allow rotamer equilibration (at least in fluid solutions).

### 5. Pyrenyl Derivatives

Only preliminary information is available for *trans*-1-StPy.<sup>109</sup> Its fluorescence decay is monoexponential



## SCHEME II

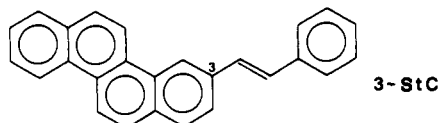


( $\tau = 4.5$  ns in MCH) as expected for this compound where the nonbonded interactions between the aryl and ethylene hydrogens resemble those typical of 1-StN (high  $\Delta H$  between the two rotamers).

In the case of a naphthyl derivative, 2,1'-NPyE, for which only two "naphthyl" conformers should be expected for the same steric reasons, the Fischers<sup>91</sup> actually observed, in addition to the two (slightly shifted) A and B spectra, a third emission spectrum at much longer wavelengths (first peaks at 419, 428 and 465 nm, respectively). The authors assigned the latter to a less favored C rotamer, which could differ considerably from A and B and also exhibit a larger Stokes shift, analogous to sterically hindered *trans*-stilbene derivatives.<sup>110</sup>

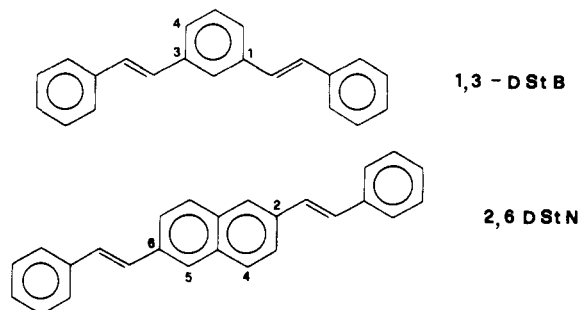
### 6. Chrysenyl Derivatives

Only preliminary results are available on DAEs bearing a chrysenyl group.<sup>109</sup> For 3-StC, two rotamers were clearly evidenced by the biexponential fluorescence decay ( $\tau_A = 7.3$  ns,  $\tau_B = 19.2$  ns in toluene at room temperature). However, the small spectral changes observed by changing  $\lambda_{exc}$  did not give any information on the composition of the mixture.



### 7. Distyrylnaphthalenes and -benzenes

As shown in the formula scheme, 2,6-distyrylnaphthalene (2,6-DStN) and analogous compounds should also exist in solution as an equilibrium mixture of three rotamers. This was indeed observed<sup>22,111</sup> as



illustrated in Figure 29, where the emission spectrum of 2,6-DStN is seen to vary with  $\lambda_{exc}$ , and suitable  $\lambda_{exc}$ 's could be found, yielding almost pure emission spectra of the three individual rotamers. Oxygen only slightly affected the shape of the emission spectrum, indicating similar decay rates for the excited rotamers. As expected by analogy with 1-StN, neither 1,4- nor 1,5-DStN exhibited any  $\lambda_{exc}$  dependence of their emission spectra.<sup>111</sup> Other related compounds, where the two phenyl

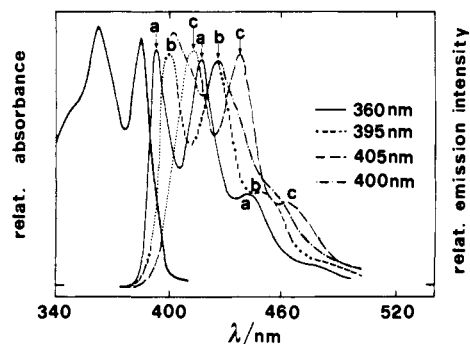


**Figure 29.** Emission (uncorrected) and absorption spectra of *trans*-2,6-DStN in toluene at 183 K. The three sets of emission peaks corresponding to the three rotamers are denoted by a, b, and c in the order of increasing wavelength. Dotted lines denote interpolated parts of the emission curves in the wavelength regions inaccessible because of scattered exciting light (adapted from ref 111).

groups were para substituted ( $\text{CH}_3\text{O}$ , isopropyl) or replaced by naphthyl or thienyl groups, were also studied and gave more or less similar results.<sup>111</sup>

Regarding distyrylbenzenes (DStBs), only the 1,3- and 1,4-substituted ones are expected to form isoenergetic rotamers, as in the above naphthyl analogues. In practice, a  $\lambda_{exc}$  dependence was observed<sup>112</sup> only with the 1,3-derivative.

### 8. Dimethylstilbenes

Of the symmetrically substituted *n,n'*-dimethylstilbenes (*n,n'*-DMSs), which were considered in connection with the problem of rotamerism, only 3,3'-DMS is expected to exist in solution as an equilibrium mixture of three almost isoenergetic rotamers (Scheme II). The other two symmetrical derivatives are not expected to display multicomponent behavior, because the 4,4'-DMS does not give rise to distinguishable conformers and the 2,2'-DMS for steric reasons which make the tc and cc components lie at very high relative energies.

The presence of the three rotamers of *trans*-3,3'-DMS was indirectly evidenced by the ENDOR studies of its radical anion at low temperature<sup>51</sup> (indicating the cc species as the most stable one) and by the different products obtained by dehydrophotocyclization of the corresponding cis isomer (see Introduction).<sup>14</sup> However, the observation of the rotamers by the usual fluorimetric technique met with serious difficulties. In fact, no dependence of the emission spectrum on  $\lambda_{exc}$  was observed at room temperature, slight shifts of the emission peaks being detectable only at low temperature (<150 K) when exciting in the long- $\lambda$  edge of the absorption spectrum.<sup>27,28</sup> This unexpected behavior was recently explained in a picosecond fluorescence investigation by Park and Waldeck.<sup>113</sup> These authors found that the decay profile was fitted by three exponentials at low

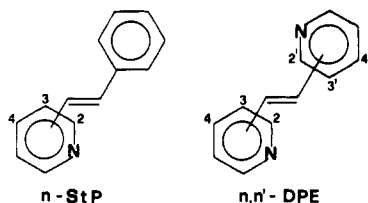
temperature, while only two exponentials appeared to be needed at higher temperatures (>273 K) and a quasi-limiting case was reached at 343 K with a 96% contribution of the fast-decaying component.<sup>113</sup> This behavior led to the conclusion that at the higher temperatures investigated the interconversion of the excited-state rotamers occurs on a shorter time scale than the nonradiative decay. These findings, taken on the whole, indicate that the NEER assumption does not hold for this system. In order to justify this behavior, the authors advanced the hypothesis (based on the observed torsional frequencies of stilbene from jet-cooled spectroscopy<sup>46,47</sup>) of very low energy barriers of 0.9 and 2.1 kcal mol<sup>-1</sup> in the ground and first singlet-excited states, respectively. However, all available theoretical data as well as other experimental observations point to considerably higher energy barriers for *t* ↔ *c* interconversion of arylethylenes (see also Figures 3, 7, and 8 and refs 100, 101, and 103). We can conclude that this puzzling problem deserves further theoretical and experimental investigation.

## B. Heteroatom-Containing Compounds

After the detailed survey on rotamerism of the hydrocarbon DAEs, which have been the object of extensive investigations with various techniques, we will now examine the rotameric behavior of their hetero analogues. Evidence for the occurrence of rotameric equilibria in these compounds, as obtained by fluorimetry, as well as by other experimental and theoretical techniques, generally parallels those described in section III.A. However, in this case, the data reported in the literature are not as exhaustive. Weaker experimental evidence was sometimes obtained while the scanty theoretical studies appear to be in a rather preliminary stage.

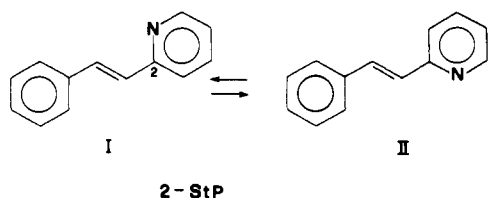
### 1. Azastilbenes

The most studied *trans*-DAEs of this class are the *n*-styrylpyridines (*n*-StPs) and the symmetrical *n,n'*-dipyridylethylenes (*n,n'*-DPEs).



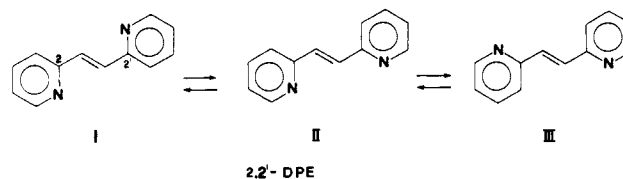
As mentioned in the Introduction, rotamerism of azastilbenes was hypothesized before the systematic experimental study by fluorimetric techniques was begun. Reasoning based on estimation of nonbonded interactions and measurements of electric moments of *trans*-StPs led to the assumption that in 2-StP the less strained, more coplanar rotamer (I in Scheme III)

SCHEME III



predominates in solution, while similar contributions of the two modifications would be present for 3-StP<sup>9</sup> due to their equivalent steric interactions. Analogously, by a comparison of the measured and calculated chemical shifts of the ethylenic protons of 2-StP and 2,2'-DPE,<sup>13</sup> the less strained structures (I in Schemes III and IV) were shown to be the predominant species in solution.

SCHEME IV



A thorough investigation of the  $\lambda_{\text{exc}}$  dependence of the fluorescence spectra of StPs was reported by Bartocci and Mazzucato.<sup>24a,114,115</sup> Some anomalies observed in 3-StP and 3,3'-DPE, in particular the marked decrease in the fluorescence quantum yield (which is already very small at room temperature) when the  $\lambda_{\text{exc}}$  was around 290 nm, were first assigned to a hidden absorption to a nonemitting state rather than to the presence of conformers, mainly because the room temperature excitation and emission spectra were found to be practically independent of  $\lambda_{\text{em}}$  and  $\lambda_{\text{exc}}$ .<sup>114</sup> Given the rather speculative character of this interpretation, the authors initiated a detailed study of the absorption and fluorescence spectra as a function of temperature in various solvents and in rigid matrices of EPA at 77 K.<sup>115</sup> In the latter conditions, more or less clear  $\lambda_{\text{exc}}$  effects on the emission spectra were observed for all three isomeric *n*-StPs (*n* = 2,3,4). The hidden absorption, not accompanied by a detectable emission at room temperature, was explained by the excitation of a second rotational conformer with very short  $\tau$  and low  $\phi$ , which becomes highly fluorescent only at high viscosity and low temperature when the internal rotation around the double bond is inhibited. The spectra obtained by slowly cooling (which should enable rotamer equilibration) to 77 K in EPA are shown in Figure 30. The spectra of the rotamers are similar in shape and shifted only in energy. By excitation at the long-wavelength edge of the absorption spectrum ( $\lambda_{\text{exc}} = 338$  nm), a bathochromically shifted spectrum was obtained. It seemed to correspond to an almost pure species that, by analogy with the case of the hydrocarbon compounds, will hereafter be called A species (B for the short- $\lambda$  absorbing species). It must be noted that such analogy refers to the spectral position and not to the  $\tau_{\text{F}}$  values since only single lifetimes were generally found for these compounds. The A spectrum was then subtracted from the emission spectrum of the A + B mixture obtained at a shorter  $\lambda_{\text{exc}}$ . The resulting emission spectrum should be that of the almost pure B species. The excitation spectrum of B was obtained by using  $\lambda_{\text{em}}$  near the blue edge of the corresponding emission spectrum while that of the A species remained hidden in the spectrum of the mixture. A net shift of about 10 nm was found between the emission spectra of the two rotamers of 2-StP and 3-StP while a smaller shift of about 3 nm was found for isomer 4. A tentative explanation for the observation of the phenomenon in 4-StP (where distinct rotamers are not expected) is that



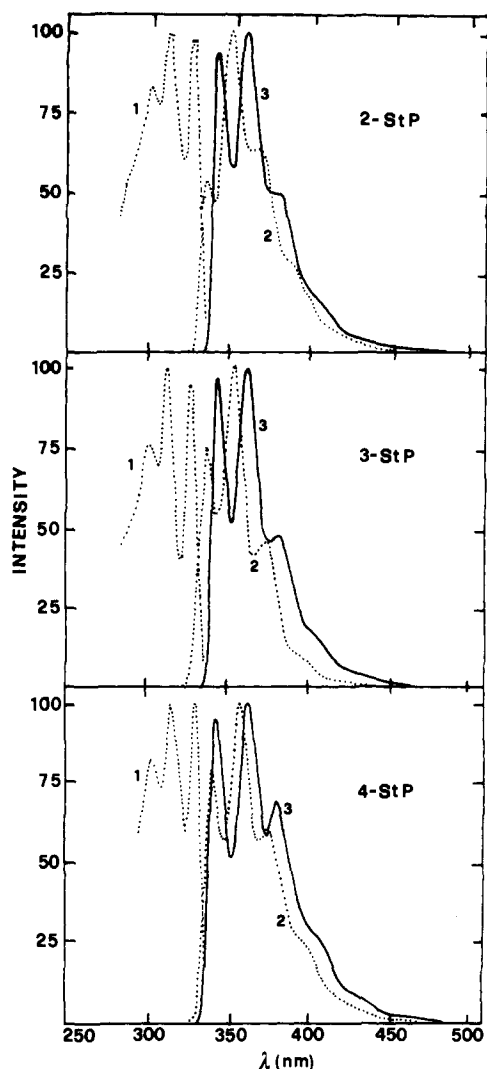


**Figure 30.** Fluorescence excitation (1) and emission (2, 3) spectra of almost pure conformers of *trans*-StPs in EPA at 77 K obtained by selective excitation (see text) (solid curve: conformer A; dotted curve: conformer B) (reprinted from ref 115; copyright 1982 Elsevier (Amsterdam)).

some degrees of disrotatory (or conrotatory) twisting of the two rings induced by the rigid matrix might lead to at least two discrete conformations.<sup>115</sup>

A similar behavior was observed for the *n,n'*-DPEs (*n,n'* = 2,3,4) but the  $\lambda_{\text{exc}}$  effects were even smaller than in the case of StPs.<sup>116</sup>

In all these compounds, the fluorescence decay measured at different  $\lambda_{\text{exc}}$ 's in EPA at 77 K could be represented satisfactorily by single exponential functions. However, in the case of 2-StP and 3-StP a somewhat better fit was obtained by deconvoluting the signal decay with a biexponential function. Correspondingly, the  $\phi$  values, measured under the same conditions, did not show any  $\lambda_{\text{exc}}$  dependence. On the other hand, for other compounds, e.g. for 2,2'- and 3,3'-DPE, some  $\lambda_{\text{exc}}$  effect was found for  $\phi$  but not for  $\tau$ . The apparent divergencies of these results are probably related to the fact that the effects being dealt with are at the limit of experimental uncertainty. Spectral analysis, with the help of the vibronic structure, is, in this case, more powerful than that based on the  $\phi$  and  $\tau$  values for resolving the presence of multiple emissions. In fact, the latter values refer to integrated quantities (defined by a single parameter) and thus do

not offer the best way to discriminate between different conformations.<sup>116</sup>

In an attempt to rationalize the above experimental observations, Marconi et al.<sup>66</sup> carried out a theoretical work using the MNDO method to calculate the ground-state properties of the distinct rotameric forms and the INDO/S method to evaluate their  $S_0 \rightarrow S_n$  transition properties. The results of the MNDO calculations, including empirical corrections for solvent effects, predicted that, in the 2-derivatives of both StP and DPE, the I forms are the most stable ones. In 2-StP, the form II was predicted to lie  $\sim 2$  kcal mol<sup>-1</sup> above the stable modification, thus implying a relative abundance of just 3.4%. Similarly, in 2,2'-DPE, the forms II and III were found at  $\sim 3$  and  $\sim 5$  kcal mol<sup>-1</sup>, respectively, above the form I. Although these energy differences are probably overestimated, they qualitatively explain the very weak manifestations of multi-component behavior of these molecules.

As far as the excited states are concerned, a basic consideration in ref 66, derived from previous INDO/S<sup>65</sup> and CNDO/S<sup>117</sup> calculations, was that the lowest lying singlet-excited state should be  $\pi\pi^*$  in character, at least in the *o*- and *m*-azastilbenes. According to this prediction, the INDO/S results on the  $S_0 \rightarrow S_1$  transition properties of the different rotamers were analyzed with no reference to a possible involvement of  $n\pi^*$  states. Briefly, the  $S_0 \rightarrow S_1$  absorption band of the stable forms (I) of the ortho derivatives were found to be slightly red-shifted with respect to those of the unstable ones (II). This formally enabled the authors to identify the I rotamers of 2-StP and 2,2'-DPE as the A species. This assignment, however, should be considered with caution because the observed red-shifts in rigid matrix<sup>115,116</sup> are decidedly higher than the calculated ones (800–850 cm<sup>-1</sup> instead of 50–55 cm<sup>-1</sup>).

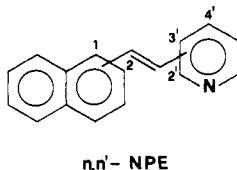
As for the meta isomers of StP and DPE, where the steric interactions are practically the same in all the planar conformers, MNDO calculations predicted the different rotamers to be almost isoenergetic. In the case of 3-StP, the form II was found to be  $\sim 0.3$  kcal mol<sup>-1</sup> more stable than I (when including the solvent effect). Thus the fractions of the two species are expected to be  $\sim 0.6$  and  $\sim 0.4$ , respectively, in the room temperature equilibrium mixture and this may explain why the  $\lambda_{\text{exc}}$  dependence of the photophysical properties is more evident for 3-StP than for 2-StP. In 3,3'-DPE, where the solvent effects were estimated to be almost the same for the three rotamers, the corresponding energy differences came out to be still lower, and hence all modifications should be expected to be present with comparable abundances at ordinary temperatures. Thus, the fact that only two species were experimentally distinguished could be attributed to the close similarity in the photophysical properties between two of the three rotamers. Regarding the relative shifts of the rotamer spectra, the INDO/S values were again quite underestimated with respect to the experimental values, so no clear structural identification was reached.

To conclude, it should be noted that the theoretical and fluorimetric results, considered together, do not provide a satisfactory and consistent description of the rotational isomerism in these compounds. Possible reasons for this situation could involve two complicating phenomena, both related to the fact that  $\lambda_{\text{exc}}$  effects

were only observed in frozen media. A first possibility could be the occurrence of thermal equilibration of the excited rotamers in fluid solutions contrary to the NEER assumption, as already discussed for 3,3'-DMS (section III.A.8). An alternative explanation, already proposed in the case of *p*-azastilbenes, is that the matrix rigidity could induce preferential trapping of discrete conformations, which do not necessarily correspond to the conformers which exist in fluid media. Therefore, further work is needed to better interpret the rotamerism associated with the internal rotation of the pyridyl chromophore.

## 2. Naphthyl-Pyridyl Derivatives

Some *trans* isomers of *n,n'*-naphthylpyridylethylenes (*n,n'*-NPEs) were studied in detail by Mazzucato et al.<sup>16,24,32</sup> The interest in these compounds lies in the



fact that the presence of two asymmetric chromophoric groups (1- and 2-naphthyl, 2'- and 3'-pyridyl) can in principle give rise to four different species. A preliminary investigation, mainly concerned with the photochemical behavior of the 3'-pyridyl derivatives,<sup>16</sup> showed that the "naphthyl conformers" (due to the rotation of the naphthyl group) behave similarly to the corresponding hydrocarbons while the characterization of the "pyridyl conformers" (due to the rotation of the pyridyl group) is practically impossible, at least in fluid solutions, because the dependence of the fluorescence properties on  $\lambda_{\text{exc}}$  is too small, as already seen for StPs and DPEs.<sup>115,116</sup> Since the rotamer behavior is controlled by the rotation of the naphthalene moiety, one expects to find evidence of two main conformers in the case of the 2-naphthyl derivatives and only one for the 1-naphthyl derivatives, as in the case of 1-StN (section III.A.1). The consequences of this working hypothesis, which has also been applied to related systems (anthryl derivatives containing the naphthyl or thienyl groups),<sup>98</sup> seemed to be justified based on the results obtained for StNs and StPs. It was also confirmed by a photophysical behavior qualitatively similar to that of *n*-StNs, in which a biexponential decay occurred only in the case of the 2-naphthyl derivatives.<sup>32</sup> Actually, some incongruity exists in that the results of the KFA method do not fit well with the expectation that the NPEs' rotamerism is controlled by the rotation of the naphthyl group. In fact, the different behavior of the 2,3' isomer (extent of the  $\lambda_{\text{exc}}$  effect similar to that of 2-StN but  $\Delta H$  value sensibly smaller) and of the 2,2' and 2,4' isomers (negligible  $\lambda_{\text{exc}}$  effect but higher  $\Delta H$  values, similar to that of 2-StN) indicates that the above assumption is probably an oversimplification and that the rotamerism of NPEs is also affected by the presence and the position of the nitrogen atom. In any case, the results obtained are interesting and will be described briefly.

A common feature of the three isomeric *trans*-2,*n'*-NPE was the absence of isoemissive frequencies in the normalized (to equal absorbed quanta) fluorescence spectra of the mixture.<sup>32</sup> Therefore, application of the

**TABLE X. Photophysical Parameters, Arrhenius Parameters for Photoisomerization, Enthalpy Difference, and Relative Concentrations of the Rotamers of *trans*-2,3'-NPE in *n*-Hexane at Room Temperature, as Derived from the KFA Method (from ref 32)**

parameter	A rotamer	B rotamer
$\phi$	0.25	0.85
$\tau$ , ns	4.9	14.9
$k_F$ , $10^7$ s <sup>-1</sup>	5.1	5.7
$\Delta E_{t \rightarrow p}$ , kcal mol <sup>-1</sup>	6.7	7.3
log $A_{t \rightarrow p}$	12.8	12.4
$\Delta H$ , cal mol <sup>-1</sup>	270	
relative abundance, %	62	38

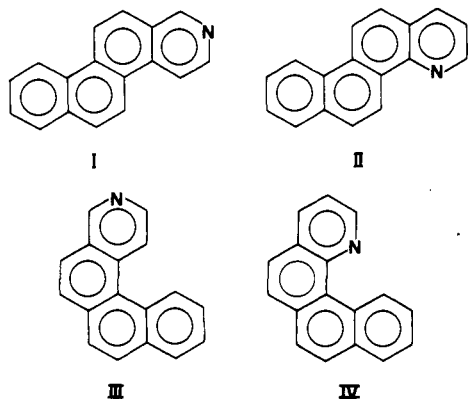
KFA method required, as in the case of 3-StPh,<sup>39,72</sup> the special procedure reported in section II.A.5.a. However, the weak sensitivity of the emission spectra to  $\lambda_{\text{exc}}$  for the 2,2' and 2,4' isomers, in addition to a relatively high  $\Delta H$  (see below) which shifts the equilibrium toward the more stable rotamer, practically limited the applicability of the analysis to the fluorescence behavior of the 2,3' isomer. On the basis of the  $\lambda_{\text{exc}}$  effect on the decay kinetics of the latter compound, the fast decay component (A) was related to the bathochromic rotamer and the slow decay component (B) to the hypsochromic one, as in the case of 2-StN.<sup>20,25,31</sup> The assignment was supported by the time-resolved spectra measured in *n*-hexane.<sup>32</sup>

The results of the analysis are collected in Table X. The main difference with respect to the corresponding hydrocarbon, 2-StN, is the similarity of the radiative rate constants, the larger difference in  $\phi$  being here responsible for the ratio  $\tau_B/\tau_A \approx 3$ . In this case, the A rotamer has a much higher non-radiative rate parameter, probably related to the *trans*  $\rightarrow$  *perp* internal rotation. In fact, the activation energies and frequency factors for the isomerization in the singlet manifold, obtained from the study of the temperature effect on the  $\tau$  values, confirmed this result indicating a faster photoreactivity of the short-lived rotamer (see Table X). From the plot of log  $\gamma$  against  $1/T$  (see section II.A.5.a) the A - B enthalpy difference  $\Delta H = 270$  cal mol<sup>-1</sup> was obtained, a value noticeably smaller than that found for 2-StN. From this result, neglecting entropy terms, the predominant species in solution is the A species,<sup>32</sup> unlike the parent hydrocarbon where the longer lived and hypsochromic B rotamer was the more stable species.<sup>31</sup> According to simple consideration of the nonbonded interactions occurring in the two planar rotamers, we should then conclude that, in this case, the A species (short- $\tau$  and long- $\lambda$ ) is identifiable as the more elongated species. This should not be surprising because the lowest excited states of the two rotamers have, unlike in 2-StN, the same character (probably <sup>1</sup>L<sub>b</sub> naphthalenic) as shown by their very similar and rather low  $k_F$  values.

Since the analysis was not applicable to the 2,2' and 2,4' isomers, only the distinct lifetimes of the rotamers and the ratios of the corresponding preexponential factors were obtained from the deconvolution of the fluorescence decay curves. The enthalpy difference and the relative concentrations were obtained from the temperature effect on the preexponential factors of the decay curves.<sup>32</sup> In these two compounds the shorter lived A rotamer was also found to be the more abundant species at room temperature and characterized by a higher rate constant for the photoisomerization to the

cis form. It was concluded that only at low temperatures (<200 K) does the triplet mechanism become operative.

Qualitative information on the rotamerism of the nonfluorescent cis isomers was obtained from a study of the dehydrophotocyclization of *n*,3'-NPE (*n* = 1,2).<sup>16</sup> For both compounds, only two cyclization products were isolated from the photoreaction mixture, namely 2- and 4-azachrysene (I and II) from the 1-naphthyl derivative and 1- and 3-azabenzoc[*c*]phenanthrene (III and IV) from the 2-naphthyl isomer. In both cases, the



compounds with the quinoline-type structure (II and IV) were found in a much smaller chemical yield (slightly  $\lambda_{\text{exc}}$  dependent) compared to the analogues with the isoquinoline-type structure (I and III). The cyclization products of 2,3'-NPE derived from the two pyridyl isomers of the cis rotamer corresponding to trans B, while those derived from the cis rotamer corresponding to trans A were not detected in the photoreaction mixture. Inertness toward ring closure leading to highly quinoid structures of the intermediate dihydro derivative (which would then dehydrogenate to the final benzanthracenes), already reported for related compounds,<sup>14</sup> was also verified in the present case.<sup>16</sup>

Also from the quasi line spectra in Shpol'skii matrices of *n*-hexane at 5 K evidence for only two rotamers of 2,2'-NPE was reported.<sup>45</sup> In a *n*-decane matrix, the spectrum of only one rotamer was clearly observed. The close similarity between the emission spectra and that of 2-StN helped in characterizing the behavior of the A and B rotamers. A time-resolved experiment with laser excitation yielded a shorter  $\tau$  for the red-shifted A species in agreement with results obtained in *n*-hexane fluid solution.<sup>32</sup> Obviously, the  $\tau$  value was much longer (>30 ns) in the rigid matrix due to the absence of the concurrent trans  $\rightarrow$  cis photoisomerization.

### 3. Phenanthryl-Pyridyl Derivatives

A phenanthryl analogue of 3-StP, the 3,3'-PhPE was studied by Fischer.<sup>118</sup> Relatively modest  $\lambda_{\text{exc}}$  effects on the fluorescence spectra were observed. By exciting at 330 and 345 nm, the distinct emissions of the short- and long-wavelength absorbing species were roughly estimated.

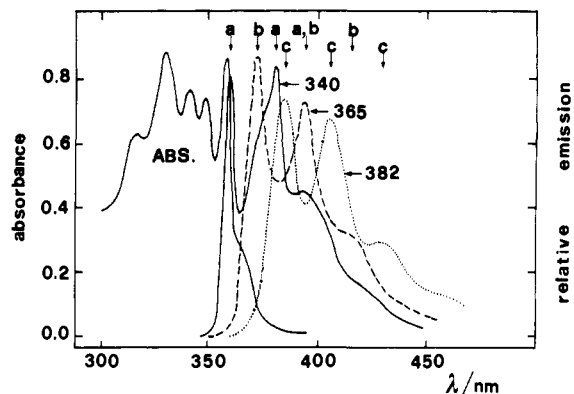
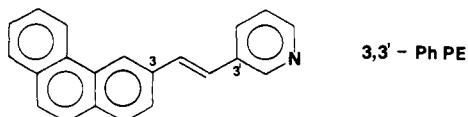
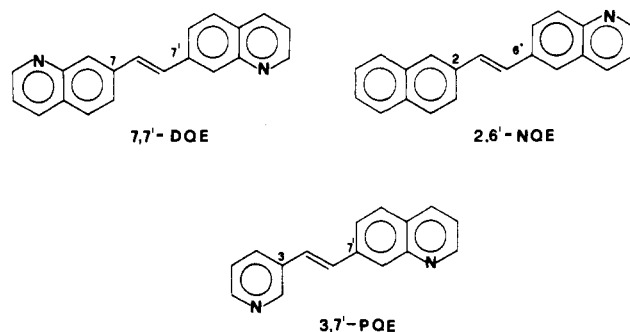


**Figure 31.** Emission spectra of the almost pure three conformers of 7,7'-DQE in MCH at 203 K observed by selective excitation at the  $\lambda_{\text{exc}}$  (nm) indicated. The absorption spectrum of the mixture is also reported for comparison (adapted from ref 118).

### 4. Quinoly and Isoquinoly Derivatives

Some quinoly derivatives, 2,6'-NQE, 3,7'-PQE, and 7,7'-DQE, were investigated by Fischer<sup>118</sup> in several inert solvents at temperatures of 203 K and lower. A



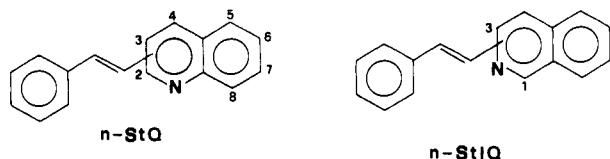
pronounced spectral variation with  $\lambda_{\text{exc}}$  was found for all these compounds but the results with 7,7'-DQE were particularly interesting since they gave the most clear-cut evidence of a three-component system. The spectra of Figure 31 show three distinct emission spectra characterized by sets of peaks shifted toward each other by 10–15 nm, the first peak being observed at 359, 370 and 380 nm for the three species in a 2:1 MCH–2MP mixture. The c emission underwent preferential quenching by oxygen, indicating a substantially longer  $\tau$ .

*trans*-2,6'-NQE was also studied by Ghiggino.<sup>28</sup> A two-exponential decay was observed ( $\tau_A = 2.5$  ns and  $\tau_B = 16$  ns in cyclohexane at room temperature) but, as in the case of 2,2'-DNE, the bad fit ( $\chi^2 > 2$ ) provided some evidence for more than two components (four expected). Also, fluorescence-quenching experiments with  $\text{CCl}_4$  showed deviations from the Stern–Volmer behavior and a  $\lambda_{\text{exc}}$ -dependent quenching efficiency indicating the presence of at least three differently quenchable entities.

Muszkat and Wisniewski-Knittel<sup>44</sup> studied 7,7'-DQE and 2,6'-NQE in polycrystalline *n*-hexane matrices at 5 K and compared them to 2,2'-DNE. These compounds showed strikingly similar quasi line spectra with minimal Stokes shifts. The analysis of the vibronic bands led to the conclusion that they deviate slightly from planarity and that the quasi line spectra are due to the more planar short-wavelength absorbing rotamer. Lamotte, Muszkat, et al.<sup>45</sup> used the same matrix to

study 7-StQ. Here again, as for 2-StN, such experiments allowed the quasi line spectra of the distinct rotamers to be obtained and assigned on the basis of the close resemblance to 2-StN. A time-resolved experiment with laser excitation showed no variation in the relative intensities of the two spectra up to a 40-ns delay, implying that the two lifetimes are similar and longer than the laser pulse duration.

A more systematic study of the conformers of *trans*-StQs and -StIQs, including specific solvent effects, was carried out by Gennari et al.<sup>119-123</sup> A general



characteristic of these molecules is the strong dependence of their photochemical and photophysical behavior on the nature of the solvent, in particular on its polarity and hydrogen-bonding ability. It should be noted that the exceedingly high basicity of  $S_1$  for some StQs leads to their direct protonation by various alcohols.<sup>122</sup> When the styryl group is linked to the ring containing the heteroatom, the fluorimetric behavior roughly parallels that of the corresponding StPs. In fact, 2-StQ has a very low  $\bar{\phi}$  and isomerizes in low yield while 4-StQ has a higher  $\phi_{t \rightarrow c}$  but is scarcely fluorescent.<sup>123</sup> On the other hand, 3-StQ has relatively high  $\bar{\phi}$  and  $\phi_{t \rightarrow c}$  and is more suitable for a study of rotamerism. When the styryl group is linked to the ring which does not contain the nitrogen atom, fluorescence becomes the main deactivation process.<sup>123</sup>

*trans*-3-StQ was studied more thoroughly.<sup>119,120</sup> Changing  $\lambda_{exc}$  produced some variations in the relative height of its emission peaks. More detailed information was obtained from the fluorescence excitation spectra monitored at different wavelengths,  $\lambda_{em}$ 's. By changing  $\lambda_{em}$ , two almost-pure excitation spectra of the two rotamers were obtained, showing the shape of their absorption spectra. The influence of  $\lambda_{exc}$  on the spectra was also reflected on the emission quantum yield. The minimum  $\bar{\phi}$  value was obtained at  $\lambda_{exc} = 315$  nm and corresponded to a maximum  $\phi_{t \rightarrow c}$  value (0.49). Excitation at longer wavelengths led to an increase in  $\bar{\phi}$  and a decrease in  $\phi_{t \rightarrow c}$  indicating that one of the excited conformers (the bathochromic one) deactivates mainly through fluorescence emission while the other one deactivates mainly through the photochemical channel. While the absorption spectrum was only slightly shifted to the red in polar solvents, the emission spectra were markedly shifted to the red, particularly in alcohols, where hydrogen bonding phenomena are probably concurrent. Similar  $\lambda_{exc}$  effects on fluorescence were also observed in aqueous solutions at various pH values. Measurements of the protonation constants for the ground and  $S_1$  states of 3-StQ ( $pK_a = 4.8$ ,  $pK_a^* = 12.7$ ) indicated that the fraction of excited molecules equilibrated with the proton depends on  $\lambda_{exc}$  and that the less fluorescent conformer is the more abundant at acidic pH values. The effects were, however, relatively modest and clear interpretations were difficult. Fluorescence decay measurements on 3-StQ also gave indication of two species ( $\tau_A = 0.4$  and 1.7 ns;  $\tau_B = 2.3$  and 5.7 ns at room temperature in CH and at 77 K in

a matrix of 3-MP containing 5% vol of MTHF, respectively). Changes of the rotamer composition in different solvents was hypothesized to partially explain the spectral shifts and changes in  $\bar{\phi}$  observed. The short A lifetime prevented the authors from applying the KFA method for a quantitative estimation of these changes in composition.<sup>120</sup>

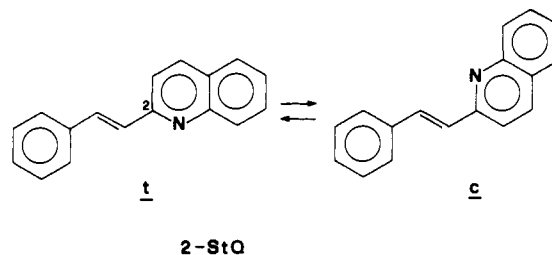
Even the spectral properties of the protonated molecule, 3-StQH<sup>+</sup>, display a strong dependence on the solvent though no clear correlations with the solvent properties were found.<sup>120</sup> The effects of solvent composition and  $\lambda_{exc}$  on the emission properties seemed to give some indication of a two-component system. The decay was, however, monoexponential, and the authors concluded that, in practice, only one conformer emits at room temperature. It could also be that the equilibrium is shifted toward one configuration of the cation.

For other *n*-StQs, in particular for the 6 and 7 isomers, a  $\lambda_{exc}$ -dependent dual emission was also found and assigned to two distinct conformational isomers.<sup>122,123</sup>

For 1-StIQ,<sup>121</sup> the main deactivation process of  $S_1$  is internal conversion to the ground state caused by an intramolecular hydrogen bond between the ethylenic hydrogen and the heteroatom that forces the molecule into a configuration which inhibits isomerization to *cis*. In hydroxylic solvents, intermolecular hydrogen bonds compete with the intramolecular bond and favor an efficient *trans*  $\rightarrow$  *cis* conversion. For this molecule, however, a  $\lambda_{exc}$ -independent emission was found and the fluorescence excitation spectrum was identical to the absorption spectrum.<sup>121</sup> As in the case of 1-StN, the equilibrium is largely shifted toward the more stable rotamer for steric reasons.

A detailed study of 2-StQ was recently carried out by Shim et al.<sup>124</sup> Here the styryl group is in ortho position with respect to the heteroatom and the molecule is then expected to show somewhat different steric nonbonded interactions compared to 2-StN and 3-StQ. Contrary to most DAEs, the less elongated rotamers (*c*) (named B in ref 124) may have more planar geometry than the *t* rotamer (named A) and thus becomes the more stable configuration (Scheme V). This species was identified

#### SCHEME V

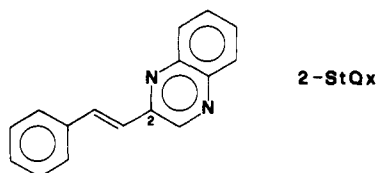


as the long- $\lambda$  absorbing component, the assignment being made by comparison with the conformationally restricted analogue, 3-methyl-2-StQ, where practically only the *c* rotamer, which is more planar because of less steric repulsions, is present in solution. Interestingly, only one conformer was observed in ethanol with a single excited state lifetime (0.3 ns). It was assigned to the *t* configuration which is stabilized by intermolecular hydrogen bonding between the protic solvent and the heteroatom. Such interaction is unfavorable in the *s-cis* configuration. Quantum mechanical calculations of the ground-state properties using the AM1

method (a modification of the MNDO scheme)<sup>125</sup> supported the above interpretations. In fact, they predicted a lower energy for the *c* rotamer with  $\Delta H \approx 1.2$  kcal mol<sup>-1</sup>, corresponding to 88% of such configuration at room temperature. In alcohol, the *t* rotamer with a higher dipole moment ( $\mu = 1.68$  D) than the *c* rotamer ( $\mu = 1.2$  D) can be better stabilized by solvation, besides by intermolecular hydrogen bonding, thus making the more elongated *t* species predominant in solution. The energy barrier impeding *c*  $\rightarrow$  *t* isomerization was calculated as  $\sim 2.5$  kcal mol<sup>-1</sup>. This value, although probably underestimated as expected for a MNDO-type calculation (see section II.C and ref 125), qualitatively indicates that ground-state rotamers may rapidly interconvert in fluid media.

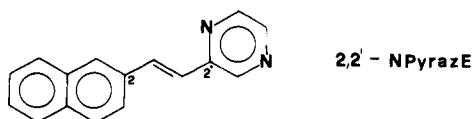
### 5. Quinoxaly and Pyrazyl Derivatives

One of the diazaanalogues of 2-StN, the *trans*-2-styrylquinoxaline (2-StQx), was studied by Shim et al.<sup>126</sup>



In ethanol, the fluorescence spectrum (and particularly the excitation spectrum) showed the usual  $\lambda_{\text{exc}}$  ( $\lambda_{\text{em}}$ ) dependence due to the presence of the two rotamers. In *n*-hexane, on the other hand, only one component was observed in the excitation spectrum. These results were interpreted as showing that both rotamers are fluorescent in ethanol but that only one rotamer is fluorescent in *n*-hexane, while a change in the position of the conformational equilibrium in different solvents was considered less probable. In ref 126, such behavior was reasonably explained by the vibronic mixing of the lowest lying <sup>1</sup>(*n*, $\pi^*$ ) and <sup>1</sup>( $\pi$ , $\pi^*$ ) states, enhancing the efficiency of the nonradiative and nonreactive decay processes in nonpolar (and nonprotic) solvents<sup>127</sup> and resulting in very low  $\bar{\phi}$  and  $\phi_{t \rightarrow c}$  values. A similar behavior had been observed for other azastilbenes (see above). The mixing becomes much weaker in hydrogen-donating polar solvents leading to a strong increase of  $\bar{\phi}$  and a smaller increase of  $\phi_{t \rightarrow c}$  (for more details, see section III.C).

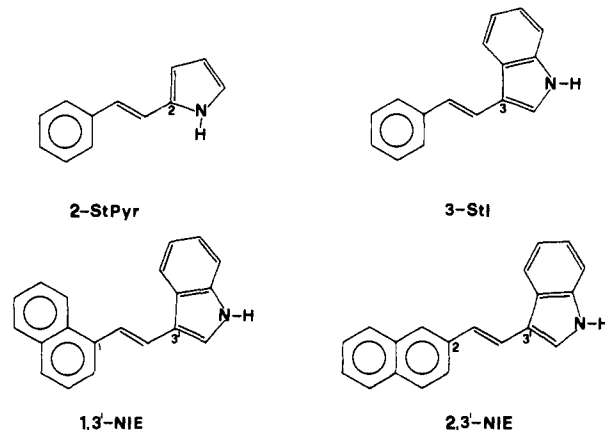
The *trans*-2,2'-naphthylpyrazylethylene (2,2'-NPyrazE) was studied by Shim and Kim<sup>128</sup> in different solvents. Two components were revealed by the  $\lambda_{\text{exc}}$  effect on the fluorescence spectra. Molecular mechanics calculations allowed their assignment to the two "naphthyl" conformers of similar energy. A large  $\Delta H$  (2.4 kcal mol<sup>-1</sup>) destabilizes one "pyrazyl" conformer making detectable only the more stable configuration.



### 6. Pyrrolyl and Indolyl Derivatives

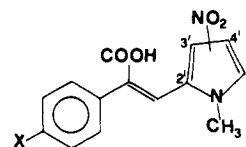
DAEs containing a pyrrolic nitrogen were recently investigated by Galiazzo et al.<sup>129</sup> Only preliminary fluorimetric results are available on rotamerism of these molecules where, contrary to the pyridyl derivatives

seen above, the heteroatom contributes a pair of non-bonding electrons to the ring thus eliminating the deactivating channel of the *n*, $\pi^*$  states by internal conversion. The compounds studied were 2-StPyr and some indolyl analogues, 3-StI, 1,3'-NIE and 2,3'-NIE.



All these compounds behave similarly to stilbene being characterized by very small  $\bar{\phi}$  ( $< 0.02$ ) and high  $\phi_{t \rightarrow c}$  ( $\sim 0.5$ ) which accounts for all absorbed quanta. As to the rotamer behavior, the small  $\lambda_{\text{exc}}$  effects observed on the fluorescence spectrum, more evident at 77 K in an alcoholic rigid matrix, were explained by the presence of at least two rotamers. The fluorescence anomalies were also observed for 3-StI, which resembles 1-StN (one-component system) but which is probably characterized by slightly reduced nonbonded interactions.

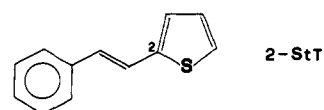
The preferred conformations of some substituted StPyr's were studied much earlier by Sciotto et al.<sup>12</sup> in the case of *trans*- and *cis*-1-phenyl-2-(*N*-methylnitro-pyrrol-2'-yl)acrylic acids on the basis of the position of the olefinic and pyrrolic protons in the NMR spectrum.



For the *cis* isomers, the heterocyclic proton in the 3' position ( $H_3$ ) was found to be remarkably shielded by the  $\pi$  electrons of the phenyl ring and no coupling was observed between the ethylene proton and  $H_5$ . Both factors indicate the existence of the *s-cis* conformation, which is more stable for steric reasons. Similar results were found for the *trans* isomers revealing, also in this case, the presence of the *s-cis* configuration.

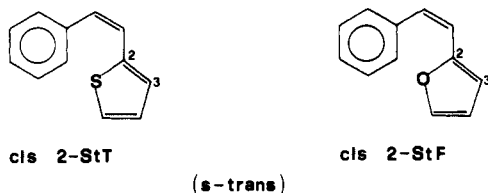
### 7. Thienyl and Furyl Derivatives

The fluorescence spectrum of *trans*-2-styrylthiophene (2-StT) showed a  $\lambda_{\text{exc}}$  dependence only at low temperature in rigid unipolar matrices.<sup>130</sup> The quantum yield

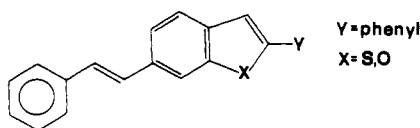


of the two competitive processes, fluorescence and photoisomerization, were affected by  $\lambda_{\text{exc}}$  in a complementary way,  $\bar{\phi}$  being greater when  $\phi_{t \rightarrow c}$  was smaller. The long wavelength absorbing species seemed to have a smaller  $\bar{\phi}$  and higher  $\phi_{t \rightarrow c}$  but no quantitative analyses were made.<sup>130</sup>

A study of the stereochemistry of the cis isomers of styrylfurane (StF) and styrylthiophene (StT) para substituted at the phenyl group ( $\text{CH}_3$ , Cl,  $\text{NO}_2$ ) and/or at the ethylenic carbon (COOH) was carried out by Sciotto et al.<sup>11,131</sup> Using the NMR technique, the authors got



structural information from the chemical shift values of the proton in the 3 position of the pentatomic ring. As expected, the NMR data did not allowed resolution of the distinct rotamers. The values of the chemical shifts for the cis isomers of StF and StT and of the acid of the thienyl derivative were found in the normal range and the shielding effects on  $\text{H}_3$  by the  $\pi$  electrons of the phenyl group were not noticed thus suggesting a predominant s-trans conformation. For the acid of the furyl derivative, the resonance line of  $\text{H}_3$  exhibited a strong shielding effect which suggests the existence of the s-cis conformation only. This behavior is probably due to destabilization of the s-trans form because of a stronger electrostatic repulsion between the negatively charged heterocyclic oxygen and the  $\pi$  electrons of the phenyl group.<sup>11</sup> Some heterocyclic analogues of 2-StN with the naphthyl group replaced by substituted benzo[b]thiophene and benzo[b]furan groups were studied by Wismontski-Knittel et al.<sup>132</sup> The  $\lambda_{\text{exc}}$  dependence



of their emission spectra was reminiscent of the general behavior of DAEs described thus far. Short-lived (<2 ns) monoexponential decays were observed with the limited time resolution of the fluorimeter. Exciplexes with amines and triplet transients were also investigated for these compounds but no information on their rotamerism was obtained.

### C. Solvent Effects

Although the effects of the solvent on the observed properties of DAE rotamers have been mentioned often in the preceding sections, some summarizing considerations may be necessary to better define the subject.

First we will refer to the direct solvent effects on the ground-state rotamers. In general, distinct conformers will undergo more or less different solvation effects, such that their relative stabilities (and hence the mixture composition at equilibrium) may change upon changing the solvent polarity. Such effect, of course, is expected to be negligible in the case of hydrocarbon DAEs, where all the envisaged rotamers are essentially apolar. As a matter of fact, the enthalpy differences between the two rotamers of 2-StN were found to be the same, within experimental error, in *n*-hexane and ethanol (Table III).<sup>31</sup> Noticeable effects may, in principle, occur in those DAEs where rotamerism is due to the presence of heteroatom-containing groups. In fact,

in these cases, different rotamers may have substantially different dipole moments, as shown, for instance, by MNDO calculations on *n*-StPs and *n,n'*-DPEs.<sup>66</sup> In the latter compounds, however, evidence for the presence of distinct rotamers is rather weak and appears only at low temperatures (see section III.B.1) when effects due to the medium rigidity are probably predominant and hence may mask effects related to the solvent polarity. Clearer effects, traceable to the solvent properties, were observed in *n*-StQs. Shifts in the conformeric equilibrium were first suggested by Gennari et al.<sup>119,120</sup> to explain the spectral shifts of 3-StQ in solvents of different polarity, but no quantitative determinations were made. A dramatic effect was recently encountered in 2-StQ<sup>124</sup> upon changing the solvent from aprotic to protic. The t conformer (A in the authors notation), the less abundant in aprotic (both polar and apolar) media, becomes the largely predominant species in alcohols due to a marked stabilization probably associated with selective hydrogen bonding between the protic solvent and the nitrogen atom in the quinoline group.

With regard to the excited states, various effects may be exerted by the solvent, all of which could affect detection of the rotamers via fluorimetric measurements. Two different cases can be distinguished, concerning the hydrocarbon and the heteroatom-containing DAEs, respectively. Of course, rather weak effects would be expected for the hydrocarbon compounds. In principle, one could envisage two mechanisms for the influence of the solvent on the relaxation kinetics of the excited rotamers. First of all, at a zero-order approximation, the two lowest singlet excited states have very different natures: one of them is a "forbidden" covalent-type state (identifiable as the  $^1L_b$  state of the polycyclic group), while the other (prevalently HOMO  $\rightarrow$  LUMO) has "allowed" and more ionic character. This situation resembles that encountered in  $\alpha,\omega$ -diphenylpolyenes having two lowest lying excited states,  $^1A_g^-$  ("covalent") and  $^1B_u^+$  ("ionic"), whose relative position depends on the polyene chain length.<sup>133</sup> In our case, however, the lack of symmetry makes the two states interact and gain mixed character when their energy gap becomes small. Now, on changing from apolar to polar solvents, the "ionic" (more polar) state is expected to undergo a relative stabilization and this may result in a varied radiative rate constant by altering the extent of mixing between  $S_1$  and  $S_2$ . Connected with the stabilization of the ionic-type state, the energy gap between  $S_1$  and the coupled triplet state may also change, thus causing a variation of the ISC efficiency.

The second mechanism is related to a lowering of the barrier which hinders the double bond trans  $\rightarrow$  cis isomerization in the  $S_1$  state by increasing the solvent polarity. Such effect, which is the equivalent of that observed in the case of stilbene<sup>134</sup> and  $\alpha,\omega$ -diphenylpolyenes,<sup>133</sup> is due to a strong stabilization of the markedly polarized twisted intermediates in polar solvents. Thus, an increase of the solvent polarity is expected to cause an enhancement of the photoisomerization rate accompanied by a reduction of the fluorescence quantum yield. Both of these mechanisms may influence the fluorimetric detection of the rotamers, since the energy gap and nature of the two lowest singlet excited states are more or less different in the

distinct species. The only detailed study of the effects of the solvent polarity on the decay kinetics of the rotamers is that reported by Bartocci et al.<sup>31</sup> for *n*-StNs. The results of ref 31 show that on changing from *n*-hexane to ethanol the difference in  $k_F$  of the two conformers of 2-StN is significantly reduced (Table III) while that in  $k_{ISC}$  is greatly enhanced. Moreover, one of the rotamers (A) is characterized by a strong increase of the *trans* → *perp* rotation rate ( $k_{t \rightarrow p}$ ) and a corresponding marked decrease of  $\phi$ . These observations suggest that both of the above described mechanisms are operative in the 2-StN rotamers, the detection of the effect being favored by the small energy gap between the two lowest lying excited states.

More marked and specific solvent dependencies of the photophysical parameters of the rotamers have recently been observed in quinolyl and quinoxalyl derivatives, in particular 2-StQx.<sup>126</sup> The main point about these compounds is the presence of a  $^1(n, \pi^*)$  state very near the lowest state of  $\pi, \pi^*$  type. The closeness of these two states of different orbital types is expected to result in a strong vibronic coupling which, in turn, leads to more efficient nonradiative deactivation ( $S_1 \rightarrow S_0$  internal conversion and, possibly,  $S_1 \rightarrow T_n$  ISC), thus providing a rationalization of the very low fluorescence quantum yields of these compounds in nonpolar and nonprotic solvents.<sup>126,127</sup> In protic and polar solvents, on the other hand, the  $^1(n, \pi^*) - ^1(\pi, \pi^*)$  energy gap may increase substantially, the two states being shifted in opposite directions.<sup>127</sup> Because of the increased energy gap, the vibronic coupling will become smaller and  $\phi$  will increase. Since different rotamers generally have unequal  $^1(n, \pi^*) - ^1(\pi, \pi^*)$  energy gaps, their photophysical parameters will exhibit different solvent dependencies. This enabled Shim et al.<sup>126</sup> to explain why only one rotamer is observed in the excitation spectrum of 2-StQx in *n*-hexane, while two rotamers are clearly detectable in ethanol.

All of the above described solvent effects on the excited state properties of the rotamers are static in nature. It is to be noted that the dynamic solvent effects on the rates of the rotamer interconversion in the  $S_1$  state,<sup>100-102</sup> are of a side interest in the present context, since they become operative when the NEER hypothesis breaks down and hence the fluorimetric methods are of little use for quantitative studies of DAE rotamerism.

#### IV. Conclusions

In this article the studies carried out during the last 15–20 years on the phenomenon of rotational isomerism in DAEs have been reviewed. Although the subject concerns specifically DAEs in their ground electronic state, the study started with the observation of emission spectroscopic anomalies in solution and most of the available information has been derived from the application of fluorimetric techniques. The success of this approach in reflecting the ground-state equilibrium composition lies in the validity of the basic NEER assumption that no equilibration occurs between the excited rotamers during the  $S_1$  lifetime. A number of photochemical laboratories have been intensely involved with the fluorimetric investigation of this subject. Significant, but less extensive, contributions have been obtained by using experimental techniques other than

fluorimetry (e.g., flash photolysis and vibrational spectroscopy) as well as by quantum mechanical treatments.

All of these studies have thus provided a large amount of information on DAE rotamers, even if some of the published work is quite scattered and of little usefulness for a general rationalization of the phenomenon. At the present, a satisfactory description appears to have been reached only in the case of the hydrocarbon DAEs thanks to a series of integrated works in which a significant set of prototype compounds were studied with many of today's available experimental and theoretical techniques. A less satisfactory and incomplete description has been obtained for the heteroatom-containing compounds because of fewer investigations, weaker experimental evidence and the lack of a thorough theoretical study.

As for future perspectives, extending qualitative observations of the rotamerism in new DAEs seems to be of lesser importance in view of the abundance of information already available. The efforts should be directed toward improving the investigation techniques already utilized, searching for new techniques, and applying them to clarify remaining ambiguities in the behavior of the most representative series of compounds.

Among the techniques mentioned in section II.A, the quantitative methods of fluorescence analysis (KFA and PCA-SM) could be extended to more cases to more thoroughly test their real limits in resolving the properties of the rotamer mixtures (photophysical and thermodynamic parameters, composition, conformation assignments). Probably, the most worthwhile aspect which should be further developed is the applicability limits of the NEER hypothesis. This problem becomes crucial in DAEs containing large aromatic substituents which have a low-energy  $S_1$  state which is practically localized in the polycyclic group. In fact, in these compounds the energy barrier to the rotamer interconversion in the excited state is expected to be similar to that of the ground state, thus making them, at least in principle, candidates for the breaking down of the NEER hypothesis. In such a situation, a low interconversion barrier around the quasi single bond(s) is generally combined with a high barrier around the ethylenic double bond, which inhibits *trans* → *cis* isomerization, thus leading to a long excited state lifetime which allows  $t \rightarrow c$  equilibration.

Important contributions are expected from spectroscopic observations in the isolated molecule conditions (Shpol'skii matrices and supersonic jets). While trapping of rotamers in *n*-alkane matrices has already provided some important structural information and seems still promising, observations by jet-cooled spectroscopy are surprisingly still lacking, in spite of the careful investigation on stilbene reported several years ago.

The direct study of the ground-state equilibrium using techniques other than fluorimetry (such as low-temperature NMR and ENDOR, IR and Raman spectroscopy) should be more extensively investigated.

Further efforts in the area of quantum mechanical calculations are required in order to improve and complete our understanding of the hydrocarbon DAE rotamers and to systematically face the treatment of the heteroatom-containing compounds for which only

scanty results have been presented to date. Cases concerning the hydrocarbons which are still open include some unclear conclusions reached in the interpretation of the photophysical properties of the anthryl derivatives and some puzzling problems such as the break down of the NEER assumption which has been proposed to occur in 3,3'-dimethylstilbene. As for the aza compounds, an important aspect to be defined concerns the relative ordering of the  $n, \pi^*$  state(s) introduced by the heteroatom(s) and the lowest  $\pi, \pi^*$ -type state.

A final relevant point, rather neglected to date and which deserves further study, is the solvent effect on the interconversion barriers and particularly on the enthalpy difference between rotamers and on their photophysical and photoreactive properties. Viscosity, polarity, and hydrogen-donating capability can play important roles in this respect. Moreover, in case of nonvalidity of the NEER principle, the adiabatic  $t \rightarrow c$  interconversion in the excited state can offer a prototype system for studying dynamic solvent effects on ultrafast chemical reactions.

**Acknowledgments.** We are grateful to Ernst Fischer for his interest in this review article manifested in many helpful suggestions and stimulating discussions. We also thank all of our co-workers named in several references of this paper, and in particular I. Baraldi and G. Bartocci for their continuous help during our study of DAE rotamerism. Thanks are also due to D. Pannacci and M. Pelliccia for the drawings and to the Italian Consiglio Nazionale delle Ricerche and Ministero per l'Università e la Ricerca Scientifica e Tecnologica for financial support.

## References

- Mulliken, R. S. *J. Chem. Phys.* **1939**, *7*, 121; *Rev. Mod. Phys.* **1942**, *14*, 265.
- Vroegop, P. J.; Lugtenburg, J.; Havinga, E. *Tetrahedron* **1973**, *29*, 1393. Jacobs, H. J. C.; Havinga, E. *Adv. Photochem.* **1979**, *11*, 305.
- Cherkasov, A. S. *Dokl. Acad. Sci. USSR* **1962**, *146*, 852.
- Cherkasov, A. S.; Voldaykina, K. G. *Bull. Acad. Sci. USSR Ser. Phys.* **1963**, *27*, 628.
- Fletcher, A. N. *J. Phys. Chem.* **1968**, *72*, 2742.
- Momicchioli, F.; Bruni, M. C.; Baraldi, I. *J. Phys. Chem.* **1972**, *76*, 3983.
- Razi Naqvi, K.; Donatsch, J.; Wild, U. P. *Chem. Phys. Lett.* **1975**, *34*, 285. Hughes, E., Jr.; Wharton, J. H.; Nauman, R. V. *J. Phys. Chem.* **1971**, *75*, 3097.
- Baraldi, I.; Bruni, M. C.; Caselli, M.; Ponterini, G. *J. Chem. Soc., Faraday Trans. 2* **1989**, *85*, 65.
- Sorriso, S.; Lumbruso, H. *Bull. Soc. Chim. France* **1973**, 1583. Favini, G.; Fasone, S.; Raimondi, M. *Gazz. Chim. Ital.* **1967**, *97*, 1434.
- Galiazzo, G.; Bortolus, P.; Masetti, F. *J. Chem. Soc., Perkin Trans. 2* **1975**, 1712.
- Fischella, S.; Mineri, G.; Scarlata, G.; Sciotto, D. *Tetrahedron* **1975**, *31*, 2445.
- Bottino, F. A.; Mineri, G.; Sciotto, D. *Tetrahedron* **1978**, *34*, 1557.
- Coletta, F.; Gambaro, A.; Pasimeni, L. *Gazz. Chim. Ital.* **1973**, *103*, 265; **1974**, *104*, 43.
- Muszkat, K. A. *Top. Curr. Chem.* **1979**, *88*, 91.
- Wismontski-Knittel, T.; Bercovici, T.; Fischer, E. *J. Chem. Soc. Chem. Commun.* **1974**, 716.
- Masetti, F.; Bartocci, G.; Mazzucato, U.; Galiazzo, G. *Gazz. Chim. Ital.* **1982**, *112*, 255.
- Hammond, G. S.; Shin, S. C.; Van, S. P. *Mol. Photochem.* **1969**, *1*, 89.
- Fischer, G.; Fischer, E. *Mol. Photochem.* **1974**, *6*, 463.
- Haas, E. See: footnote 12 in ref 18. See also: Goedicke, Ch.; Stegemeyer, H.; Fischer, G.; Fischer, E. *Z. Phys. Chem. N. F.* **1976**, *101*, 181.
- Haas, E.; Fischer, G.; Fischer, E. *J. Phys. Chem.* **1978**, *82*, 1638; Fischer, E. *J. Phys. Chem.* **1981**, *85*, 1770.
- Sheck, Yu. B.; Kovalenko, N. P.; Alfimov, M. V. *J. Lumin.* **1977**, *15*, 157. Alfimov, M. V.; Sheck, Yu. B.; Kovalenko, N. P. *Chem. Phys. Lett.* **1976**, *43*, 154.
- Fischer, E. *J. Photochem.* **1981**, *17*, 331; *J. Mol. Struct.* **1982**, *84*, 219.
- For review articles see: (a) Saltiel, J.; D'Agostino, J.; Megarity, E. D.; Metts, L.; Neuberger, K. R.; Wrighton, M.; Zaffriou, O. C. *Org. Photochem.* **1973**, *3*, 1. (b) Saltiel, J.; Charlton, J. L. In *Rearrangements in Ground and Excited States*; de Mayo, P., Ed.; Academic: New York, 1980; Vol. 3. (c) Saltiel, J.; Sun, Y.-P. In *Photochromism: Molecules and Systems*; Dürr, H.; Bouas-Laurent, H., Eds.; Elsevier: Amsterdam, 1990; Chapter 3.
- (a) Mazzucato, U. *Pure Appl. Chem.* **1982**, *54*, 1705. (b) *Gazz. Chim. Ital.* **1987**, *117*, 661.
- Birks, J. B.; Bartocci, G.; Aloisi, G. G.; Dellonte, S.; Barigelletti, F. *Chem. Phys.* **1980**, *51*, 113.
- Castel, N.; Fischer, E. *J. Mol. Struct.* **1985**, *127*, 159.
- Fischer, E. *J. Phys. Chem.* **1980**, *84*, 403.
- Ghiggino, K. P. *J. Photochem.* **1980**, *12*, 173. Matthews, A. C.; Sakurov, R.; Ghiggino, K. P. *J. Photochem.* **1982**, *19*, 235.
- McGown, L. B.; Bright, F. V. *Anal. Chem.* **1984**, *56*, 2195.
- Alfimov, M. V.; Razumov, V. F.; Rachinsky, A. G.; Listvan, V. N.; Sheck, Yu. B. *Chem. Phys. Lett.* **1983**, *101*, 593.
- Bartocci, G.; Masetti, F.; Mazzucato, U.; Marconi, G. *J. Chem. Soc., Faraday Trans. 2* **1984**, *80*, 1093.
- Bartocci, G.; Masetti, F.; Mazzucato, U.; Spalletti, A.; Bruni, M. C. *J. Chem. Soc., Faraday Trans. 2* **1986**, *82*, 775.
- Warner, I. M.; Christian, G. D.; Davidson, E. R.; Callis, J. B. *Anal. Chem.* **1977**, *49*, 564 and references cited therein.
- Saltiel, J.; Eaker, D. W. *J. Am. Chem. Soc.* **1984**, *106*, 7624.
- Sun, Y.-P.; Sears, D. F., Jr.; Saltiel, J. *Anal. Chem.* **1987**, *59*, 2515.
- (a) Saltiel, J.; Sears, D. F., Jr.; Mallory, F. B.; Mallory, C. W.; Buser, C. A. *J. Am. Chem. Soc.* **1986**, *108*, 1688. (b) Sun, Y.-P.; Sears, D. F., Jr.; Saltiel, J.; Mallory, F. B.; Mallory, C. W.; Buser, C. A. *J. Am. Chem. Soc.* **1988**, *110*, 6974.
- Sun, Y.-P.; Sears, D. F., Jr.; Saltiel, J. *J. Am. Chem. Soc.* **1988**, *110*, 6277.
- Cruciani, G.; Spalletti, A.; Bartocci, G. *Z. Phys. Chem. N. F.*, in press.
- Spalletti, A.; Bartocci, G.; Mazzucato, U.; Cruciani, G. *Chem. Phys.*, in press.
- Lawton, W. H.; Sylvestre, E. A. *Technometrics* **1971**, *13*, 617.
- Richards, J. L.; Rice, S. A. *J. Chem. Phys.* **1971**, *54*, 2014.
- Hudson, B. S.; Kohler, B. E.; Schulten, K. In *Excited States*; Lim, E. C., Ed.; Academic: New York, 1982; Vol. 6, pp 1-95.
- Muszkat, K. A.; Wismontski-Knittel, T. *Chem. Phys. Lett.* **1981**, *83*, 87.
- Muszkat, K. A.; Wismontski-Knittel, T. *J. Phys. Chem.* **1981**, *85*, 3427.
- Lamotte, M.; Morgan, F. J.; Muszkat, K. A.; Wismontski-Knittel, T. *J. Phys. Chem.* **1990**, *94*, 1302.
- Ito, M. *J. Phys. Chem.* **1987**, *91*, 517. Suzuki, T.; Mikami, N.; Ito, M. *J. Phys. Chem.* **1986**, *90*, 6431.
- Spangler, L. H.; van Zee, R.; Zwier, T. S. *J. Phys. Chem.* **1987**, *91*, 2782.
- Traetteberg, H.; Fronsten, E. B.; Mijlhoff, F. C.; Hoekstra, A. *J. Mol. Struct.* **1975**, *26*, 57.
- Ladd, J. A.; Wardale, H. W. In *Internal Rotation in Molecules*; Orville-Thomas, W. G., Ed.; Wiley: London, 1974; Chapter 5.
- Kurreck, H.; Kirste, B.; Lubitz, W. *Electron Nuclear Double Resonance Spectroscopy of Radicals in Solution*; VHC Publ.: Weinheim, 1988.
- Higuchi, J.; Ishizu, K.; Nemoto, F.; Tajima, K.; Suzuki, H.; Ogawa, K. *J. Am. Chem. Soc.* **1984**, *106*, 5403.
- (a) Park, P. J. D.; Pethrick, R. A.; Thomas, B. H. In *Internal Rotation in Molecules*; Orville-Thomas, W. G., Ed.; Wiley: London, 1974; Chapter 4. (b) Cunliffe, A. V. In *Internal Rotation in Molecules*; Orville-Thomas, W. G., Ed.; Wiley: London, 1974; Chapter 7. Allen, G.; Fewster, S. In *Internal Rotation in Molecules*; Orville-Thomas, W. G., Ed.; Wiley: London, 1974; Chapter 8.
- Scoponi, M.; Gallinella, E.; Momicchioli, F. *J. Chem. Soc., Faraday Trans. 2* **1988**, *84*, 95.
- Wismontski-Knittel, T.; Sofer, I.; Das, P. K. *J. Phys. Chem.* **1983**, *87*, 1745.
- Wismontski-Knittel, T.; Das, P. K. *J. Phys. Chem.* **1984**, *88*, 1168.
- Wismontski-Knittel, T.; Das, P. K. *J. Phys. Chem.* **1984**, *88*, 2803. For the case of 2-StN, see also ref 85.
- Fischer, E.; Castel, N. *J. Mol. Struct.* **1986**, *145*, 367.
- Krongauz, V.; Castel, N.; Fischer, E. *J. Photochem.* **1987**, *39*, 285.
- Sadley, J. *Semiempirical Methods of Quantum Chemistry*; Ellis Horwood: Chichester, 1985.
- (a) Warshel, A.; Karplus, M. *J. Am. Chem. Soc.* **1972**, *94*, 5612. (b) Warshel, A.; Levitt, M. *QCPE* No. 247, Indiana University, 1974.



- (61) Momicchioli, F.; Baraldi, I.; Bruni, M. C. *J. Chem. Soc., Faraday Trans. 2* 1972, 68, 1556.
- (62) Del Bene, J.; Jaffe, H. H. *J. Chem. Phys.* 1968, 48, 1807; 1968, 48, 4050; 1968, 49, 1221.
- (63) Ridley, J.; Zerner, M. *Theor. Chim. Acta* 1973, 32, 111; 1976, 42, 223.
- (64) Momicchioli, F.; Baraldi, I.; Bruni, M. C. *Chem. Phys.* 1983, 82, 229.
- (65) Orlandi, G.; Poggi, G.; Marconi, G. *J. Chem. Soc., Faraday Trans. 2* 1980, 76, 598.
- (66) Marconi, G.; Orlandi, G.; Poggi, G. *J. Photochem.* 1982, 19, 329.
- (67) Bartocci, G.; Masetti, F.; Mazzucato, U.; Spalletti, A.; Orlandi, G.; Poggi, G. *J. Chem. Soc., Faraday Trans. 2* 1988, 84, 385.
- (68) Momicchioli, F.; Baraldi, I.; Bruni, M. C. *Chem. Phys.* 1982, 70, 161.
- (69) Wolf, A.; Schmidtke, H. H.; Knop, J. V. *Theor. Chim. Acta* 1978, 48, 37.
- (70) Momicchioli, F.; Baraldi, I.; Fischer, E. *J. Photochem. Photobiol. A* 1989, 48, 95.
- (71) Baraldi, I.; Momicchioli, F.; Ponterini, G. *J. Mol. Struct. (THEOCHEM)* 1984, 110, 187.
- (72) Bartocci, G.; Masetti, F.; Mazzucato, U.; Spalletti, A.; Baraldi, I.; Momicchioli, F. *J. Phys. Chem.* 1987, 91, 4733.
- (73) Bartocci, G.; Masetti, F.; Mazzucato, U.; Baraldi, I.; Fischer, E. *J. Mol. Struct.* 1989, 193, 173.
- (74) Baraldi, I.; Ponterini, G. *J. Mol. Struct. (THEOCHEM)* 1985, 122, 287.
- (75) Baraldi, I.; Gallinella, E.; Momicchioli, F. *J. Chim. Phys.* 1986, 83, 653.
- (76) Baraldi, I.; Ponterini, G.; Momicchioli, F. *J. Chem. Soc., Faraday Trans. 2* 1987, 83, 2139.
- (77) Bartocci, G.; Mazzucato, U.; Masetti, F.; Aloisi, G. G. *Chem. Phys.* 1986, 101, 461.
- (78) Fischer, E. *J. Photochem.* 1985, 28, 139.
- (79) Saltiel, J. et al. See footnote 10 in ref 36b; see also ref 23c; p 143.
- (80) Becker, R. S. *Theory and Interpretation of Fluorescence and Phosphorescence*; Wiley: New York, 1969.
- (81) Mazzucato, U., et al. Unpublished results. See also: Elisei, F.; Mazzucato, U.; Görner, H. *J. Chem. Soc., Faraday Trans. 1* 1989, 85, 1469.
- (82) Momicchioli, F. Unpublished results related to ref 70.
- (83) Krysanov, S. A.; Alfimov, M. V. *Chem. Phys. Lett.* 1983, 98, 176.
- (84) Wettermark, G.; Tegner, L.; Martensson, O. *Ark. Kemi* 1968, 30, 185.
- (85) Görner, H.; Eaker, D. W.; Saltiel, J. *J. Am. Chem. Soc.* 1981, 103, 7164.
- (86) Hollas, J. M.; Ridley, T. *Chem. Phys. Lett.* 1980, 75, 94; Hollas, J. M.; Musa, H.; Ridley, T.; Turner, P. H.; Weisenberger, K. H. *J. Mol. Spectrosc.* 1982, 94, 437.
- (87) Almlöf, J. E.; Isacson, P. U.; Mjöberg, P. J.; Ralowski, W. M. *Chem. Phys. Lett.* 1974, 26, 215.
- (88) Almenningen, A.; Bastiansen, O.; Dyvik, F. *Acta Crystallogr.* 1961, 14, 1065.
- (89) McGlynn, S. P.; Azumi, T.; Kinoshita, M. *Molecular Spectroscopy of the Triplet State*; Prentice-Hall: New York, 1969.
- (90) Momicchioli, F.; Del Re, G. *J. Chem. Soc. (B)* 1969, 674. Del Re, G.; Momicchioli, F.; Rastelli, A. *Theor. Chim. Acta* 1972, 23, 316.
- (91) Fischer, G.; Fischer, E. *J. Phys. Chem.* 1981, 85, 2611.
- (92) Ham, M. S.; Ruedenberg, K. *J. Chem. Phys.* 1956, 25, 13.
- (93) Momicchioli, F. *Ric. Sci.* 1969, 39, 123; 1969, 39, 217.
- (94) Platt, J. R., et al. *Systematics of the Electronic Spectra of Conjugated Molecules: a Source Book*; Wiley: New York, 1964.
- (95) Birks, J. B. *Photophysics of Aromatic Molecules*; Wiley: London, 1970; Chapter 4.
- (96) Trotter, J. *Acta Crystallogr.* 1963, 16, 605.
- (97) Somers, J. B. M.; Laarhoven, W. H. *Rec. J. Roy. Neth. Chem. Soc.* 1980, 99, 160.
- (98) Wismontski-Knittel, T.; Das, P. K.; Fischer, E. *J. Phys. Chem.* 1984, 88, 1163.
- (99) Ghiggino, K. P.; Skilton, P. F.; Fischer, E. *J. Am. Chem. Soc.* 1986, 108, 1146.
- (100) Flom, S. R.; Nagarajan, V.; Barbara, P. F. *J. Phys. Chem.* 1986, 90, 2085.
- (101) Brearley, A. M.; Flom, S. R.; Nagarajan, V.; Barbara, P. F. *J. Phys. Chem.* 1986, 90, 2092.
- (102) Barbara, P. F.; Jarzaba, W. *Acc. Chem. Res.* 1988, 21, 195.
- (103) Arai, T.; Karatsu, T.; Sakuragi, H.; Tokumaru, K.; Tamai, N.; Yamazaki, I. *Chem. Phys. Lett.* 1989, 158, 429.
- (104) Bartocci, G.; Mazzucato, U.; Spalletti, A.; Elisei, F. *Spectrochim. Acta* 1990, 46A, 413.
- (105) (a) Karatsu, T.; Arai, T.; Sakuragi, H.; Tokumaru, K. *Chem. Phys. Lett.* 1985, 115, 9. (b) Becker, H.-D.; Andersson, K. *J. Org. Chem.* 1983, 48, 4542.
- (106) Cruickshank, D. W. J. *Acta Crystallogr.* 1956, 9, 915.
- (107) Siebrand, W. *J. Chem. Phys.* 1967, 46, 440; 1967, 47, 2411.
- (108) Görner, H.; Schulte-Frohlinde, D. *J. Phys. Chem.* 1981, 85, 1835.
- (109) Masetti, F. et al. Unpublished results.
- (110) Fischer, G.; Seger, G.; Muszkat, K. A.; Fischer, E. *J. Chem. Soc., Perkin Trans. 2* 1975, 1569.
- (111) Fischer, G.; Fischer, E. *J. Chem. Soc., Perkin Trans. 2* 1981, 1264.
- (112) Castel, N.; Fischer, E.; Bartocci, G.; Masetti, F.; Mazzucato, U. *J. Chem. Soc., Perkin Trans. 2* 1985, 1969.
- (113) Park, N. S.; Waldeck, D. H. *Chem. Phys. Lett.* 1990, 168, 379.
- (114) Bartocci, G.; Mazzucato, U. *Chem. Phys. Lett.* 1977, 47, 541.
- (115) Bartocci, G.; Mazzucato, U. *J. Lumin.* 1982, 27, 163.
- (116) Bartocci, G.; Masetti, F.; Mazzucato, U.; Dellonte, S.; Orlandi, G. *Spectrochim. Acta* 1982, 38A, 729.
- (117) Distefano, G.; Mazzucato, U.; Modelli, A.; Pignataro, S.; Orlandi, G. *J. Chem. Soc., Faraday Trans. 2* 1975, 71, 1583.
- (118) Fischer, E. *Bull. Soc. Chim. Belg.* 1979, 88, 889.
- (119) Galiazzo, G.; Gennari, G.; Bortolus, P. *J. Photochem.* 1983, 23, 149.
- (120) Gennari, G.; Galiazzo, G.; Bortolus, P. *J. Photochem.* 1986, 35, 177.
- (121) Gennari, G.; Galiazzo, G.; Bortolus, P. *J. Photochem. Photobiol. A* 1988, 43, 293.
- (122) Gennari, G.; Galiazzo, G.; Bortolus, P. *Chem. Phys. Lett.* 1989, 157, 194.
- (123) Galiazzo, G.; Bortolus, P.; Gennari, G. *Gazz. Chim. Ital.* 1990, 120, 581.
- (124) Shim, S. C.; Kim, D. W.; Kim, M. S. *J. Photochem. Photobiol. A* 1991, 56, 227.
- (125) Dewar, M. J. S.; Zoebisch, E. G.; Healy, E. F.; Stewart, J. J. P. *J. Am. Chem. Soc.* 1985, 107, 3902.
- (126) Shim, S. C.; Lee, K. T.; Bong, P.-H. *J. Photochem. Photobiol. A* 1987, 40, 381.
- (127) Lim, E. C. In *Excited States*; Lim, E. C., Ed.; Academic: New York, 1977; Vol. 3, p 305.
- (128) Shim, S. C.; Kim, M. S. *J. Chem. Soc., Perkin Trans. 2* 1989, 1897.
- (129) Galiazzo, G.; Gennari, G.; Bortolus, P. *Gazz. Chim. Ital.* 1991, 121, 67.
- (130) Gennari, G. et al. Unpublished results.
- (131) Bottino, F. A.; Scarlata, G.; Sciotto, D.; Torre, M. *Spectrochim. Acta* 1980, 36A, 205.
- (132) Wismontski-Knittel, T.; Das, P. K.; Fischer, E. *Helv. Chim. Acta* 1984, 67, 2246.
- (133) Allen, M. T.; Whitten, D. G. *Chem. Rev.* 1989, 89, 1691.
- (134) Sundström, V.; Gillbro, T. *Chem. Phys. Lett.* 1984, 109, 538.